

**Step 1**

$$\begin{aligned}W &= 1.1 \text{ } DL + 1.6 \text{ } LL \\&= 1.1 \times 12,400 + 1.6 \times 1390 = 15,865 \text{ kN}\end{aligned}$$

**Step 2**

For  $\phi = 33^\circ$ ;  $N_q = 20$ ,  $N_\gamma = 15$

For circular section,  $s_q = 1.2$ ,  $s_\gamma = 0.6$

$$d_q = d_\gamma = 1 + 0.1 \left( \frac{12.678}{5.5} \right) \tan \left( 45 + \frac{33}{2} \right)^\circ = 1.4$$

$$W' = 0.5; I_q = I_\gamma = 1$$

$$\begin{aligned}q_{\text{ult}} &= q(N_q - 1) s_q d_q I_q + 0.5 \gamma B N_\gamma s_\gamma d_\gamma I_\gamma W' + \gamma D \\&= 9.2 \times 12.678 (20 - 1) \times 1.2 \times 1.4 \times 1 + (0.5 \times 19.2 \times 5.5 \times 15 \times 0.6 \times 1.4 \\&\quad \times 0.5) + (19.2 \times 12.678) \\&= 3723 + 332.6 + 243.4 \approx 4300 \text{ kN}\end{aligned}$$

$$\frac{W}{A} = \frac{15,865}{24.42} = 649.7 \text{ kN} < \frac{430}{2}$$

Hence, it is justified.

**Step 3**

$$\begin{aligned}M_B &= \alpha WB \tan \phi \quad (\text{where } \alpha = 0.6 \times 0.61 = 0.366) \\&= 0.366 \times 15,865 \times 5.5 \tan 33^\circ \\&= 20,739 \text{ kNm}\end{aligned}$$

**Step 4**

$$\begin{aligned}M_s &= 0.1 \gamma' (K_p - K_A) LD^3 = 0.1 \times 9.2 \times 7.035 \times 0.9 \times 5.5 \times (12.678)^3 \\&= 65,280 \text{ kNm}\end{aligned}$$

$$\begin{aligned}\text{For circular well, } M_f &= 0.11 \gamma' (K_p - K_A) B^2 D^2 \sin \delta \\&= 0.11 \times 9.2 \times 7.035 \times 5.5^2 \times 12.678^2 \times \sin 20^\circ \\&= 11,839 \text{ kNm}\end{aligned}$$

$$\begin{aligned}\text{Total resisting moment, } M_r &= 20,739 + 65,280 + 11,839 \\&= 97,850 \text{ kNm}\end{aligned}$$

$$M_t = 0.7 \times 97,850 = 68,500 \text{ kNm}$$

Moment due to tilt and shift = 5500 kNm

$$\begin{aligned}\text{Equivalent } H &= 1.1 \left( \frac{5500}{24.603} \right) + 1.25 \times 1755 = 245.9 + 2193.7 \\&= 2439.6 \text{ kN}\end{aligned}$$

Applied moment =  $2439.6(24.603 - 0.2 \times 12.678)$   
 (Point of rotation  $0.2D$  above base)

$$= 53,830 \text{ kNm} < 68,500 \text{ kNm. Therefore, accepted.}$$

### Example 10.4

For the bridge considered in Example 10.3, check the adequacy of the abutment well whose elevation and nature of earth pressure diagrams have been shown in Fig. 10.12

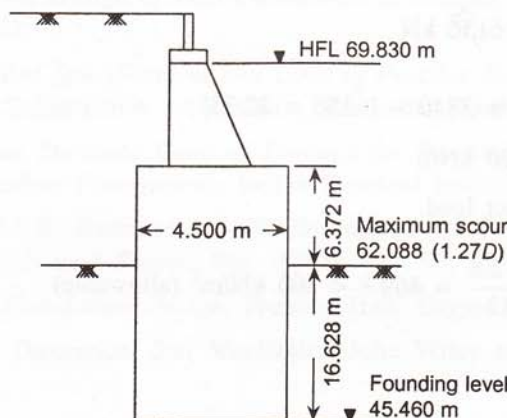


Fig. 10.12 Elevation and earth pressure for bridge in Example 10.3.

Given:

$$\text{Total Vertical Load } V = 11,472.8 \text{ kN}$$

$$\text{Horizontal Force } F_H = 3446.5 \text{ kN}$$

$$\text{Moment } M = 77,020 \text{ kNm}$$

$$\text{Moment due to tilt and shift} = 3840 \text{ kNm}$$

$$\text{Normal scour depth } d_s = 6.096 \text{ m}$$

$$p_o = 47.66 \text{ kN/m}^2$$

(refer Fig. 10.10)

### Solution

Bombay method

$$e = H_1 + D = \frac{M}{F_H} = \frac{77,020}{3446.5} = 22.35 \text{ m}$$

$$D = 16.628 \text{ m}$$

$$q_{\max} = \frac{D^2}{6(H_1 + D)} [ \gamma'(K_p - K_A) D \cos \delta - 3p_o ]$$

$$\begin{aligned}
 &= \frac{D^2}{6(H_1 + D)} [mD - 3p_o] \\
 &= \frac{(16.628)^2}{6 \times 22.35} [(9.2 \times 7.035 \times 16.628 \times 0.94) - (3 \times 47.66)] \\
 &= 1791 \text{ kN/m}
 \end{aligned}$$

$$Q_{\max} = \frac{1791 \times 5.5}{(FS=)1.6} = 6156 \text{ kN}$$

$$\begin{aligned}
 \text{Net moment} &= 77,020 + 3840 - (6156 \times 22.35) \\
 &= -56,720 \text{ kNm}
 \end{aligned}$$

∴ Consider only direct load.

$$\text{Base pressure} = \frac{11,472.8}{24.42} = 469.8 < 800 \text{ kN/m}^2 \text{ (allowable)}$$

Method based on IRC : 78

$$\begin{aligned}
 q_{\max} &= \frac{D^2}{6(H_1 + D)} (mD - 3p_o) \\
 &= \frac{mD^3}{6(H_1 + D)} - \frac{p_o D^2}{2(H_1 + D)} \\
 &= \frac{60.8 \times 16.628^3}{6 \times 22.35} - \frac{47.66 \times 16.628^2}{2 \times 22.35} \quad \text{where } m = 9.2 \times 7.035 \times 0.94 = 60.8 \\
 &= 2084.4 - 294.8
 \end{aligned}$$

With  $FS (= 1.6)$  on 1st term only,

$$q'_{\max} = \frac{2084.4}{1.6} - 294.8 = 1008 \text{ kN/m}^2$$

$$\therefore Q_{\max} = 1008 \times 5.5 = 5540 \text{ kN}$$

$$\text{Balance moment} = 80,860 - 5540 \times 22.35 = -429.5 \text{ kNm}$$

$$\therefore \text{Base pressure} = \frac{11,472.8}{24.42} = 469.8 < 800 \text{ kN/m}^2 \text{ (allowable)}$$

---

**REFERENCES**

---

- IRC: 5-1998, *Standard Specifications and Code of Practice for Road Bridges*, Section 1, General Features of Design, The Indian Roads Congress, New Delhi, 1998.
- IRC: 45-1972, *Recommendations for Estimating the Resistance of Soil below the Maximum Scour Level in the Design of Well Foundation of Bridges*, The Indian Roads Congress, New Delhi, 1972.
- IRC: 78-1983, *Standard Specifications and Code of Practice for Road Bridges*, Section: VII, Foundation and Substructure, 1st Revision, The Indian Roads Congress, New Delhi, 1994.
- IS: 6403-1971, *Indian Standard Code of Practice for Determination of Allowable Bearing Pressure on Shallow Foundations*, Indian Standard Institution, New Delhi, 1972.
- Peck, R.B. and A.R.S.S. Bazzaraf (1969), Discussion on Paper by D'Appolonia, et al., *Journal Soil Mech. and Found. Div.* ASCE, Vol. 95, SM. No. 3.
- Teng, W.C. (1962), *Foundation Design*, Prentice Hall, Englewood Cliffs, New Jersey.
- Terzaghi, K. (1943), *Theoretical Soil Mechanics*, John Wiley and Sons, New York.

# 11

# Foundations on Expansive Soils

## 11.1 INTRODUCTION

Some cohesive soils undergo swelling when they come into contact with water and shrink when water is squeezed out. Foundations built on these soils undergo movement with swelling and shrinkage of the soil. As a result, there is considerable cracking and other forms of distress in the buildings.

Expansive soils are mostly found in the arid and semi-arid regions of the world. They cover large areas of Africa, Australia, India, United States, South America, Myanmar and some countries of Europe. In India, expansive soils cover nearly 2 percent of the land area and are called *black cotton soil* because of their colour and cotton growing potential. Large areas of Deccan plateau, Andhra Pradesh, Karnataka, Madhya Pradesh, and Maharashtra have deposits of expansive soil.

Expansive soils derive their swelling potential mainly from montmorillonite mineral which is present in these soils. They are residual soils formed by the weathering of basaltic rocks under alkaline environment. Extended periods of dry climate cause desiccation of the soil but rains cause swelling near the ground surface. The depth of the swelling zone is not much—being less than 5 m in most cases. However, the active zone over which there are seasonal changes in moisture content, varies from 1.5 m to 4 m (O'Neill and Poormoayed, 1980).

## 11.2 NATURE OF EXPANSIVE SOIL

The swelling characteristics of a soil depend largely on the type of clay mineral present in the soil. Differential Thermal Analysis (DTA), X-ray diffraction, and electron microscopy are common methods of determining the proportion of different minerals present in a soil. Some simple laboratory tests are often used to determine the swelling potential of natural soil.

### 11.2.1 Free-swell Test

This test is performed by pouring 10 g of dry soil, passing 425 micron sieve, in a 100 cc graduated cylinder filled with water. The soil collects at the bottom of the cylinder and

gradually increases in volume. After 24 hours, the volume of the soil is read from the graduations in the cylinder. The percent free swell of the soil is given by

$$\text{Free swell (\%)} = \frac{\text{final volume} - \text{initial volume}}{\text{initial volume}} \times 100$$

The percent free swell of predominant clay minerals is given in Table 11.1. Kaolinite and illite have percent free swell less than 100 and are generally regarded as non-swelling minerals. Montmorillonite, on the other hand, has high swelling potential.

**Table 11.1** Free swell of clay minerals

Mineral	Percent free swell
Montmorillonite (Bentonite)	1200–2000
Kaolinite	80
Illite	30–80

Gibbs and Holtz (1956) suggested that soils having free swell above 50% may be expected to cause problem to light structures.

### 11.2.2 Differential Free Swell

Two samples of oven-dried soil (10 g) passing 425 micron sieve are taken and poured into 100 cc graduated glass cylinders—one filled with water and the other with kerosene. Kerosene, being a non-polar liquid does not cause any volume change in the soil. After 24 hours, the volumes of soil in the two cylinders are measured and the differential free swell, *DFS* is obtained

$$DFS = \frac{\text{soil volume in water} - \text{soil volume in kerosene}}{\text{soil volume in kerosene}} \times 100$$

IS 2720 (Part III-1980) gives the degree expansiveness of a soil in terms of the differential free swell, Table 11.2.

**Table 11.2** Degree of expansiveness and *DFS*

Degree of expansiveness	<i>DFS</i> (%)
Low	Less than 20
Moderate	20–35
High	35–50
Very high	Greater than 50

### 11.2.3 Unrestrained Swell Test

This test is done in the standard odometer. The soil specimen is given a small surcharge load (say, 5 kN/m<sup>2</sup>) and submerged in water. The volume expansion of the specimen is measured in terms of the increase in thickness of the specimen—the cross-sectional area remaining constant. The percent swell is expressed as

$$s_w(\%) = \frac{\Delta H}{H} \times 100$$

where,  $s_w(\%)$  = free swell,

$\Delta H$  = increase in height of soil sample, and

$H$  = original height.

Vijayvergiya and Ghazzali (1973) gave a correlation between free swell, natural moisture content, and liquid limit of some clays. This correlation is presented in Fig. 11.1.

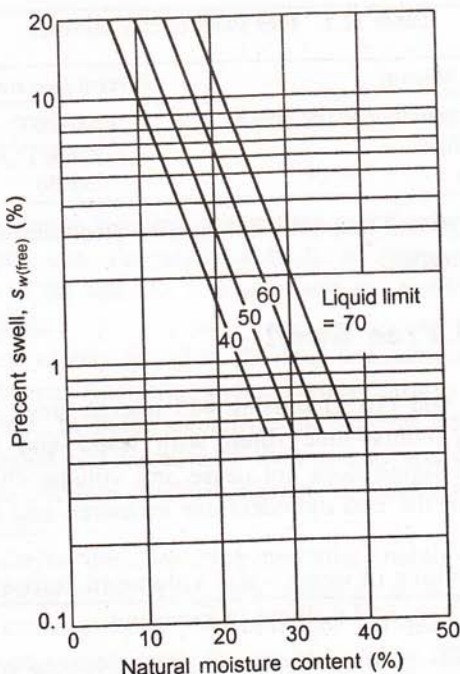


Fig. 11.1 Relationship between free swell, water content, and liquid limit  
(after Vijayvergiya and Ghazzali, 1973).

#### 11.2.4 Swelling Pressure

The swelling pressure indicates the external pressure required to prevent swelling of a soil when the latter comes into contact with water. The test is done in the consolidation apparatus. Water is added to the specimen and as it starts to swell, pressure is applied in small increments to prevent swelling. The test is continued till the sample just begins to settle. This gives the swelling pressure ( $p_s$ ) of the sample (Sridharan et al. 1986). As a general rule, a swelling pressure of 20–30 kN/m<sup>2</sup> is considered low. A highly swelling soil, for example, bentonite may have swelling pressure as high as 1500–2000 kN/m<sup>2</sup>.

Some empirical formulae have been suggested for estimating the swelling pressure of a soil from the void ratio and plasticity index of the soil (Pidgeon, 1987).

$$p_s = 2.7 - 24 \left( \frac{e_i}{PI} \right)$$

where,  $p_s$  = swelling pressure ( $\text{kg}/\text{cm}^2$ ),

$e_i$  = initial void ratio, and

$PI$  = plasticity index (%).

### 11.2.5 Classification of Swelling Potential

Potential swell is defined as the vertical swell under a pressure equal to overburden pressure. A number of classification systems for the swelling potential have been proposed (Seed et al. 1962; Sowers and Sowers, 1970; Chen, 1988; Vijayvergiya and Ghazzali 1973). These are generally based on the Atterberg Limits of the soil. O'Neill and Poormoayed (1980) summarized the U.S. Army Waterways Experiment Station criterion based on plasticity index and the potential swell. This classification of expansive soil is expressed in Table 11.3.

Table 11.3 Classification of expansive soil

Liquid limit	Plasticity index	Potential swell	Swelling potential
< 50	< 25	< 0.5	Low
50–60	25–35	0.5–1.5	Marginal
> 60	> 35	> 1.5	High

USBR (1960) gives similar criteria for clays based on colloid percent (less than 0.001 mm) and shrinkage limit of the soil, which are shown in Table 11.4.

Table 11.4 Criteria for expansive clays

Colloid content (%)	Plasticity index	Shrinkage limit	Probable expansion (%)	Degree of expansiveness
> 28	> 35	< 11	> 30	Very high
20–30	25–41	7–12	20–30	High
13–23	15–28	10–16	10–20	Medium
< 15	> 10	> 15	< 10	Low

### 11.3 EFFECT OF SWELLING ON BUILDING FOUNDATIONS

In tropical countries, the soil near the ground surface dries up during the summer as a consequence of intense heat and recession of ground water table. The soil becomes stiff and cracks and fissures open up. When rains come, the soil gets wet by the precipitation and with time, the ground water table also rises. This causes increase in water content of the soil and hence, swelling of the soil. The structure built on the soil protects the soil from the heat but nonetheless water tends to accumulate from the surrounding areas and contributes to swelling. The depth over which such variation in water content occurs depends on the nature of soil and climatic conditions but an active zone of 3.5–4 m has generally been observed.

The movement of the foundation with swelling and shrinkage of the soil causes the floor slabs of buildings to lift up and develop a dome shaped deformation pattern. This leads to cracks in the floor and external walls. The differential movement also causes diagonal

cracks in the walls and at the corner of doors and windows, as shown in Fig. 11.2 Utilities buried in the soil get damaged and the leakage of water into the soil results in further swelling. The effect is more pronounced in the one or two storey buildings where the foundation pressure is often less than the swelling pressure. For tall structures, foundation pressure generally exceeds the swelling pressure and the swelling potential reduces.

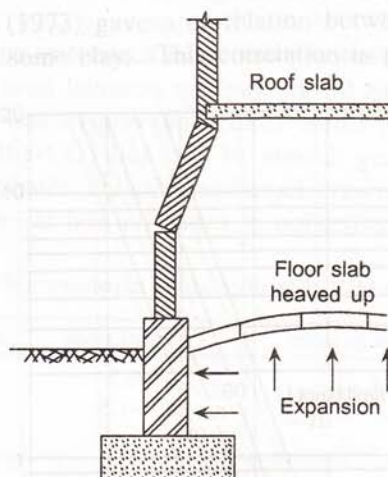


Fig. 11.2 Distress in buildings due to swelling.

## 11.4 FOUNDATION DESIGN IN EXPANSIVE SOIL

Foundation design in expansive soil needs a different approach as compared to that in non-swelling soil. It must be realized that limiting the safe bearing pressure to a low value does not help to counteract the swelling pressure. Rather, design should be done with a high enough bearing pressure and following the criteria of bearing capacity failure and permissible of settlement, so that chances of swelling are minimized.

Foundation design in expansive soil can be done in the following ways:

1. Isolating the foundation from the swelling soil,
2. Taking measures to prevent the swelling, and
3. Employing measures to make the structure withstand the movement.

### 11.4.1 Isolating the Foundation from the Swelling Zone: Under-reamed Piles

A common method of building foundation in expansive soil is to provide under-reamed piles below the foundation. Here, the structural load is transferred to the soil beneath the zone of fluctuation of water content. The piles are taken to depths of 5–6 m, that is, well beyond the expansive zone. These piles are bored cast-in-situ piles with the lower end enlarged to form under-reamed bulbs with the help of special tools, Fig. 11.3. The piles generally have shaft

diameter of 300 mm and bulb diameter of 750 mm, as depicted in Fig. 11.4. The piles are fixed at the top to RCC plinth beams. A gap of 75–100 mm is kept between the plinth beam and the soil which is filled with granular material to permit swelling of the underlying soil without straining the plinth beams. The piles are adequately reinforced to take care of the uplift forces caused by the swelling action of the soil.

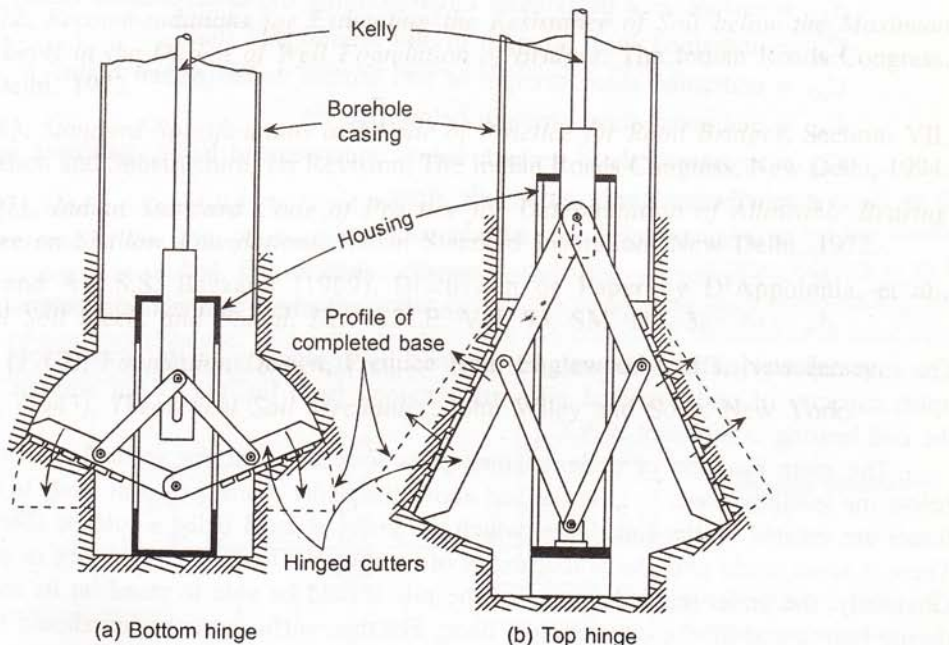


Fig. 11.3 Tools for bulb formation in under-reamed piles. (after Tomlinson, 1994)

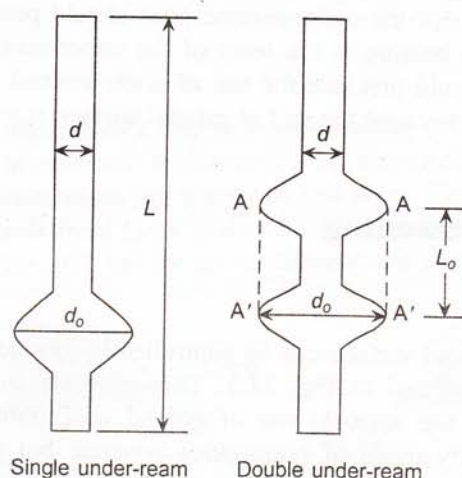


Fig. 11.4 Typical under-reamed pile foundation.

The ultimate bearing capacity of an under-reamed pile is determined from static analysis as already discussed in Chapter 9.

$$Q_u = \alpha C_{a1} A_{f1} + C_{a2} A_{f2} + A_p N_c C_{p1} + A_u N_c C_{p2} \quad (11.1)$$

where,  $A_{f1}$  = surface area of pile stem,

$A_{f2}$  = surface area of cylinder circumscribing the under-reamed bulbs,

$C_{a1}$  = undrained shear strength of soil around pile shaft,

$C_{a2}$  = undrained shear strength of soil around under-reamed bulbs,

$C_{p1}$  = undrained shear strength below pile tip,

$C_{p2}$  = undrained shear strength below under-reamed bulbs,

$\alpha$  = adhesion factor along pile stem,

$A_p$  = cross-sectional area of pile toe,

$N_c$  = bearing capacity factor, usually taken as 9.0, and

$A_u = (\pi/4)(D_u^2 - D^2)$  where  $D_u$  and  $D$  are the bulb and stem diameters respectively.

The safe capacity of the pile may be obtained by applying a factor of safety of 2.5–3. The uplift capacity of under-reamed piles are obtained from Eq. (11.1) but without considering the end bearing component  $A_p N_c C_{p1}$ .

The main function of under-reamed piles is to transmit the vertical load into the soil below the swelling zone. In case the soil above the under-reamed section tends to swell, uplift forces are created on the foundation which the under-reamed bulbs would be able to counter. There is some doubt over the practicability of forming the under-reamed bulbs in granular soil. Obviously, the under-reamed section of the pile should be able to stand on its inclined faces during boring and till the concreting is done. For this, sufficient cohesion should be available. Clayey soil provides this cohesion without much difficulty. But the formation of bulb in granular soil is not free from uncertainties. Field experiments have shown that the sand tends to disintegrate during the stand up time and no bulb is really formed.

It should also be noted that the under-reamed piles should penetrate well into the firm ground to give sufficient end bearing at the level of the under-reams. Presence of soft clay beneath the expansive soil would preclude the use of under-reamed piles. Indiscriminate use of under-reamed piles simply because the soil at ground surface is expansive in nature, often serves no useful purpose.

#### 11.4.2 Controlling Swelling

##### Impervious apron

Swelling of soil near the ground surface can be controlled by providing an impervious apron around the structure as illustrated in Fig. 11.5. This prevents surface precipitation from penetrating into the soil but the seasonal rise of ground water table is not controlled. The impervious apron is generally made of bituminous concrete but it should be sufficiently flexible to prevent cracking and distress due to soil movement caused by swelling. It is necessary for the apron to penetrate sufficiently into the foundation to prevent ingress of water into the soil during inundation.

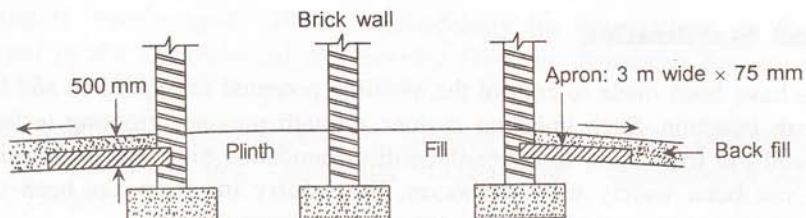


Fig. 11.5 Impervious apron for controlling swelling.

### **Surcharge loading**

Swelling can also be controlled by applying a pressure on the ground at least equal to the swelling pressure of the soil. Attempts have been made to apply a surcharge on the footing area but this does not prevent the swelling between foundations. If surcharge loading is to be applied, this should be done to cover the entire building area by a suitable non-swelling soil. The depth of surcharge should, of course, be such that the surcharge pressure is at least equal to the swelling pressure of the soil. Surcharge loading is depicted in Fig. 11.6.

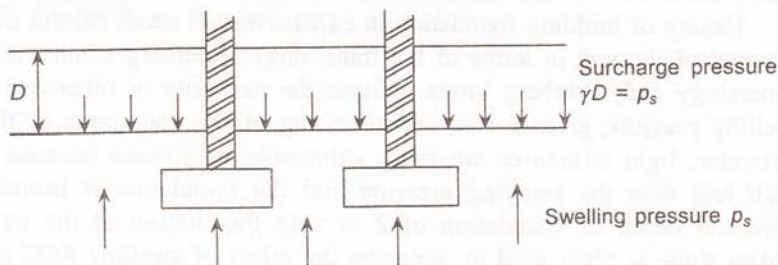


Fig. 11.6 Surcharge loading to control swelling.

### **CNS layer**

Katti (1979) proposed the use of a cohesive non-swelling (CNS) layer to reduce the effect of swelling. A clay soil of adequate thickness having non-swelling clay minerals, is placed on the subgrade and the foundations are placed on this layer. The optimum thickness of the CNS layer is to be determined from large scale tests. The method has been used in canal lining works, as shown in Fig. 11.7 but its use in foundations is still limited.

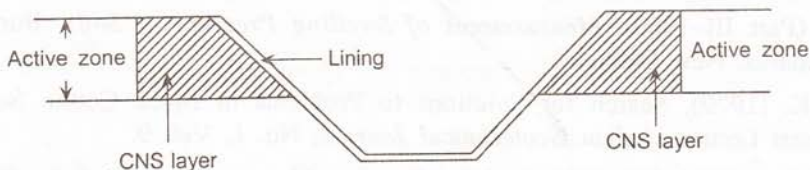


Fig. 11.7 Use of CNS layer in canal lining.

### Chemical Stabilization

Attempts have been made to control the swelling potential of expansive soil by lime-slurry or lime-flyash injection. Such injection is done through pressure grouting technique on a close grid around the foundation to cover the entire foundation area. But the method is expensive and has not been widely used. However, lime slurry injection has been used to stabilize foundations on expansive soil after occurrence of distress.

#### 11.4.3 Measures to Withstand Settlement

The foundation may be made sufficiently rigid by providing interconnected beams and band lintel to withstand the effects of differential movement on the structure. Stiffened mat foundations (Lytton, 1972) have also been adopted to counter the effect of differential ground movement. Premlatha (2002) carried out a study on the use of stiffened mat for low rise structures in Chennai, based on evaluation of heave of the soil. A three dimensional soil structure interactive analysis was done to suit the loading, climate, and environmental conditions of Chennai. However, these methods are rather expensive and have not been widely used for low to medium structures.

Design of building foundation in expansive soil needs careful evaluation of the swelling potential of the soil in terms of the mineralogy, Atterberg Limits, and the swelling pressure. Mineralogy and Atterberg limits indicate the necessity or otherwise of special design. Only swelling pressure gives a true understanding of the magnitude of the swelling potential. In particular, light structures are more vulnerable to distress because the bearing pressure is often less than the swelling pressure and the foundation is prone to uplift forces. For a minimum depth of foundation of 2 m with the bottom of the trench filled with sand, a broken stone is often used to minimize the effect of swelling RCC plinth beams. Band lintel also helps to withstand the effect of swelling.

Under-reamed piles and surcharge loading seem to be the most suitable methods of countering the effect of swelling. In addition, good surface drainage and impervious paving around the site help to prevent water percolation in the soil.

### REFERENCES

- Chen, F.H. (1988), *Foundations on Expansive Soils*, Elsevier, Amsterdam.
- Gibbs, H.J. and W.G. Holtz (1956), *Engineering Properties of Expansive Clays*, Transactions ASCE, New York. Vol. 121, pp. 641–663, Paper No. 2814, Discussion, pp. 664–777.
- IS 2720 (Part III–1980), *Measurement of Swelling Pressure of Soils*, Bureau of Indian Standards, New Delhi.
- Katti, R.K. (1979), Search for Solutions to Problems in Black Cotton Soils, First IGS Annual Lecture, *Indian Geotechnical Journal*, No. 1, Vol. 9.
- Lytton, R.L. (1972), *Design Method for Concrete Mats on Unstable Soils*, Proceedings 3rd American Conference on Materials Tech., Rio-de-Janeiro, Brazil, pp. 171–177.

- O'Neill, M.W. and N. Poormoayed, (1980), Methodology for Foundations on Expansive Clays, *Journal of the Geotechnical Engineering Division*, American Society of Civil Engineers, Vol. 106, No. GT12, pp. 1345–1367.
- Pidgeon, J.T. (1987), *A Comparison of Existing Methods for the Design of Stiffened Raft Foundation on Expansion Soil*, Proceeding 7th Regional Conference of Africa on SMFE, pp. 277–289.
- Premlatha, K. (2002), *Prediction of Heave Using Soil-Water Characteristics and Analysis of Stiffened Raft on Expansive Clays of Chennai*, Ph. D. Thesis, Anna University, Chennai.
- Seed, H.B., R.J. Woodward, Jr., and R. Lundgren (1962), Prediction of Swelling Potential for Compacted Clays, *Journal of the Soil Mechanics and Foundations Division*, American Society of Civil Engineers, Vol. 88, No. SM3, pp. 53–87.
- Sowers, G.B. and G.F. Sowers (1970), *Introductory Soil Mechanics and Foundations*, 3rd ed., New York, Macmillan.
- USBR (1960), *Earth Manual*, U.S. Bureau of Reclamation, Denver, Colorado, July, 1960.
- Vijayvergiya V.N. and O.I. Ghazzali (1973), *Prediction of Swelling Potential of Natural Clays*, Proceedings 3rd International Research and Engineering Conference on Expansive Clays, pp. 227–234.

**Step 4:**

$$\frac{mM}{I} = \frac{1 \times 48,680}{972.45} = 50 \cdot \gamma^2 (K_p - K_A) = 9.2 \times 7.035 = 64.7$$

with seismic,  $1.25/(K_p - K_A) = 1.25 \times 64.7 = 80.88 < 50$

**Step 5:**

$$\sigma_{x_1, 0_1} = \frac{W - \mu' p}{A/B}$$

$$= \frac{13,790 - 0.364 \times 5641}{24.42} = \frac{48,680 \pm 5.5}{2 \times 972.45}$$

$$= 465.8 \pm 137.7$$

$= 603.5, 328.1 \text{ kN/m}^2 \leq 800 \text{ kN/m}^2$ . Hence, it is acceptable.

Method based on IRC-45 (Ultimate)

# 12

# Ground Improvement Techniques

## 12.1 INTRODUCTION

Soils are deposited or formed by nature under different environmental conditions. Man does not have any control on the process of soil formation. As such the soil strata at a site are to be accepted as they are and any construction has to be adapted to suit the subsoil condition. The existing soil at a given site may not be suitable for supporting the desired facilities such as buildings, bridges, dams, and so on because safe bearing capacity of a soil may not be adequate to support the given load. Although pile foundations may be adopted in some situations, they often become too expensive for low to medium-rise buildings. In such cases, the properties of the soil within the zone of influence have to be improved in order to make them suitable to support the given load.

Ground improvement for the purpose of foundation construction essentially means increasing the shear strength of the soil and reducing the compressibility to a desired extent. A number of ground improvement techniques have been developed in the last fifty years. Some of these techniques need specialized equipment to achieve the desired result. In this chapter, only the common ground improvement techniques which use simple mechanical means to improve soil properties for low to medium-rise structures are considered. For tall structures, pile foundations with or without basement would generally give the most economic foundations.

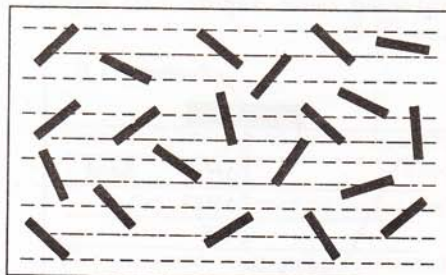
## 12.2 PRINCIPLES OF GROUND IMPROVEMENT

The mechanics of ground improvement depends largely on the type of soil—its grain-size distribution, water content, structural arrangement of particles and so forth. In general, ground improvement is called for in soft cohesive soil with low undrained shear strength ( $c_u < 2.5 \text{ t/m}^2$ ) and loose sand ( $N < 10$  blows per 30 cm). The mechanics of ground improvement can be understood in terms of the structural arrangement of particles constituting the soil deposit.

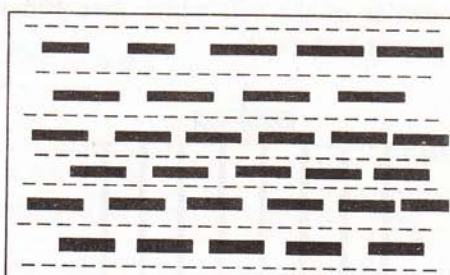
### (a) Cohesive soil

Sedimentary (alluvial or marine) clays during deposition under flowing water have the flexible flake shaped particles arranged at random flocculated structure with large void spaces

filled with water. Figure 12.1(a) depicts the flocculated structure of cohesive soil. Such structural arrangement with high water content is unstable and gives high compressibility. Under the influence of increasing overburden pressure or external load, the soil consolidates and the particles tend to re-orient themselves along horizontal planes (that is, perpendicular to the line of action of the applied load). Such a dispersed structure is more stable and the reduction of water content brings the particles closer together to reduce compressibility, as shown in Fig. 12.1(b). Thus, reduction of water content through application of external load would cause improvement of engineering properties of cohesive soil.



(a) Flocculated structure.



(b) Dispersed structure.

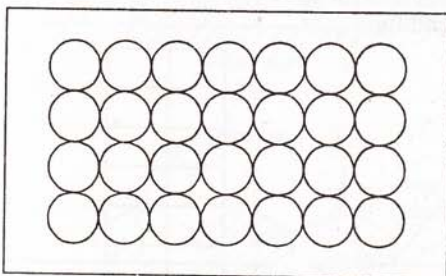
**Fig. 12.1 Structure of cohesive soil.**

Cohesive soil can be improved using

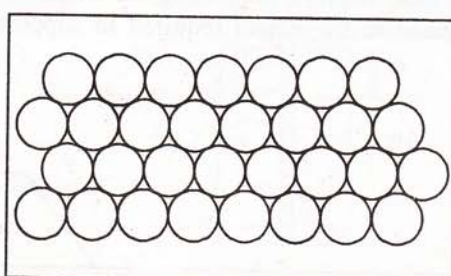
- Preloading with vertical drains and
- Soil reinforcement with stone columns.

### **(b) Granular soil**

Particles of granular soil such as sand and gravel, have three-dimensional structure. For the purpose of understanding, they can be represented by spheres which in loose condition are arranged one on top of the other as shown in Fig. 12.2(a). Granular soils in this condition have low relative density. The shear strength is also low because of the tendency of the particles to roll over one another under the influence of shearing stresses. If the same particles are rearranged as shown in Fig. 12.2(b), the void space decreases and the relative



(a) Loose structure.



(b) Dense structure.

**Fig. 12.2 Structure of granular soil.**

density increases with corresponding increase of shear strength. Thus, properties of granular soil can be improved by increasing its relative density by external means. Following ground improvement techniques are used for granular soil:

- Compaction with drop hammer and
- Deep compaction by compaction piles or vibrofloatation.

Apart from these, soil reinforcement by inserting stiffer materials within the soil fabric such as metallic strips, compacted granular piles, geotextiles, and so on would also improve the properties of the soil which then behave as reinforced mass. Figure 12.3 depicts soil reinforcement technique.

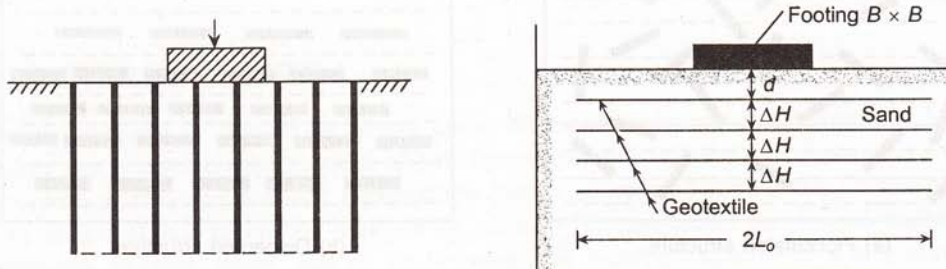


Fig. 12.3 Soil reinforcement.

Chemical injection and grouting are also adopted as methods of ground improvement. In these cases, the chemicals penetrate into the voids and get set to strengthen the soil fabric. Normally, these techniques require specialized equipment to achieve success in the field. These methods are not discussed in this chapter.

## 12.3 GROUND TREATMENT IN COHESIVE SOIL

### 12.3.1 Preloading with Vertical Drains

The most common method of ground treatment in cohesive soil is to reduce the void ratio or water content of the soil by preconsolidation. This increases the shear strength of the soil and reduces the compressibility even before construction of the building is commenced. Figure 12.4 displays preloading for building foundations. Soil properties are improved under the preload to the extent required to support the building.

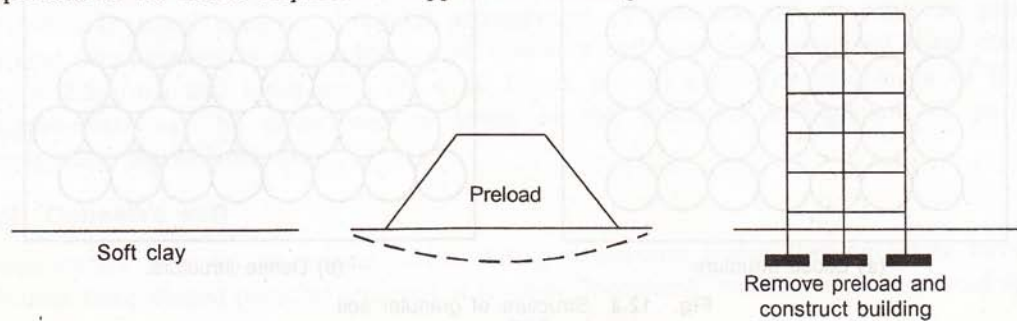


Fig. 12.4 Preloading for building foundations.

The mechanics of ground improvement by preloading may be discussed with reference to the void ratio versus effective stress relationship of a normally consolidated clay, as shown in Fig. 12.5.

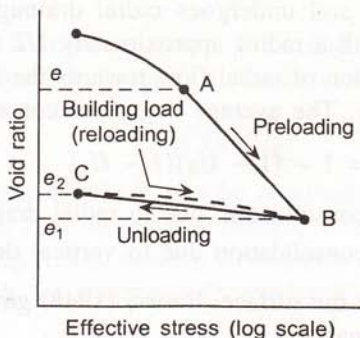


Fig. 12.5 Pressure versus void ratio relationship for normally consolidated clay.

The pressure void ratio relationship of a normally consolidated clay follows the virgin consolidation curve from A to B during preloading. There is large settlement consequent upon the change of void ratio from  $e$  to  $e_1$ . When the preload is removed, the soil undergoes swelling from B to C and the void ratio increases from  $e_1$  to  $e_2$ . Thereafter, when the building is erected, the same intensity of pressure  $\Delta p$  is applied but now the settlement is a function of the change of void ratio corresponding to reloading, that is,  $e_2$  to  $e_1$ . So the settlement of the building is reduced considerably. In effect, the potential settlement of the ground under the building load is made to occur under the preload prior to construction of the building.

In direct preloading, the time for consolidation may run into years because of the low permeability of the clay and long drainage path. To reduce the time for consolidation, vertical drains with a drainage blanket on top are used. This is illustrated in Fig. 12.6.

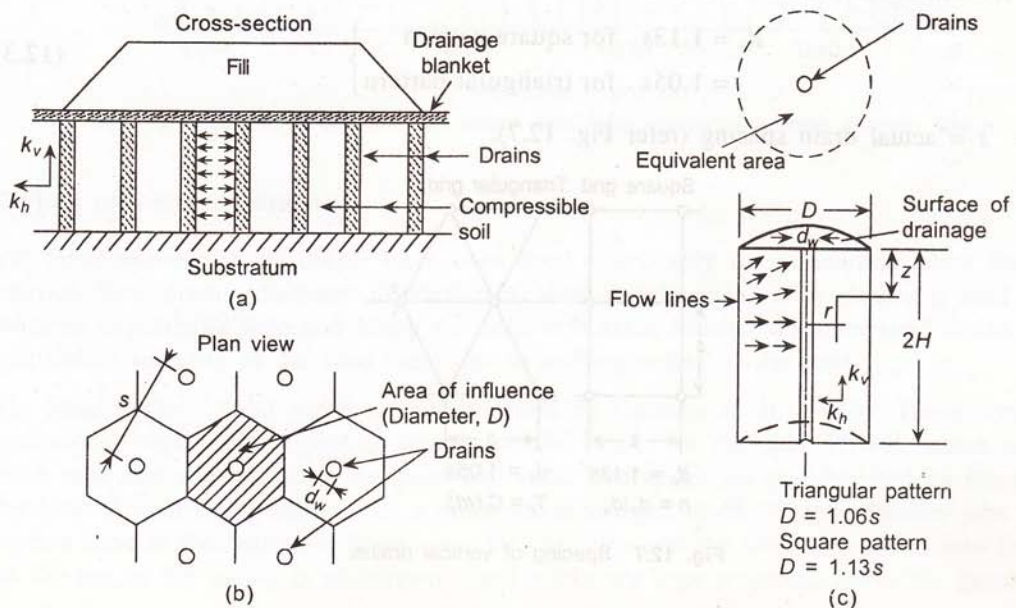


Fig. 12.6 Preloading with vertical drains.

In the earlier days, sand drains, 300–500 mm diameter, were installed by filling with sand the vertical holes made into the soil at predetermined spacing. Nowadays sand wicks and prefabricated vertical drains (PVD), e.g., band drains are mostly used to have more efficient consolidation under the preload. When a soil is preloaded by dead weight, the horizontal drainage path is reduced and the soil undergoes radial drainage. Each drain well has an axisymmetric zone of influence with a radius approximately 1/2 times the well spacing. The flow within the zone is a combination of radial flow towards the sand drain and vertical flow towards the free-draining boundary. The average degree of consolidation is then given by,

$$\bar{U} = 1 - (1 - U_R)(1 - U_Z) \quad (12.1)$$

where  $U_R$  = average degree of consolidation due to radial drainage and

$U_Z$  = average degree of consolidation due to vertical drainage.

Assuming uniform vertical strain at the surface, Barron (1948) gave the expression for degree of consolidation due to radial drainage as,

$$U_R = 1 - \exp\left(-\frac{8T_r}{F_a}\right) \quad (12.2)$$

where  $F_a = \left(\frac{n^2}{n^2 - 1}\right) \log_e n - \left(\frac{3n^2 - 1}{4n^2}\right)$ ,

$n = \frac{d_e}{d_w} = \frac{\text{equivalent drain spacing}}{\text{drain diameter}}$ , and

$$T_r = \frac{C_r t}{d_e^2} = \text{radial time factor.}$$

The drains may be installed in either square or triangular grid. Considering the influence area of each drain to be circular, we have

$$\left. \begin{aligned} d_e &= 1.13s && \text{for square pattern} \\ &= 1.05s && \text{for triangular pattern} \end{aligned} \right\} \quad (12.3)$$

where  $s$  = actual drain spacing (refer Fig. 12.7).

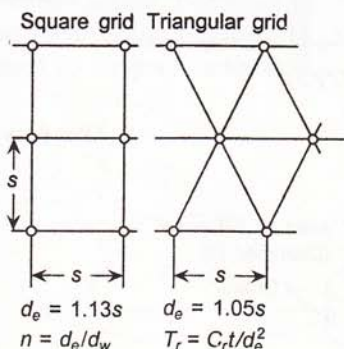


Fig. 12.7 Spacing of vertical drains.

Coefficient of radial consolidation,

$$C_r = \frac{k_h}{\gamma_w m_v} \quad (12.4)$$

In field problems,  $U_z$  is small compared to  $U_r$  and is often neglected. Therefore, for a time  $t$  and knowing ( $C_r$ ), the time factor ( $T_r$ ) can be calculated and degree of consolidation obtained from Eq. (12.5) as,

$$U = T_r - U_R \quad (12.5)$$

The relationship between  $U$  and  $T_r$  can be obtained by solving Eq. (12.2) for different values of  $n$ , as shown in Fig. 12.8. In practical design, for a given drain diameter  $d_w$ , a spacing  $d_e$  is chosen, and the time required to achieve 90% degree of consolidation is calculated. If the time is too little or too much, the spacing is changed and calculations are repeated.

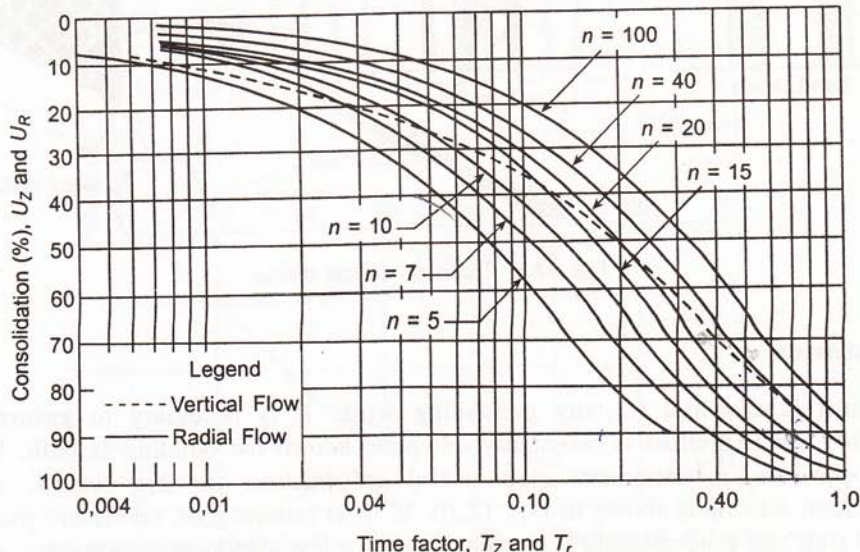


Fig. 12.8 Degree of consolidation versus time factor for radial average (Barron, 1948).

### Types of vertical drains

(a) *Sand drains*: Sand drains have been used extensively for preloading since the early thirties. Sand drains (diameter 300–500 mm) were mostly installed by driving a steel casing with an expendable shoe and filling the hole with sand. Smaller diameter sand drains would not ensure integrity of the sand drain due to arching action of the sand.

(b) *Sand wicks*: Sand wicks were introduced by Dastidar et al. (1969). These consist of cylindrical bags made of jute or any permeable fabric, for example, HDPE, which is filled with sand and stitched along the sides and ends. The wicks are prefabricated on the ground by manual sand filling and kept in a water vat to saturate. A 65–75 mm diameter pipe casing with a shoe at the bottom is driven into the soft clay and the wick introduced into the hole at the top as the casing is withdrawn. Sand wicks are kept projected above the ground and

covered with a drainage blanket. The sand wicks may be of 55–75 mm diameter and can be installed at spacing of 1–2 m.

(c) *Band drains:* Band drains or fabric drains are usually 75–100 mm wide and 3–5 mm thick made of synthetic fabric with high permeability. They are installed in the ground by special mandrel and cranes.

In addition to the above cardboard drains (Kjellman, 1948) and rope drains have also been used. Different types of vertical drains are shown in Fig. 12.9.

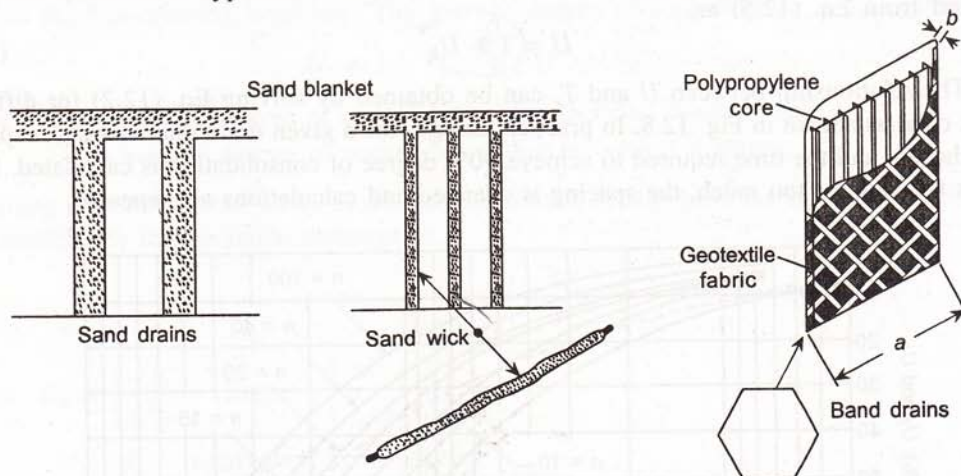


Fig. 12.9 Types of vertical drains.

### Case histories

Field control is essential for any preloading work. It is necessary to ensure that the consolidation under preload is essentially complete before the building is built. Settlement and pore-pressure measurement give useful information in this regard. A simple instrumentation scheme is shown in Fig. 12.10. In most routine jobs, settlement measurement on vertical rods and pore-pressure measurement with a few standpipe piezometers, around the periphery of the preload should be sufficient.

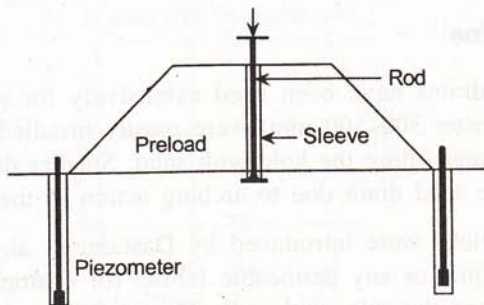


Fig. 12.10 Preloading: field measurement scheme.

Dastidar et al. (1969) described preloading with sand wicks for four storey residential buildings at Salt Lake, Kolkata. Salt Lake is a vast stretch of low lying marshy land in the eastern side of Kolkata which originally served as a natural drainage outfall of the city. The area was reclaimed by filling with dredged fine sand and silt from the river Hooghly in the early sixties.

The reclaimed fill varies in thickness from 1.5–3.0 m. The subsoil, at a depth of about 12 m from the present GL is soft and organic in nature with shear strength seldom exceeding  $1.5 \text{ t/m}^2$ , as depicted in Fig. 12.11. Below this layer, there is stiff clay with shear strength of  $5\text{--}10 \text{ t/m}^2$ . This is underlain by medium/dense brown silty sand below a depth of 16 m.

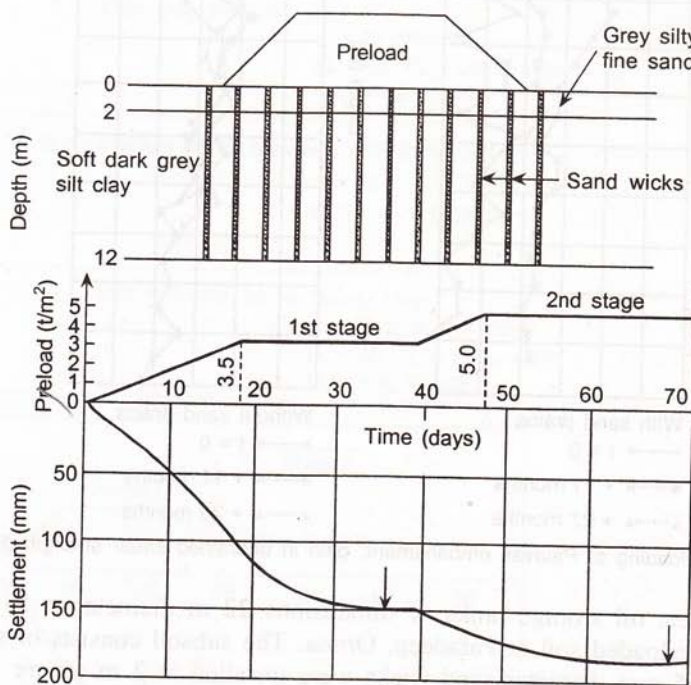


Fig. 12.11 Preloading at Salt Lake, Kolkata (Dastidar et al. 1969).

It is obvious that the soft clay would be liable to undergo excessive settlement even under low to medium-rise buildings on shallow foundations. Preloading is primarily aimed at consolidating the soft clay and making it strong enough to support the building. As an experiment, 75 mm diameter sand wicks were provided at 1.5 m square grid to accelerate the consolidation. Loading was done upto  $50 \text{ kN/m}^2$  in two stages. It was found that consolidation under each stage of loading was completed in 5–6 weeks. The buildings founded on spread footings on the preloaded soil.

Pilot (1977) reported the case history of preloading the Palavas embankment. Vane shear test was done before and after preloading to determine the gain in shear strength of the soil. The measurement showed increased undrained shear strength of the soil throughout the depth of sand drains while in the area without sand drains, the strength gain was limited to the top 4 m of the soil where consolidation was only effective in the first 26 months. This is presented in Fig. 12.12.

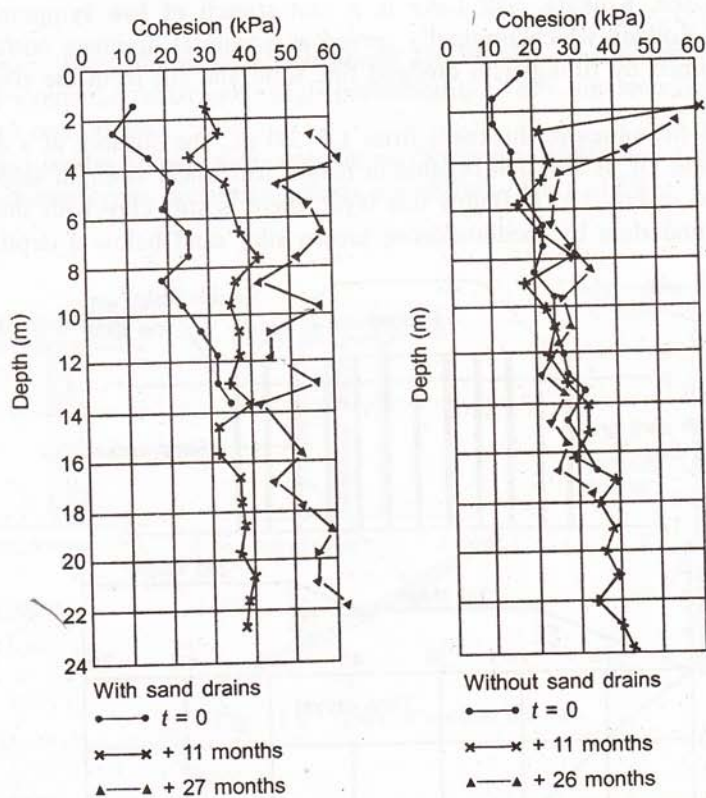


Fig. 12.12 Preloading of Palavas embankment: gain in undrained shear strength (Pilot, 1977).

In recent times, oil storage tanks of dimensions 22 m diameter  $\times$  15 m height have been founded on preloaded soil at Paradeep, Orissa. The subsoil consists of soft marine clay in the top 10 m. 65 mm diameter sand wicks were installed at 2 m square grid. Two stage preloading was done upto a pressure of 96 kN/m<sup>2</sup>. Figure 12.13 depicts the preloading. Thereafter, the tank was built on compacted sand pad foundation. The gain in strength was sufficient to give adequate bearing capacity of the soil to support the tank load of 160 kN/m<sup>2</sup>. Also, settlement of the untreated soil under the design load was estimated as 1000 mm. With a preload of 96 kN/m<sup>2</sup>, 600 mm settlement was made to occur during preloading. The tank settlement during hydro test was, thus, restricted to 350 mm at the centre and 200 mm at the periphery. Further, the settlement of the tank during hydro test indicated fairly uniform settlement within permissible limits.

Dastidar (1985) reported extensive preloading at Salt Lake, Calcutta and Haldia. He suggests a consolidation time of 20–120 days for spacing of 55 mm sand wicks between 1.2 m to 2.5 m in the predominantly alluvial deposits of Haldia and Calcutta. Table 12.1 presents the relevant data.

Table 12.1 Spacing of sand wicks and time for settlement

Location	Salt Lake, Calcutta		Haldia	
Spacing of 55 mm diameter sand wicks	1.2 m	1.5 m	2.2 m	2.5 m
Time for 95% consolidation (days)	20	24	80	120

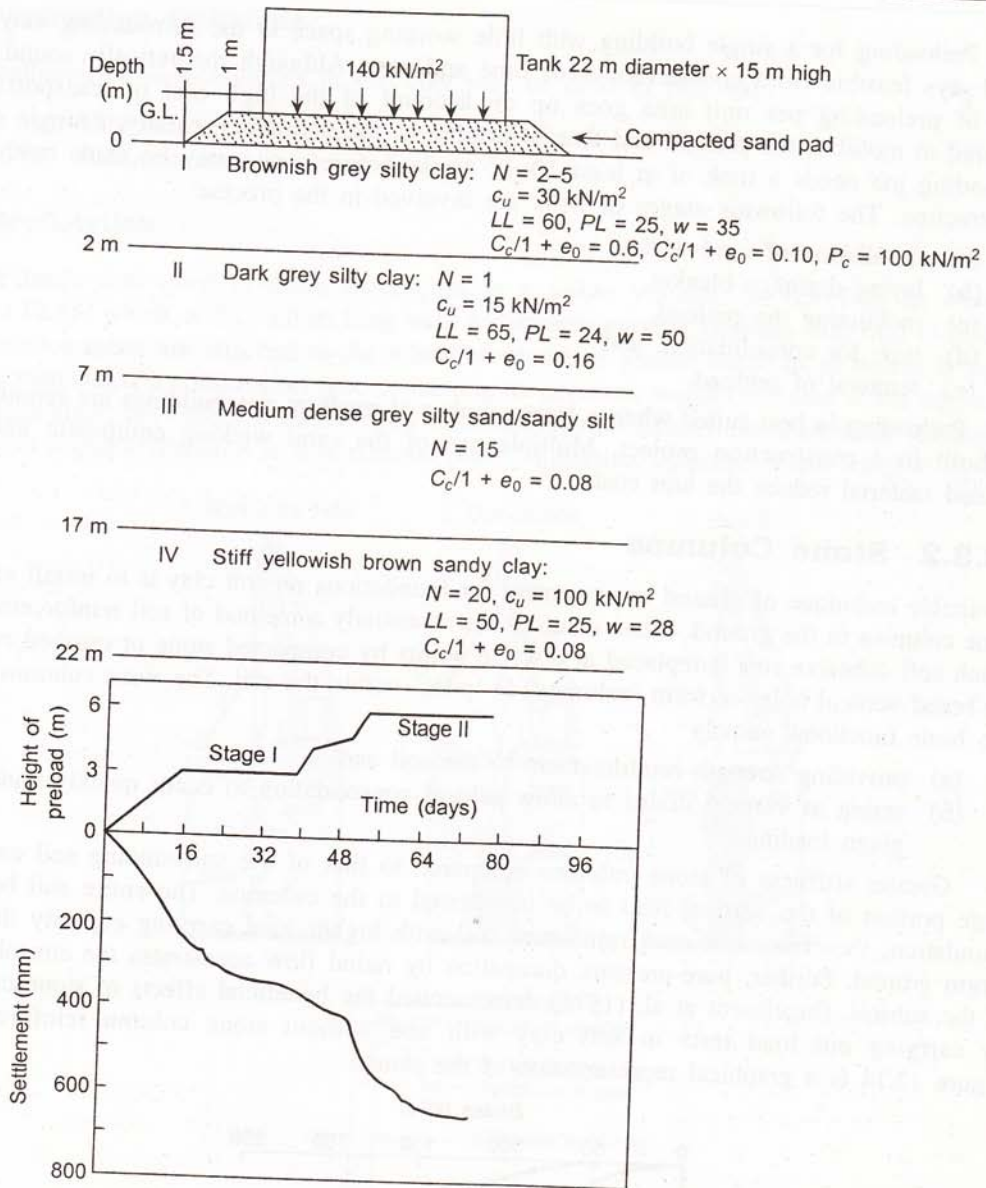


Fig. 12.13 Preloading for 22 m diameter  $\times$  15 m high storage tanks at Paradip.

### Field control

Preloading is done in the field by assembling dead weight in the form of earth fill, sand bags, brick, stone blocks and other construction materials. Sand bags are the most common method of applying the preload. However, it is difficult to assemble very high preload, requiring more than 5 to 6 m of fill. This would restrict the preload intensity  $80-100 \text{ kN/m}^2$  which should be sufficient for low to medium-rise buildings. Tall buildings would require much higher preload which is difficult to mobilize.

Preloading for a single building with little working space in the surrounding may not be always feasible from considerations of time and cost. Although theoretically sound, the cost of preloading per unit area goes up on account of the high cost of transportation required to mobilize the preload and then to dispose of the preload. Typically, a single stage preloading job needs a time of at least 10–12 weeks before a site may be made ready for construction. The following stages of work are involved in the process:

- installation of sand wicks,
- laying drainage blanket,
- mobilizing the preload,
- time for consolidation, and
- removal of preload.

Preloading is best suited when a large number of medium-rise buildings are required to be built in a construction project. Multiple use of the sand wicking equipment and the preload material reduce the unit cost.

### 12.3.2 Stone Columns

A suitable technique of ground improvement for foundations on soft clay is to install vertical stone columns in the ground. Stone columns are essentially a method of soil reinforcement in which soft cohesive soil is replaced at discrete points by compacted stone or crushed rock in pre-bored vertical holes to form 'columns' or 'piles' within the soil. The stone columns serve two basic functions, namely

- providing strength reinforcement to the soil and
- acting as vertical drains to allow subsoil consolidation to occur quickly under any given loading.

Greater stiffness of stone columns compared to that of the surrounding soil causes a large portion of the vertical load to be transferred to the columns. The entire soil below a foundation, therefore, acts as a reinforced soil with higher load carrying capacity than the virgin ground. Further, pore-pressure dissipation by radial flow accelerates the consolidation of the subsoil. Engelhardt et al. (1974) demonstrated the beneficial effects of stone columns by carrying out load tests in soft clay with and without stone column reinforcement. Figure 12.14 is a graphical representation of the same.

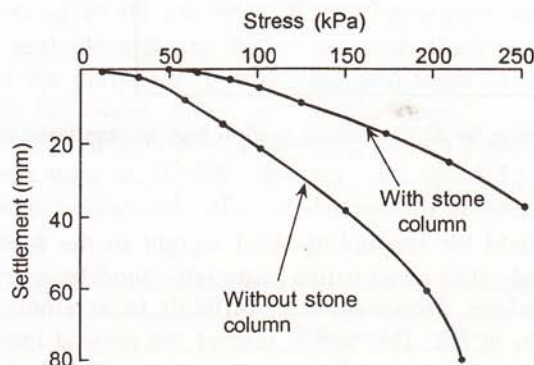


Fig. 12.14 Effectiveness of stone columns (Engelhardt et al., 1974).

## Construction technique

Installation of stone columns in soft clay may be done in two ways:

- Vibratory technique using vibroflot and
- Rammed stone column technique.

### Vibroflotation

The basic tool used in these techniques is a poker vibrator or vibroflot, as shown in Fig. 12.15, which is 2.0–3.0 m long with a diameter varying between 300 mm to 500 mm. Extension tubes are attached to the vibroflot whenever greater depth of treatment is needed. The vibroflot is a hollow steel tube containing an eccentric weight mounted at the bottom of a vertical shaft; the energy is imparted by rotational motion through the shaft while the eccentric weight imparts vibration in a horizontal plane. Vibration frequencies are fixed at 30 Hz or

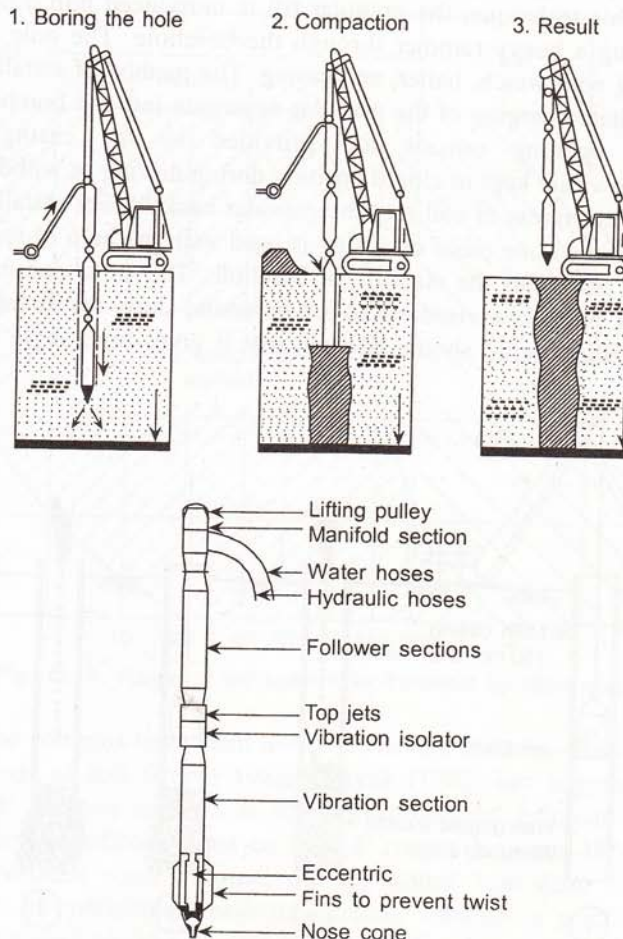


Fig. 12.15 Stone column installation by vibroflotation.

50 Hz to suit electric power cycles. The free fall amplitude varies between 5–10 mm. The machine is suspended from a vibration damping connector by follower tubes through which power lines and water pipes pass. These allow simultaneous release of water jets to remove the soil around the vibroflot as the latter makes its way into the hole under vertical pressure from the top. When the vibroflot reaches the desired depth, the water jet at the lower end is cut off and granular backfill is poured through the annular space between the hole and the vertical pipe by head load or conveyor as the vibratory poker is withdrawn. Well graded stone backfill of size 75 mm to 2 mm is used and compaction is achieved by vibration of the poker as it is lifted up. Due to compaction, the stones are pushed sideways into the soft soil to produce a stone column of diameter larger than the diameter of the borehole. Normally, 600–900 mm diameter stone column can be obtained for 300–500 mm diameter vibroflot.

### Rammed stone column

This installation technique was proposed by Datye and Nagaraju (1977) and developed further by Nayak (1983). In this technique, the granular fill is introduced into a pre-bored hole and compacted by operating a heavy rammer through the borehole. The hole is made by using normal bored piling rig with winch, bailer, and casing. The method of installation is illustrated in Fig. 12.16. To facilitate charging of the granular aggregate into the borehole, windows with hinged flap valves opening outside are provided to the casing at interval of 2 m or so. These windows are kept in closed position during driving or withdrawal of casing by screwing nuts to prevent ingress of soil into the granular backfill. For installing stone columns to greater depths, more than one piece of casing is used with the help of special quick release couplings. The casing maintains the stability of borehole. The stone columns are required to function as drain wells and it is advised not to use bentonite slurry for maintaining the stability of the borehole. Backfill material should be such that it gives high angle of internal friction

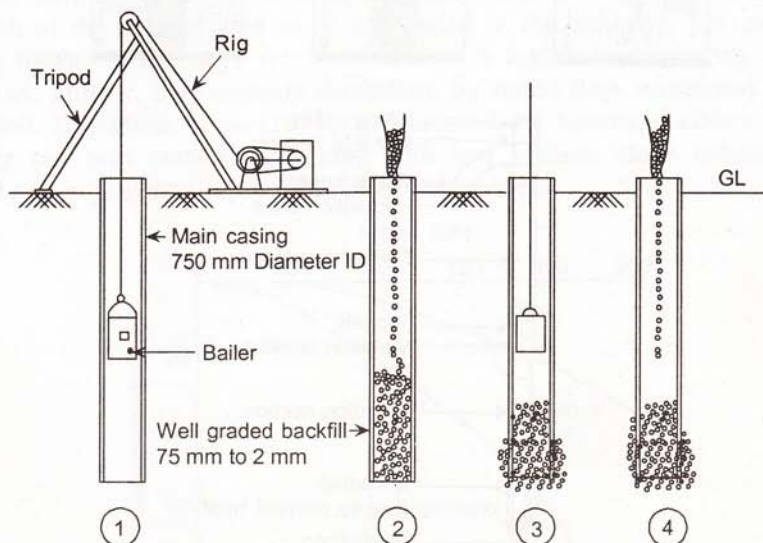


Fig. 12.16 Stone column installation by ramming method.

under given energy of compaction. Sometimes the mixtures of stone aggregate and sand, generally in proportion of 2:1, are used as backfill material. It is observed that sand is utilized mainly in filling the voids in gravel skeleton. Gravel backfill of aggregate size 75 mm to 2 mm is generally recommended. The gravel should be well graded and preferably angular shaped for good interlock. The main purpose of compaction is to rearrange the stone particles so that very good interlocking between particles is obtained to give high angle of internal friction. Too much ramming, however, crushes the aggregate. For a given compaction energy, greater weight and smaller drop of the rammer give better results.

### Comparison of construction techniques

All the installation techniques for stone columns in soft clay are self-adjusting in the sense that enlargement of the column during ramming or vibration occurs depending on the soil consistency. Figure 12.17 shows the range of soil suitable for such a treatment by stone columns.

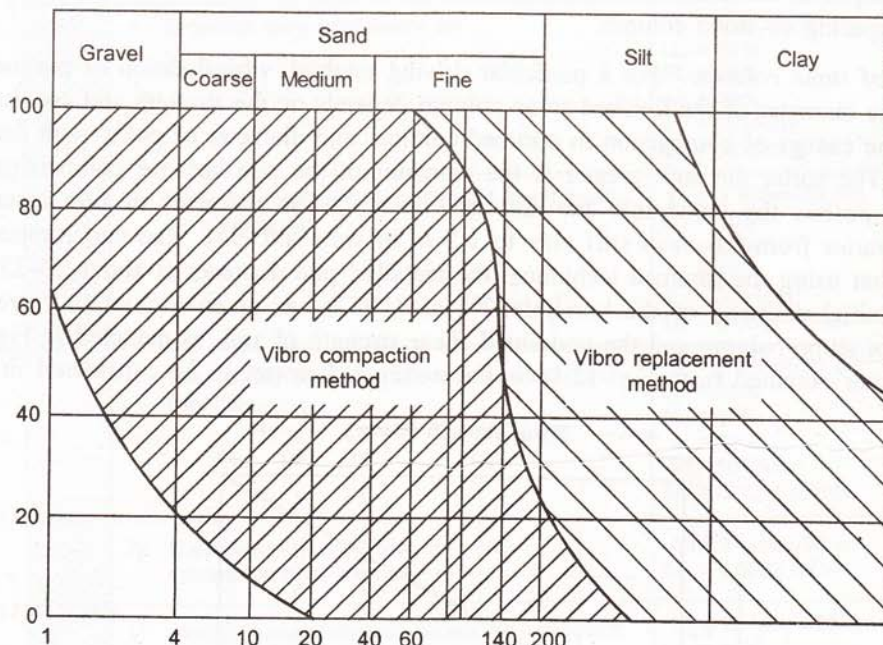


Fig. 12.17 Range of soil suitable for treatment by stone columns.

Rammed stone columns have been used extensively in India. They are found to be quite suitable for all kinds of soil (Datye 1982). Nayak (1982) has suggested that the angle of internal friction,  $\phi'$  may be as high as  $45^\circ$  for compacted granular fill in rammed stone column, whereas for vibrofloated stone column  $\phi'$  ranges between  $38^\circ$ - $42^\circ$ . It is also to be noted that in vibrofloated stone column, the top about 1 m deep does not get properly compacted for lack of confinement near the surface, whereas in practice this portion of the stone column is required to take greater load intensity. In case of rammed stone column, proper compaction can be achieved even for this length because of lateral confinement of the

casing pipe. With vibroflot, there is no harm in using high energy of compaction. Rather, it results in larger diameter of the stone column and better compaction of aggregate to give higher value of angle of internal friction. Net effect of this is to increase the load carrying capacity of the stone column. But for rammed stone column, such high compaction energy may crush the aggregates, resulting in lower value of  $\phi'$  and lower capacity of the stone columns. In general, however, vibroflotation needs skilled labour and better quality control while the installation of rammed stone columns needs greater manpower. Overall, rammed stone column appears to be more economical although it is a very slow process compared to vibroflotation.

### Design principles

The design of stone column foundation involves the assessment of

- (i) diameter of stone column,
- (ii) depth of stone column, and
- (iii) spacing of stone column.

*Diameter of stone column:* For a particular driving method, vibroflotation or rammed stone column, the diameter of the finished stone column depends on the strength and consistency of the soil, the energy of compaction in rammed column, and diameter of poker with fins of the vibroflot. The softer the soil, greater is the diameter of the pile because compaction of the aggregate pushes the stone into the surrounding soil. The diameter of pile installed by vibroflot varies from 0.6 m in stiff clay to 1.1 m in very soft clay. Rao and Ranjan (1985) reported that using the rammed technique, the installed pile diameter is about 20–25% more than the initial diameter of the borehole. Nayak (1982) has given a chart to correlate the diameter of stone column and the undrained shear strength of soil, as depicted in Fig. 12.18. The diameter obtained from Fig. 12.18 is the nominal diameter to be considered in design.

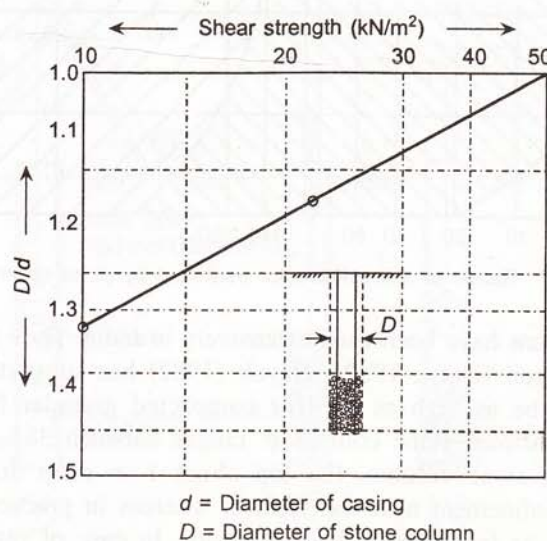


Fig. 12.18 Shear strength of soil versus diameter of stone column (Nayak, 1982).

**Depth of stone column:** The stone column is installed below a foundation upto the depth of soft compressible strata within the zone of influence in the subsoil. In addition to carrying vertical load, stone columns function as drainage path to dissipate excess pore water pressure and hence, accelerate the rate of consolidation. This requires the stone columns to be taken down to the depth of major compressible strata which make significant contribution to the settlement of the foundation.

This point can best be understood by determining the contribution of each layer of soil towards the settlement of the foundation. For example, in the subsoil condition at Haldia (refer Fig. 12.19), the depth of soil contributing to 90% of the total settlement works out to 17 m for 50 m diameter storage tanks. Accordingly, stone column depths of 17 m were adopted for these foundations. However, in some stratified deposits, the nature of stratification more or less determines the depth of stone column. For example, a 10 m thick clay deposit followed by hard clay or dense sand would require stone column depth of 10 m irrespective of the size of foundation.

Depth (m)	Description	Soil properties
0	Top soil	—
1	I Brownish grey silty/clayey silt	$N = 5 \text{ blows/30 cm}$ $LL = 50\%$ $PL = 22\%$ $w = 29\%$ $c_u = 50 \text{ kN/m}^2$ $M_v = 0.0003 \text{ m}^2/\text{kN}$
4	II Grey silty clay with decomposed wood and silt laminations	$N = 3 \text{ blows/30 cm}$ $LL = 50\%$ $PL = 24\%$ $w = 40\%$ $c_u = 30 \text{ kN/m}^2$ $M_v = 0.0007 \text{ m}^2/\text{kN}$
10	III Grey clayey silt/sandy silt with laminations of silty clay	$N = 5 \text{ blows/30 cm}$ $LL = 50\%$ $PL = 22\%$ $w = 29\%$ $c_u = 50 \text{ kN/m}^2$ $M_v = 0.0004 \text{ m}^2/\text{kN}$
14	IV Grey/Brownish grey silty clay with calcareous nodules	$N = 9 \text{ blows/30 cm}$ $M_v = 0.0002 \text{ m}^2/\text{kN}$
17	V Mottled brown/yellowish brown silty clay with nodules and rusty brown patches	$N = 20 \text{ blows/30 cm}$ $LL = 46\%$ $PL = 18\%$ $w = 24\%$ $c_u = 85 \text{ kN/m}^2$ $M_v = 0.0001 \text{ m}^2/\text{kN}$
25	VI Brown silty fine sand with lenses of clay	$N = 40 \text{ blows/30 cm}$
29	VII Brown silty fine sand	$N = 50 \text{ blows/30 cm}$
29	Very stiff to hard silty clay	—

Fig. 12.19(a) Settlement calculation for 50.m diameter × 11.4 m height tank at Haldia.

Stratum	Thickness $H_z$ (m)	$\Delta\sigma_z = I_q \times q_{net}$ (kN/m <sup>2</sup> )	$M_v$ (m <sup>2</sup> /kN) $\times 10^{-4}$	$\delta$ (m)	Cumulative settlement (%)
I	1.0	96.6	3.0	0.030	4.0
II	3.0	91.4	3.0	0.083	14.2
III	6.0	87.7	7.0	0.368	65.0
IV	4.0	83.0	4.0	0.133	83.0
V	3.0	78.5	2.0	0.047	89.3
VI	8.0	69.2	1.0	0.055	96.7
VII	4.0	54.1	0.5	0.011	98.2
VIII	11.0	41.5	0.3	0.014	100.0
				0.740	

Fig. 12.19(b) Table for settlement calculation for 50 m diameter  $\times$  11.4 m height tank at Haldia.

*Spacing of stone columns:* The design of stone column foundation primarily involves determination of a suitable spacing of stone column for a chosen diameter and length of the latter. It depends on the required load bearing capacity of the foundation and the allowable time for consolidation by radial drainage through stone columns. It can be worked out in terms of the degree of improvement required for providing a satisfactory foundation for the design load. The settlement improvement ratio of the reinforced ground to untreated ground is a function of pile spacing as shown in Fig. 12.20 (Greenwood, 1970). Mitchell and Katti (1981) have suggested typical pile spacing for rectangular and square grid depicted in Fig. 12.21.

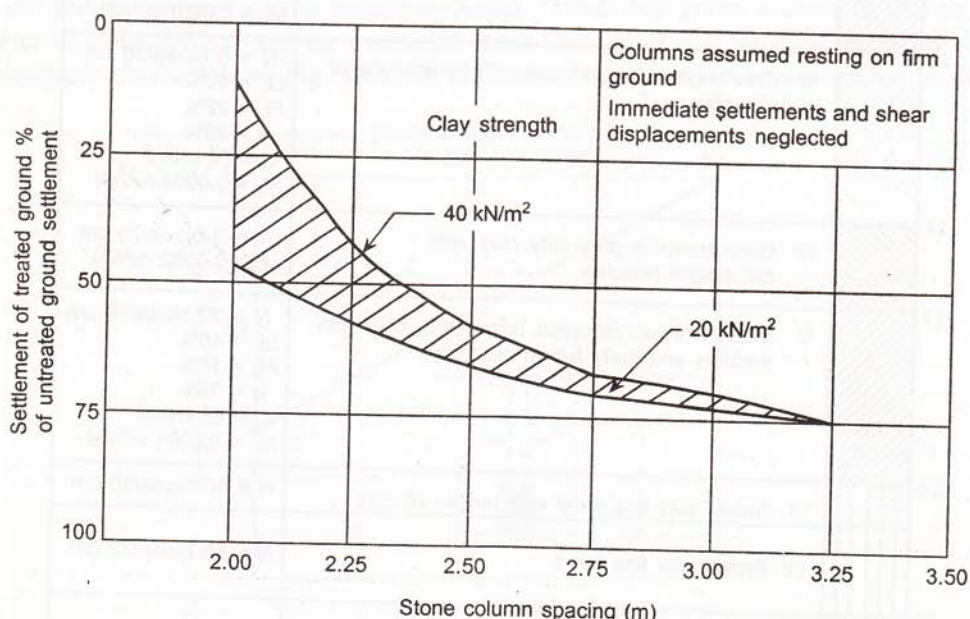


Fig. 12.20 Effect of stone column on anticipated settlement (Greenwood, 1970).

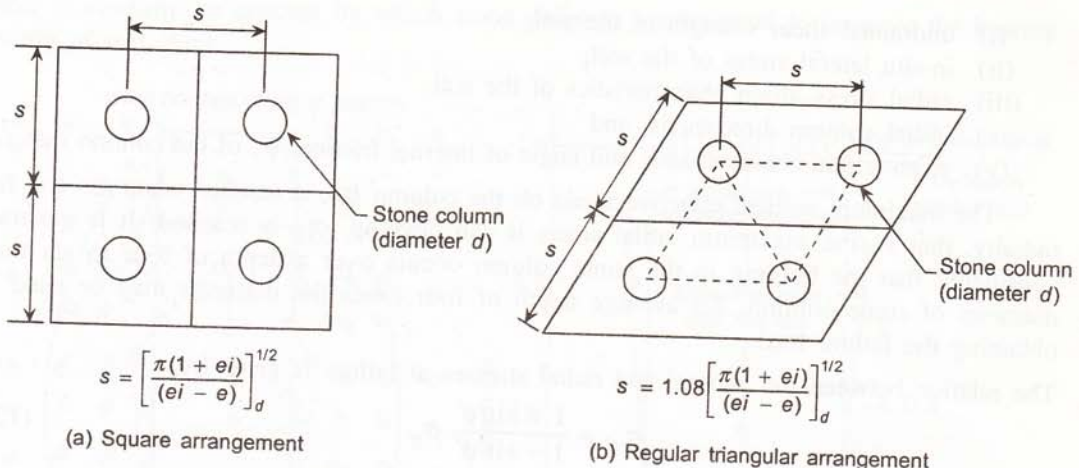


Fig. 12.21 Spacing of stone columns.

Analysis of granular pile foundations for triangular grid of piles show that significant reduction in settlement occurs only if the spacing of stone column is close ( $s/d \leq 4$ ) and the piles are installed to full depth of consolidating layer. However, too close a spacing ( $s/d \leq 2$ ) is not feasible from construction point of view. Thus, a stone column spacing ( $s/d$ ) of 2.5–4 is adopted for most practical problems. Also it has been recognized that closer spacing is preferred under isolated footing than beneath large rafts (Greenwood, 1970).

### Load carrying capacity of individual stone columns

A stone column is subjected to a stress condition much alike that imposed in the standard triaxial test as shown in Fig. 12.22. A vertical stress,  $\sigma_v$  is applied by surface loading, and a radial effective stress,  $\sigma_r$ , results from the horizontal reaction of the ground. Therefore, the factors which govern the soil–column behaviour are (Hughes et al., 1975):

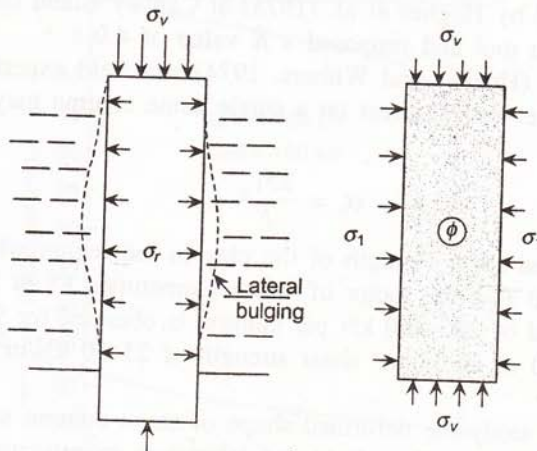


Fig. 12.22 Stresses acting on stone column.

- (i) undrained shear strength of the soil,
- (ii) in-situ lateral stress of the soil,
- (iii) radial stress-strain characteristics of the soil,
- (iv) initial column dimensions, and
- (v) stress-strain characteristics and angle of internal friction,  $\phi'$ , of the column material.

The maximum vertical effective stress on the column  $\sigma_{vf}$ , is reached when the soil fails radially, that is, the maximum radial stress it can develop,  $\sigma_{rf}$ , is reached. It is generally considered that the bulging in the stone column occurs over a depth of four to six times diameter of stone column. An average depth of four times the diameter may be used for obtaining the failure load.

The relation between the vertical and radial stresses at failure is given by,

$$\sigma_{vf} = \frac{1 + \sin \phi'}{1 - \sin \phi'} \sigma_{rf} \quad (12.6)$$

The value of  $\sigma_{rf}$  can be expressed in terms of the initial radial stress,  $\sigma_{ro}$  as

$$\sigma_{rf} = \sigma_{ro} - u + Kc_u \quad (12.7)$$

From Eqs. (12.6) and (12.7),

$$\sigma_{vf} = \frac{1 + \sin \phi'}{1 - \sin \phi'} (\sigma_{ro} - u + Kc_u) \quad (12.8)$$

where  $c_u$  is the undrained shear strength of the clay,

$\sigma_{ro}$  is the initial total radial stress,

$u$  is the pore-pressure,

$\phi'$  is the angle of internal friction of the material of the column, and

$K$  is an earth pressure coefficient.

Measurements carried out by Hughes and Withers (1974) in soft clay using a selfboring pressuremeter (Camkometer) yielded  $K$  values of about 4.0, whereas Menard had earlier used a conventional pressuremeter to obtain values of about 5.5. The full-scale loading tests on stone columns performed by Hughes et al. (1975) at Canvey Island confirmed the reliability of Eq. (12.8) as a design tool and proposed a  $K$  value of 4.0.

Both limit analysis (Hughes and Withers, 1974) and field experience (Thorburn 1975) suggest that the allowable vertical stress on a single stone column may be obtained from the empirical expression

$$\sigma_v = \frac{25 c_u}{F} \quad (12.9)$$

where  $c_u$  is the undrained shear strength of the clay in the region where the bulging of the stone column occurs and  $F$  is the factor of safety (sometimes  $FS$  or  $F_s$ ).

Typical design load of 200–400 kN per column is obtained for 900 mm diameter stone columns in cohesive soil of undrained shear strength of 25–50 kN/m<sup>2</sup> and a factor of safety of 2.0.

It is interesting to study the deformed shape of stone column as observed after failure by Hughes and Withers (1974). Both field and laboratory investigations show geometrically similar deformed shapes with bulging in the upper region, as visible in Fig. 12.23. The data

appear to confirm the concept by which stone columns are believed to improve the bearing capacity of soft clays.

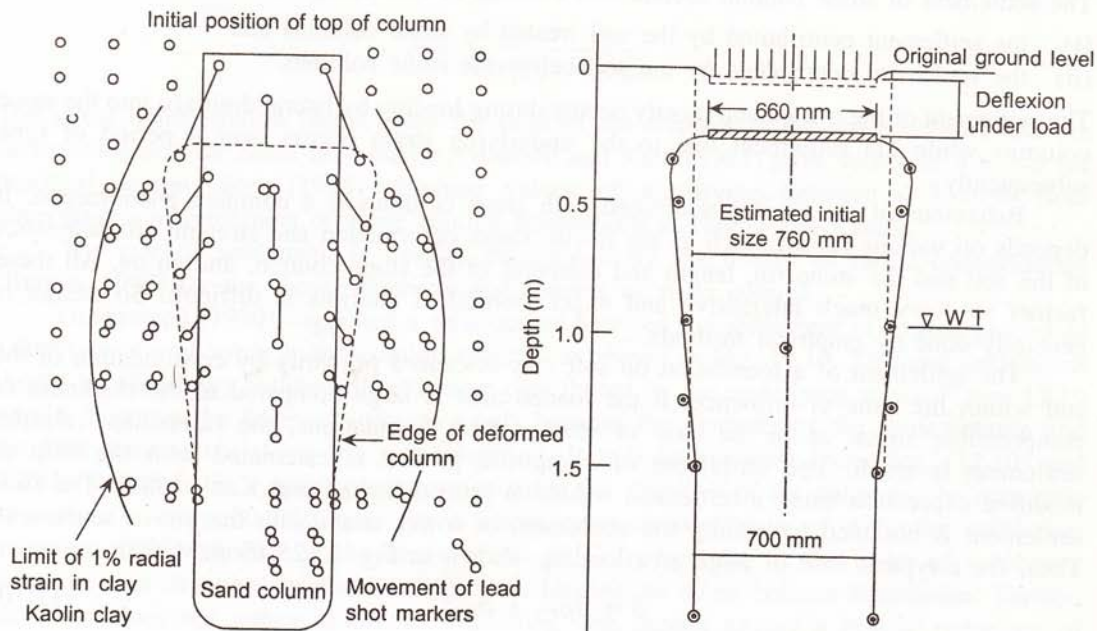


Fig. 12.23 Deformation of stone column (Hughes and Withers, 1974).

Figure 12.24 shows a typical load versus settlement curve of a test column loaded to failure at a site in Haldia. The failure load compares well with the predictions based on Eq. (12.8). A factor of safety of 2 gives the safe load on the test column.

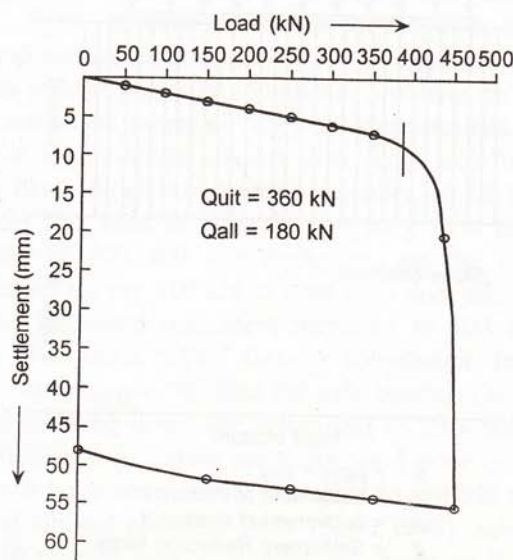


Fig. 12.24 Load settlement relationship of single stone column.

### Settlement of stone column foundations

The settlement of stone column foundations consists of two components:

- the settlement contributed by the soil treated by stone columns and
- the settlement contributed by the soil below the stone columns.

The settlement of the treated soil mostly occurs during loading by lateral drainage into the stone columns while the settlement due to the underlying strata occurs over a period of time subsequently.

Behaviour of the ground reinforced with stone columns is a complex phenomenon. It depends on various factors, such as the in-situ stress deformation and strength characteristics of the soil and the stone fill, length and diameter of the stone column, and so on. All these factors are very much interactive and exact theoretical analysis is difficult. So design is generally done by empirical methods.

The settlement of a foundation on soft clay is caused primarily by consolidation of the soil within the zone of influence. If the loaded area is large compared to the thickness of compressible strata, as in the case of storage tank foundations, the immediate (elastic) settlement is small. The settlement of composite ground is calculated with the help of modified expression using a settlement reduction ratio (Mitchell and Katti, 1981). The final settlement is obtained by adding the settlement of lower strata with the above settlement. Thus, for a typical case of large area loading, shown in Fig. 12.25 (Som, 1995),

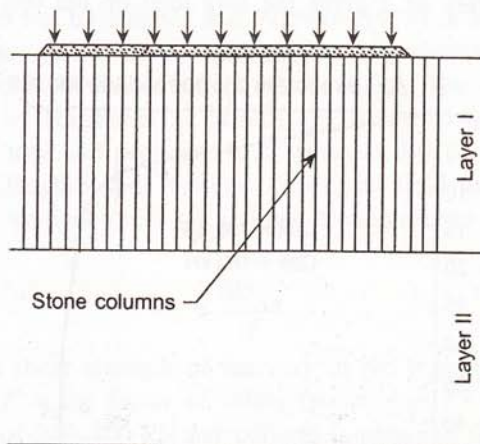
$$\delta = \beta \rho_{C1} + \rho_{C2} \quad (12.10)$$

where  $\delta$  = settlement of foundation

$\rho_{C1}$  = settlement of untreated soil within the depth of stone column treatment

$\rho_{C2}$  = settlement of untreated soil below the stone columns, and

$\beta$  = settlement reduction ratio for stone column treatment.



$$\begin{aligned}\delta &= \beta \rho_{C1} + \rho_{C2} \\ \rho_{C1} &= \text{Settlement of stratum I} \\ \rho_{C2} &= \text{Settlement of stratum II} \\ \beta &= \text{Settlement Reduction factor}\end{aligned}$$

Fig. 12.25 Settlement of stone column foundation.

The settlement reduction ratio is a function of the area ratio of stone column installation  $A_c$ , and the stress concentration ratio  $\eta$ , Eq. (12.11).

$$\beta = \frac{1}{1 + (\eta - 1)A_c} \quad (12.11)$$

The stress concentration factor gives the ratio of the stresses in the stone column and the surrounding soil for equal deformation. Mitchell and Katti (1981) gave values of  $n = 3-5$  for practical design. Som (1995) obtained values of  $n$  varying between 4–7 from field observations of settlement of stone column foundations at Haldia and Kandla.

The rate of settlement is usually determined by the theory of radial consolidation (Barron, 1948) for the chosen diameter and spacing of stone column.

Greenwood (1970) suggested a relationship between the settlement of treated ground as a function of soil strength and column spacing, as shown in Fig. 12.19. To these settlements should be added any anticipated settlement contributed by the underlying strata. Figure 12.19 should, however, be taken as indicative only because the diameter of the stone column and the area ratio is not taken into consideration. It will be apparent from Eqs. (12.10) and (12.11) that even for a spacing as close as twice the diameter of the columns, the area ratio  $A_c$  comes to only 20–25% and for a stress concentration ratio of 4–6, the settlement reduction ratio will vary in the range of 40–50%. In fact, this is the order of settlement reduction that can be expected for large area loading on stone column foundation. Further, reduction does not appear possible. Therefore, one cannot expect a drastic reduction of settlement by providing stone column foundation beneath a foundation.

### Practical applications

Flexible large area loading provides ideal situation for stone column foundations on soft cohesive soil. Thick deposits of clay are abundant along the coastal and alluvial plains of India, as shown in Fig. 12.19. In most cases, the clay layer is 10–15 m thick, somewhat desiccated near the ground surface and underlain by firm clay/dense sand/weathered rock, and so on. Such clay deposits present perennial foundation problems on account of low undrained shear strength and high settlement potential. They are characterized by water content close to the liquid limit often with high organic content. Any large area loading by way of rigid or flexible raft foundation has typical safe bearing capacity of 50 kN/m<sup>2</sup> from shear failure consideration. Even under this kind of pressure, the long term consolidation settlement is likely to be of the order of 200–400 mm depending on the size of foundation. If the foundation pressure increases to, say 100 kN/m<sup>2</sup>, not only does the safe bearing capacity falls appreciably short but the estimated settlement increases to 500–1000 mm which will not generally be acceptable even for a highly flexible foundation. In order to have optimum improvement of the soil, for example, to raise the safe bearing capacity of the foundation to say 100–150 kN/m<sup>2</sup> and to bring down the settlement to 250–500 mm various alternative methods of ground improvement, including preloading and stone columns have been tried. In recent years, stone columns have been extensively used to provide foundations for large area loading in the coastal and alluvial plains of India (Som, 1999). Some typical settlement data for a 50 m diameter × 10 m high tank at Kandla are shown in Fig. 12.26.

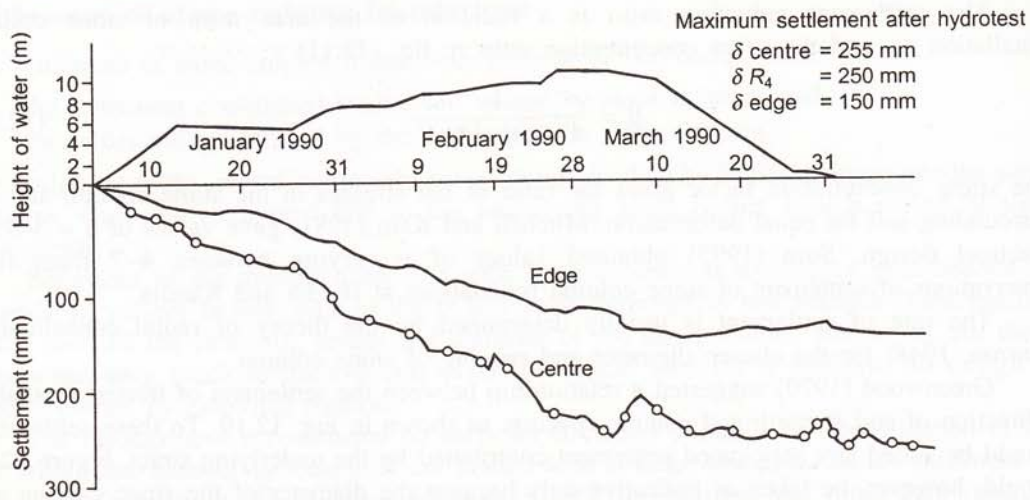


Fig. 12.26 Stone column foundation for large diameter storage tanks at Kandla: settlement during hydrotest.

## 12.4 GROUND IMPROVEMENT IN GRANULAR SOIL

Numerous methods of ground improvement in predominantly cohesionless soil using the principle of vibration are in practice today. Loose granular soil with ' $N$ ' less than 10, is characterized by low shear strength and low bearing capacity. In order to improve its strength, the soil is compacted. This increases its relative density with consequent increase of angle of shearing resistance.

The compaction of soil is achieved either by repeated hammer blows on the ground or by insertion of probes within the soil which are then vibrated. The depth and extent of vibration to be imparted depend on the nature of foundation problem encountered in a given situation.

### 12.4.1 Heavy Tamping or Drop Hammer

The heavy tamping or drop hammer method of ground compaction employs repeated blows of a heavy weight on the ground surface. In small works, a hammer (20–80 kN) is dropped from a height of 4–8 m with the help of a driving rig or a tripod stand. The hammer is made of RCC in the shape of a truncated cone with a low centre of gravity, as shown in Fig. 12.27. The repeated blows of the hammer transmit vibration into ground which improves the relative density of the soil in the upper layers and to a lesser degree in the lower layers. Ramming is associated with gradual depression of the ground surface. With each successive impact, the depression reduces in magnitude. After 5–10 blows, it remains essentially constant. The ramming is then continued in the adjacent areas. The ground is considered to be compacted if the dry density of the soil achieves the following values:

$$\begin{array}{ll} \text{Sandy silt} & : 15.5-16 \text{ kN/m}^3 \\ \text{Sand} & : 16-16.5 \text{ kN/m}^3 \end{array}$$

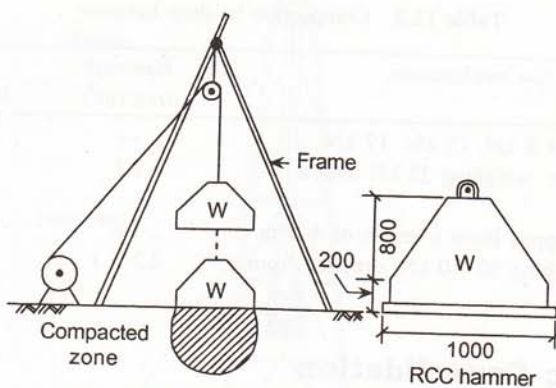


Fig. 12.27 Compaction by drop hammer.

Ground improvement by the method of drop hammer is usually achieved in the top 2.5–3 m of the soil. Deep compaction is not possible by this method. This is clear from the pre and post compaction density tests reported by Tsytovich et al. (1974) at a site in Russia, which are presented in Fig. 12.28. The method is, therefore, suitable for small foundations only.

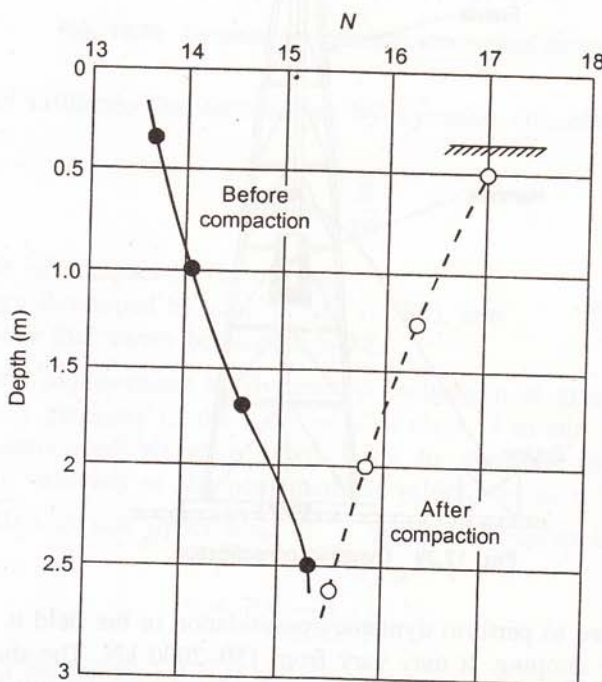


Fig. 12.28 Density versus depth in compaction by drop hammer (Tsytovich, 1974).

Based on experiences in Russia, Tsytovich (1974) suggested the depth to which significant improvement can be achieved by drop hammer technique. Table 12.2 presents compaction by drop hammer in a tabulated manner.

Table 12.2 Compaction by drop hammer

<i>Ground compaction mechanisms</i>	<i>Rammed area (m<sup>2</sup>)</i>	<i>Depth of layer compaction (m)</i>
Drop-weight rollers of 8 kN, 12 kN, 17 kN	—	1.0–1.5
Double-acting hammer, weighing 22 kN with a metal bottom plate	2.1	1.2–1.4
Hammers 24 kN, dropped from a height of 4–5 m	1.6	1.6–2.2
Heavy hammers weighing 50–70 kN, dropped from a height of 6–8 m	2.2–3.1	2.7–3.5

### 12.4.2 Dynamic Consolidation

Dynamic consolidation is the name given to the procedure of deep compaction of soils by repeated blows of a hammer falling from a height of 30–40 m. The technique, pioneered by Louis Menard, is used for compaction of soils 30 m below GL. Figure 12.29 is a diagrammatic representation of dynamic consolidation set up.

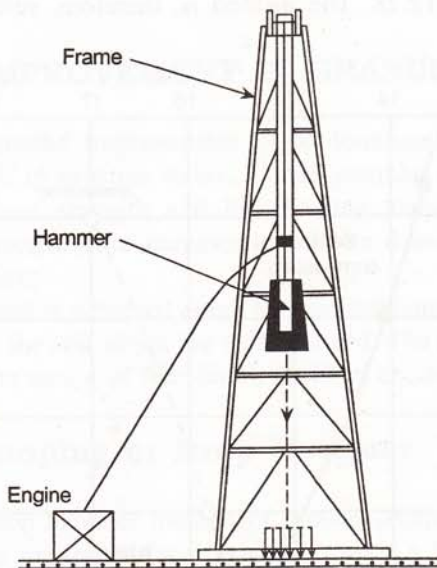


Fig. 12.29 Dynamic consolidation.

Hammer weight used to perform dynamic consolidation in the field is many times more than that used for heavy tamping. It may vary from 150–2000 kN. The shape of the contact surface and the cross-sectional area of the hammer are chosen to suit the soil type and reaction of the ground to the impact energy. Dynamic consolidation can also be done in saturated cohesive soil provided the formation is varved and contains continuous sand partings to facilitate pore-pressure dissipation. In homogeneous cohesive soil, dynamic consolidation may be done with pre-installed vertical sand drains to effect drainage, as depicted in Fig. 12.30.

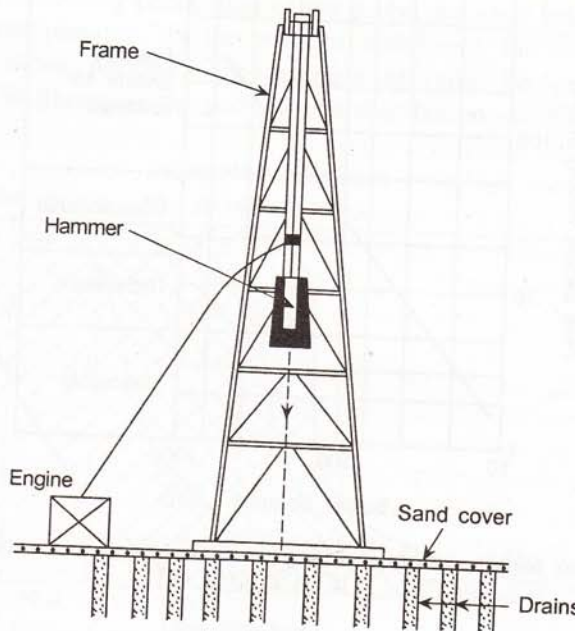


Fig. 12.30 Dynamic consolidation with vertical drains.

The depth of influence for compaction by dynamic consolidation is given by the expression:

$$D = \alpha \sqrt{\frac{E}{10}} \quad (12.12)$$

where  $D$  = depth of compaction (in metres),

$E$  = energy developed by each impact (in KJ), and

$\alpha$  = a factor that varies between 0.5–0.8.

The extent of ground improvement by dynamic consolidation as given by the improvement of bearing capacity is generally of the order of 2 in clays, 3 in silts, and 4 in sand. Heavy tamping and the associated vibration often leads to damages to adjoining structures. Figure 12.31 shows variation of the peak particle velocity  $v$ , as a function of the scaled energy factor ( $\sqrt{E/D}$ ). A safe upper limit of ' $v$ ' is generally taken as:

$$v = 70 \left( \frac{E}{10D^2} \right)^{0.56} \quad (12.13)$$

where  $E$  = energy per blows (in KJ) and

$D$  = distance between impact centre and observation point.

If the permissible maximum peak particle velocity is taken as 50 mm/s, the following relationship may be used to limit the effect of applied energy on nearby buildings.

$$E \leq 5.5 D^2 \quad (12.14)$$

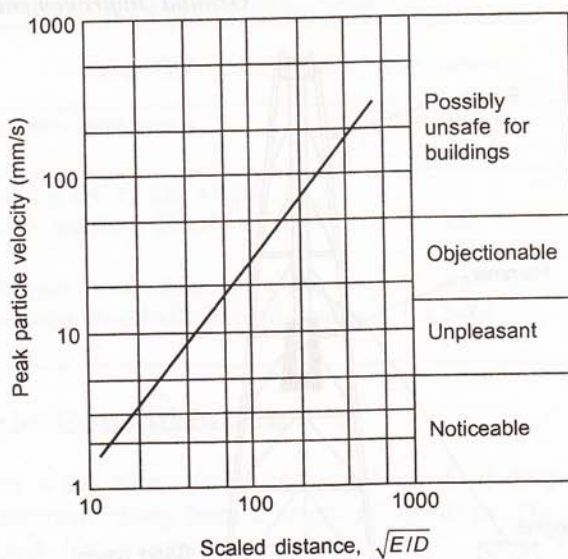


Fig. 12.31 Peak particle velocity versus single impact energy and distance from impact point [ $E$  (in J),  $D$  (in m)].

### 12.4.3 Vibrocompaction

This is method of deep compaction of granular soils where a probe is inserted into the soil and then vibrated. Compaction is brought about by vibration, as displayed in Fig. 12.32. The process is essentially similar to vibroflotation as adopted for installation of stone columns in cohesive soil described earlier.

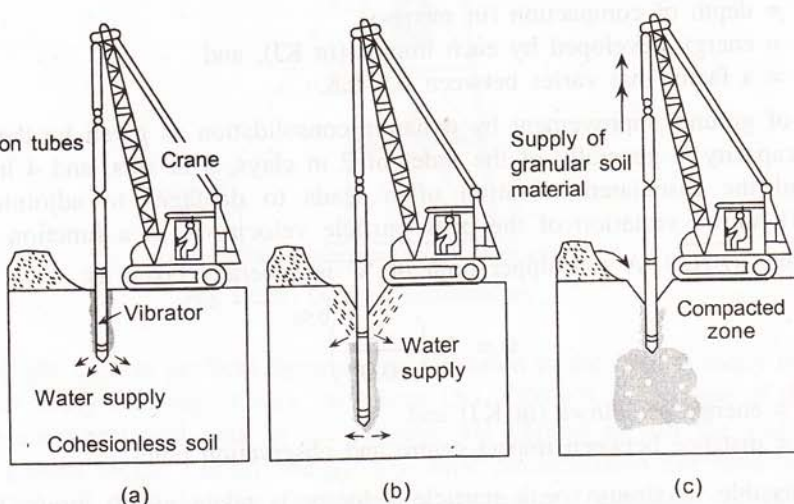


Fig. 12.32 Vibrocompaction.

The range of soil particle size that can be compacted by vibrocompaction is shown in Fig. 12.33 (Brown, 1978). During penetration of the probe, the sand below WT liquefies due to increase of pore water pressure. As the probe is withdrawn, the soil particles rearrange themselves to give a dense packing. The presence of fines, however, may inhibit the compaction. Figure 12.34 illustrates the particle size distribution suitable for the process.

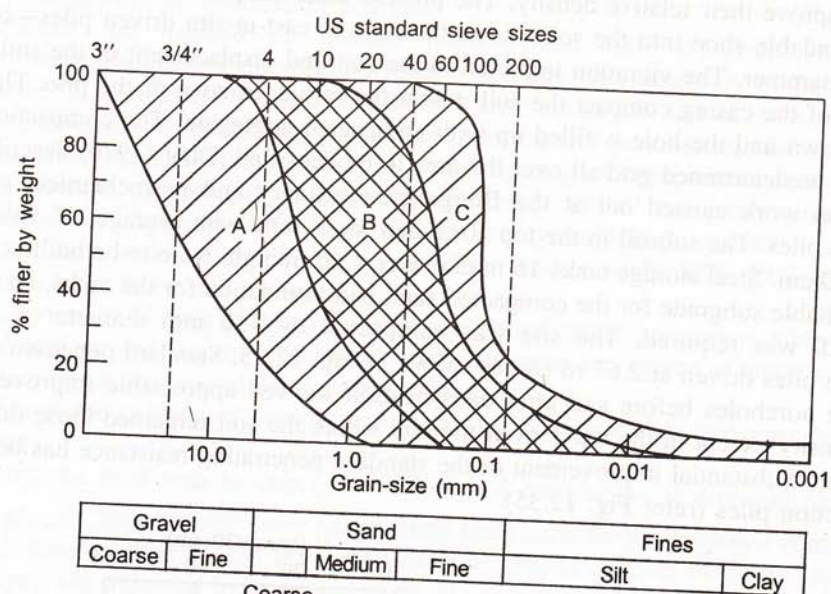


Fig. 12.33 Particle size distribution suitable for vibrocompaction.

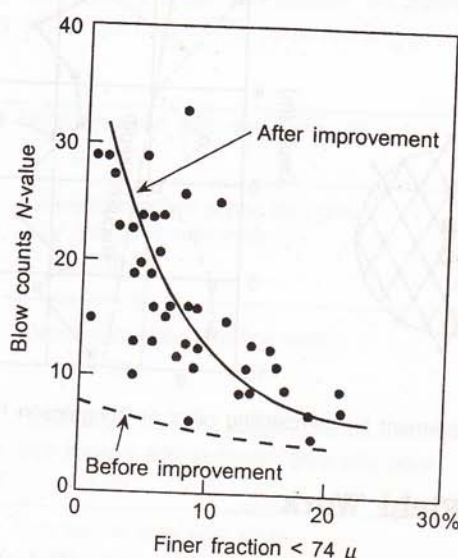


Fig. 12.34 Effect of fines content on the extent of improvement by vibrocompaction.

### 12.4.4 Compaction Piles

Densification of loose sand by compaction piles has been done for many years. Loose sand strata are liable to liquefaction during earthquake and they often need densification by artificial means to improve their relative density. The process essentially involves driving a casing that has an expendable shoe into the soil—as in the case of cast-in-situ driven piles—by repeated blows of a hammer. The vibration imparted to the soil and displacement of the soil caused by the driving of the casing compact the soil within the influence zone of the pile. The casing is then withdrawn and the hole is filled up with compacted aggregate. The compaction piles are driven on a predetermined grid all over the area to be densified. Dhar (1976) describes the soil densification work carried out at the Bongaigaon refinery and petrochemical complex by compaction piles. The subsoil in the top 10 m had loose sand with average 'N' value less than 10 blows/30 cm. Steel storage tanks 16 m diameter  $\times$  10 m high, were to be built at the site. To obtain a suitable subgrade for the compacted sand pad foundation for the tanks, an average 'N' value of 20 was required. The site was compacted by 450 mm diameter  $\times$  10 m deep compaction piles driven at 2.67 m c/c, as shown in Fig. 12.35. Standard penetration tests done in adjacent boreholes before and after densification showed appreciable improvement in the relative density except in the top 1 m of the soil where the soil remained loose due to lack of confinement. Substantial improvement of the standard penetrating resistance has been achieved by compaction piles (refer Fig. 12.35).

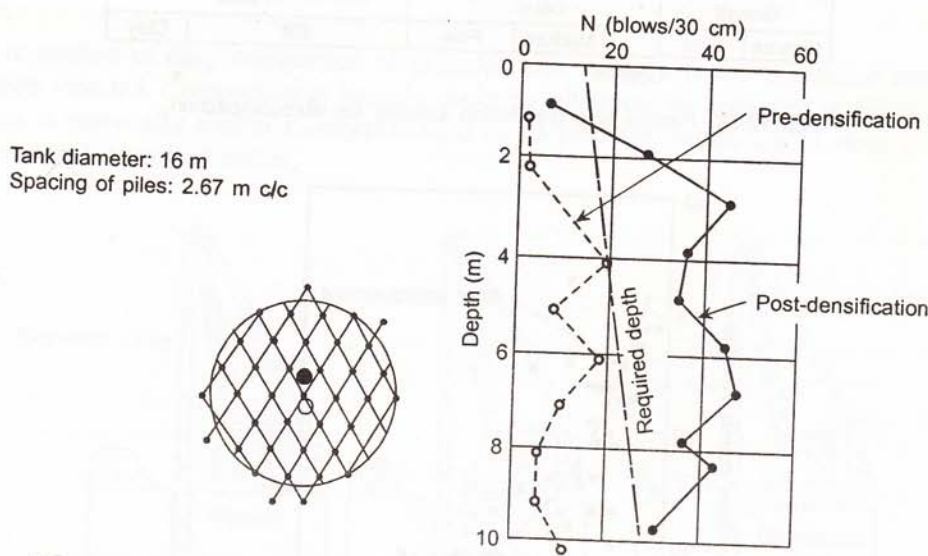


Fig. 12.35 Ground improvement by compacting piles at Bongaigaon Refinery (Dhar, 1976).

### 12.4.5 Control of Field Work

Field compaction of granular soil by mechanical vibration either at the surface or inside the ground needs adequate control to achieve the desired result. There is no mathematical approach to determine the nature and extent of ground improvement required. The problem

has to be approached on a trial and error basis with past experiences serving as useful guide. A suitable approach may be to

- (a) carry out detailed soil exploration by conducting standard penetration tests or cone penetration tests within the influence zone below the proposed foundations.
- (b) determine the extent of improvement required in terms of increased  $N$  or  $N_c$  value from appropriate foundation analysis.
- (c) choose the method of ground improvement, say, dynamic consolidation, vibrocompaction, or compaction piles depending on availability of facilities.
- (d) select a representative area close to the construction site and carry out trial ground improvement work varying the construction control parameters, such as weight of hammer, height of fall, number of blows, spacing of compaction piles, and so on. In general, the weight of hammer and height of fall are predetermined as per equipment capacity. Before starting the trial ground improvement scheme, make sure that predensification properties of the soil, namely SPT, CPT data, and so forth have to be determined.
- (e) carry out field tests to determine the post densification parameters after completion of trial ground improvement work and determine the extent of improvement as a function of spacing of compaction piles.
- (f) choose the spacing of compaction piles on the basis of pre and post densification data.
- (g) carry out field tests to check the efficacy of compaction at different locations.

A trial ground improvement work has recently been done for the proposed construction of a 120 m high temple about 75 km from Kolkata. The subsoil consists of a thin layer of firm silty clay/clayey silt followed by a deep deposit of loose to medium silty fine sand to 25 m below GL. Thereafter, a thin layer of stiff clay is found and the same is followed by dense to very dense sand. The soil condition at the temple site is shown in Fig. 12.36. In view of the high foundation loading anticipated from the temple structure, the sandy soil immediately beneath the top silty clay 12–14 m below GL required improvement.

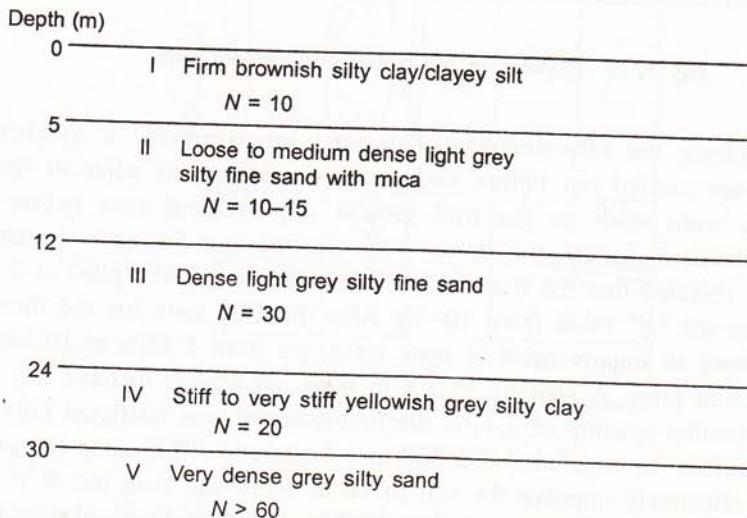


Fig. 12.36 Soil condition at temple site.

Trial ground improvement was done at a suitable location near the proposed temple structure. The area was divided into three sections shown in Fig. 12.37 and compaction was done with pile spacing of  $2.8 \text{ m} \times 2.8 \text{ m}$ ,  $2 \text{ m} \times 2 \text{ m}$ , and  $1.4 \text{ m} \times 1.4 \text{ m}$ . The method essentially consisted of driving a steel casing,  $500 \text{ mm diameter} \times 8\text{--}12 \text{ m long}$  with expendable shoe at the bottom and then filling the hole with compacted stone as the casing was withdrawn. The loose stone inside the casing was compacted in layers by 30 blows of a  $10 \text{ kN}$  hammer falling through a height of  $2 \text{ m}$ .

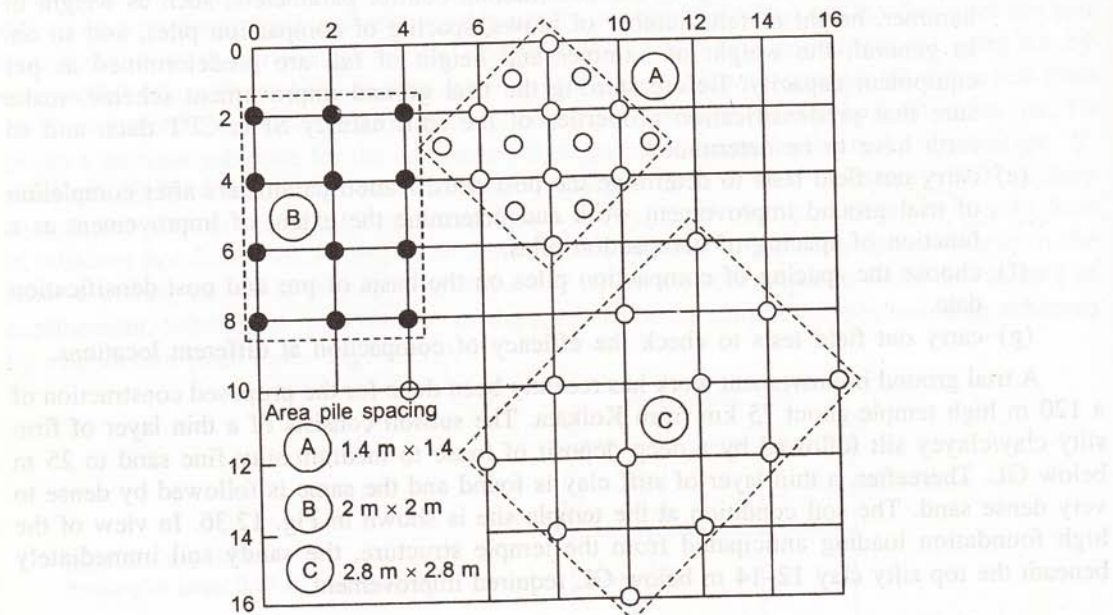


Fig. 12.37 Planning of trial ground improvement work.

In order to check the effectiveness of ground improvement, a number of cone penetration tests were carried out before and after compaction, at adjacent locations. In addition, boreholes were made in the trial ground improvement area before and after compaction and standard penetration tests were carried out in each borehole (refer Fig. 12.37). It was revealed that the trial compaction with compaction piles at  $2 \text{ m}$  spacing effectively increases the ' $N$ ' value from 10–30. Also the CPT data for the three different spacings clearly shows an improvement of cone resistance from  $5 \text{ MPa}$  to  $10 \text{ MPa}$  for  $2 \text{ m}$  spacing of compaction piles. A spacing of  $2.8 \text{ m}$  does not appear to have any significant effect while for a smaller spacing of  $1.4 \text{ m}$ , the improvement was restricted only in the top  $4\text{--}5 \text{ m}$ . It may, therefore, be concluded that  $500 \text{ mm diameter} \times 10 \text{ m}$  deep compaction piles at  $2 \text{ m} \text{ c/c}$  would effectively improve the soil to  $10 \text{ m}$  depth and both the  $N$  value and the cone resistance would be doubled in the process. The results of trial ground improvement are shown in Fig. 12.38.

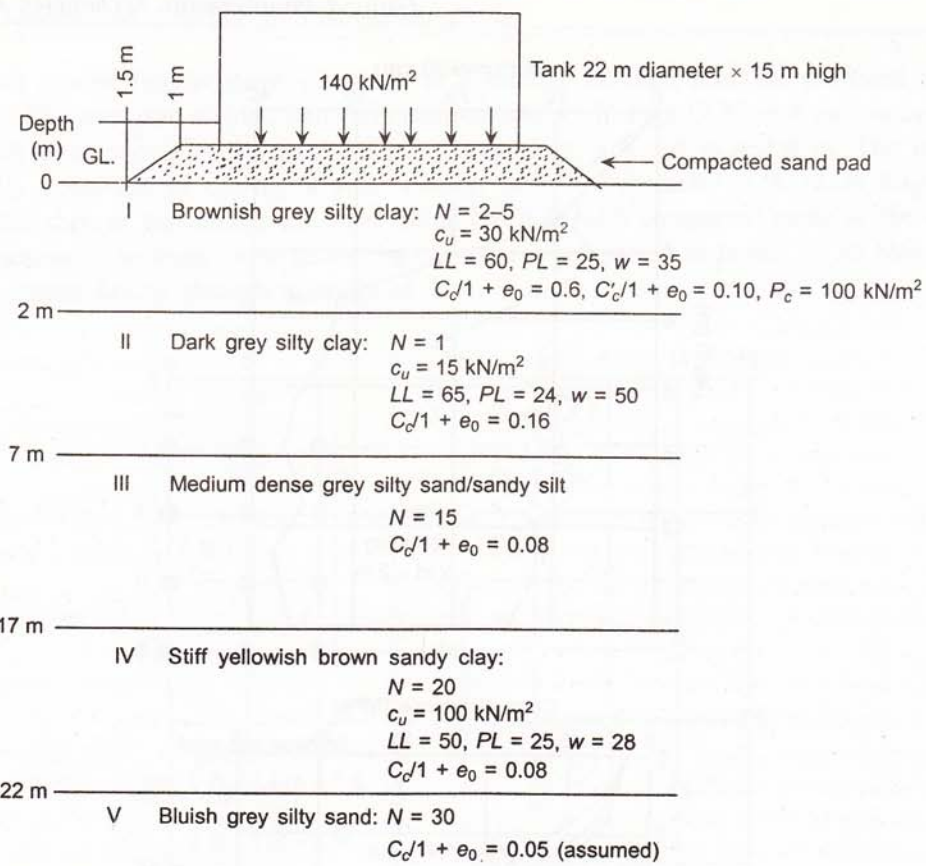


Fig. 12.39 Subsoil condition (Example 12.1).

**Solution**

- (a) Net foundation pressure, considering 45° dispersion of water load (140 kN/m<sup>2</sup>) through compacted sand pad.

$$q_n = \frac{140 \times 22^2}{(22 + 3)^2} + (1.5 \times 20) \text{ (sand pad)}$$

$$= 108 + 30 = 138 \text{ kN/m}^2$$

Average  $c_u$  of strata I and II

$$= \frac{(30 \times 2) + (15 \times 5)}{7}$$

$$= 19.3 \text{ kN/m}^2$$

$$q_{ult}(n) = c_u N_c$$

$$= 19.3 \times 6 = 116 \text{ kN/m}^2 < 138 \text{ kN/m}^2$$

$$\text{Settlement of untreated soil, } \delta = \sum \frac{C_c}{1 + e_0} H \log \frac{p_o + \Delta p}{p_o}$$

Layer	$H(m)$	$p_o$ (kN/m $^2$ )	$\Delta p$ (kN/m $^2$ )	$\frac{C_c}{1 + e_0}$	$\delta$ (m)
I	2	8	138	0.06	0.151
II	5	36	132 (0.96) + 138	0.16	0.535
III	10	96	89	0.08	0.227
IV	5	156	44	0.08	0.043
V	15	236	40	0.05	0.051
					$\Sigma 1.007 \text{ m}$ $(\approx 1000 \text{ mm})$

The subsoil of strata I and II are too weak to support the given load. Also strata I and II would contribute 70% of the total settlement.

- (b) Consider preloading the soil by installing 65 mm diameter sand wicks, 8 m long. Use two stage preloading (3 m + 3 m) with sand bags or sand fill.

The average consolidation pressure in strata I and II  
(refer Fig. 5.12, Chapter 5)

$$\text{Therefore, } P_c = 50 + 50 = 100 \text{ kN/m}^2$$



### Stratum I

$$\Delta p_1 = 100 \text{ kN/m}^2$$

Increased shear strength after consolidation by two stage preloading,  
 $\Delta c_u = 0.3 \times 100 = 30 \text{ kN/m}^2$

### Stratum II

$$\Delta p_1 = 0.96 \times 100 = 96 \text{ kN/m}^2$$

Increased shear strength,  $\Delta c_u = 0.3 \times 96 = 28.8 \text{ kN/m}^2$

Additional load during hydrotest =  $138 - 100 = 38 \text{ kN/m}^2$

Consider 90% consolidation during hydrotest. Sand wicks are to be designed accordingly.  
After consolidation,

### Stratum I

$$\Delta p = \left( \frac{38 \times 25^2}{26^2} \right) \times 0.9 = 31.6 \text{ kN/m}^2$$

$$\Delta c_u = 0.3 \times 31.6 = 9.5 \text{ kN/m}^2$$

**Stratum II**

$$\Delta p = \frac{38 \times 25^2}{29.5^2} \times 0.9 = 24.6 \text{ kN/m}^2$$

$$\Delta c_u = 0.3 \times 24.6 = 7.4 \text{ kN/m}^2$$

Hence, strength after hydrotest for

$$\text{Stratum I} : 30 + 30 + 9.5 = 69.5 \text{ kN/m}^2$$

$$\text{Stratum II} : 15 + 28.8 + 7.4 = 51.2 \text{ kN/m}^2$$

$$\text{Weighted average of } c_u = \frac{69.5 \times 2 + 51.2 \times 5}{7} = 56.4 \text{ kN/m}^2$$

$$q_{ult}(n) = 56.4 \times 6 = 338 \text{ kN/m}^2$$

$$FS = 338/138 = 2.5$$

(c) Settlement during preload

$$\text{Stage I: } P_c = 50 \text{ kN/m}^2$$

$$\delta = \sum \frac{C_c}{1 + e_0} H \log \frac{p_o + \Delta p}{p_o}$$

Layer	$H(\text{m})$	$p_o (\text{kN/m}^2)$	$\Delta p (\text{kN/m}^2)$	$\frac{C_c}{1 + e_0}$	$\delta (\text{m})$	
I	2	8	48	0.06	0.102	
II	5	36	46	0.16	0.288	0.390
III	10	96	31	0.08	0.096	
IV	5	156	15	0.08	0.016	
V	15	236	14	0.05	0.018	0.130
					$\Sigma 0.520 \text{ m}$	
					$(\approx 520 \text{ mm})$	

Consider 90% consolidation of strata I and II, 30% in stratum III, and 10% in stratum IV and V.

$$\begin{aligned} \text{Settlement at tank centre} &= (0.390 \times 0.9) + (0.3 \times 0.096) + (0.1 \times 0.034) \\ &= 0.383 \text{ m} = 383 \text{ mm} \end{aligned}$$

(d) Settlement during preload

$$\text{Stage II: } P_c = 50 \text{ kN/m}^2$$

$$\delta = \sum \frac{C_c}{1 + e_0} H \log \frac{p_o + \Delta p}{p_o}$$

Layer	$H(m)$	$p_o$ (kN/m <sup>2</sup> )	$\Delta p$ (kN/m <sup>2</sup> )	$\frac{C_c}{1 + e_0}$	$\delta$ (m)
I	2	56	48	0.6	0.031
II	5	82	46	0.16	0.152
III	10	127	31	0.08	0.076
IV	5	171	15	0.08	0.015
V	15	250	14	0.05	0.018
					$\Sigma 0.292 \text{ m}$
					(≈ 290 mm)

[Note: Effective overburden pressure  $p_o$  after stage I preload has been determined for full consolidation under the preload. In reality, for strata III, IV and V,  $p_o$  values would be less due to lower degree of consolidation.]

Consider residual settlement of stage I preload occurring in stage II and settlement for stage II preload as

*Stage I :* 10% of stratum I and II  
30% of stratum III  
10% of stratum III and IV

*Stage II:* 90% of stratum I and II  
30% of stratum II  
10% of stratum III and IV

$$\begin{aligned} \text{Settlement at centre} &= (0.1 \times 0.390) + (0.3 \times 0.096) + (0.1 \times 0.034) \\ &\quad + (0.9 \times 0.183) + (0.3 \times 0.76) + (0.1 \times 0.033) \\ &= 0.262 \text{ m} \approx 260 \text{ mm} \end{aligned}$$

Total settlement during stage I and stage II preload at centre is

$$383 + 260 = 643 \text{ mm}$$

(e) Settlement of tank centre during hydrotest:  $\Delta p = 38 \text{ kN/m}^2$

$$\delta = \sum \frac{C_c}{1 + e_0} H \log \frac{p_o + \Delta p}{p_o}$$

Layer	$H(m)$	$p_o$ (kN/m <sup>2</sup> )	$\Delta p$ (kN/m <sup>2</sup> )	$\frac{C_c}{1 + e_0}$	$\delta$ (m)
I	2	104	37	0.10	0.026
II	5	128	35	0.16	0.084
III	10	158	20	0.08	0.04
IV	5	186	17	0.08	0.03
V	15	266	11	0.05	0.025
					$\Sigma 0.205 \text{ m}$
					(≈ 205 mm)

[Note given in (d) above is valid for this case also.]

Total settlement during hydrotest at centre of tank

$$\begin{aligned}
 & 30\% \text{ of stage I preload (strata II), } 0.3 \times 0.096 = 0.029 \text{ m} \\
 & 10\% \text{ of stage I preload (strata III and IV), } 0.1 \times 0.034 = 0.0034 \text{ m} \\
 & 10\% \text{ of stage II preload (strata I and II), } 0.1 \times 0.183 = 0.018 \text{ m} \\
 & 20\% \text{ of stage II preload (strata III, IV, V), } 0.2 \times 0.110 = 0.022 \text{ m} \\
 & 90\% \text{ of hydrotest load (strata I and II), } 0.9 \times 0.110 = 0.099 \text{ m} \\
 & 30\% \text{ of hydrotest load (strata III), } 0.3 \times 0.04 = 0.012 \text{ m} \\
 & 20\% \text{ of hydrotest load (strata IV and V), } 0.2 \times 0.055 = 0.011 \text{ m} \\
 & \hline
 & \quad \quad \quad = 0.195 \text{ m} \\
 & \quad \quad \quad (\approx 200 \text{ mm})
 \end{aligned}$$

(f) Design of sand wicks

Diameter of sand wicks = 65 mm, length = 8 m

Take spacing at 1.2 cm c/c square grid

$$n = \frac{d_e}{d_w} = \frac{1.13 \times 1.2}{0.065} = 20.9$$

For 90% consolidation,  $U = 0.9$

Therefore, time factor,  $T_{90} = 0.7$

Radial coefficient of consolidation,  $C_r = 0.075 \text{ m}^2/\text{day}$

Therefore, time for 90% consolidation (for  $n = 20.9$  and  $T_{90} = 0.7$ ) is

$$\begin{aligned}
 t_{90} &= \frac{T_{90} \times d_e^2}{C_r} \\
 &= \frac{0.7 \times 1.26^2}{0.075} = 15 \text{ days}
 \end{aligned}$$

### Example 12.2

A steel storage tank, 24 m diameter  $\times$  18 m high, is to be founded on the subsoil shown in Fig. 12.40. The formation level of the ground is to be raised by a 2 m sand fill prior to construction. The soil is proposed to be treated by 0.5 m diameter stone column. Design suitable foundation for the storage tank.

#### Solution

- The subsoil will be preconsolidated under the load of 2 m sand fill with preinstalled stone columns accelerating the consolidation by sand drain effect. This will increase the shear strength of the subsoil and also help in reducing consolidation under tank load.
- The tank load (that is hydrotest load) will be dispersed through the sand pad/sand fill and the subsoil will be consolidated under the dispersed load during hydrotest. The reinforcing action of the stone columns will help to increase the overall bearing capacity of the soil and reduce settlement.
- Ground settlement under 2 m sand fill for  $\Delta p = 40 \text{ kN/m}^2$  is

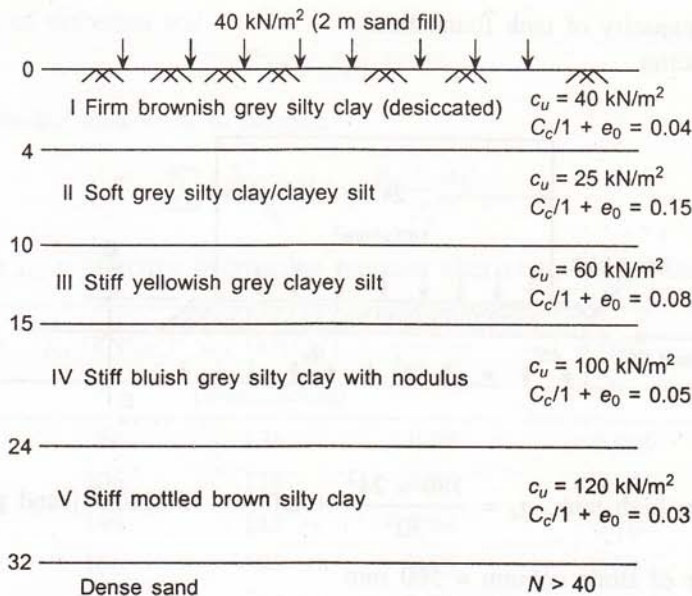


Fig. 12.40 Subsoil condition (Example 12.2).

$$\delta = \sum \frac{C_c}{1 + e_0} H \log \frac{p_o + \Delta p}{p_o}$$

Layer	$H(\text{m})$	$p_o (\text{kN/m}^2)$	$\Delta p (\text{kN/m}^2)$	$\frac{C_c}{1 + e_0}$	$\delta (\text{m})$
I	4	16	40	0.04	0.087
II	6	56	40	0.15	0.210
III	5	100	40	0.08	0.058
IV	9	156	40	0.05	0.045
V	8	224	40	0.03	0.017
					$\Sigma 0.417 \text{ m}$ $(\approx 420 \text{ mm})$

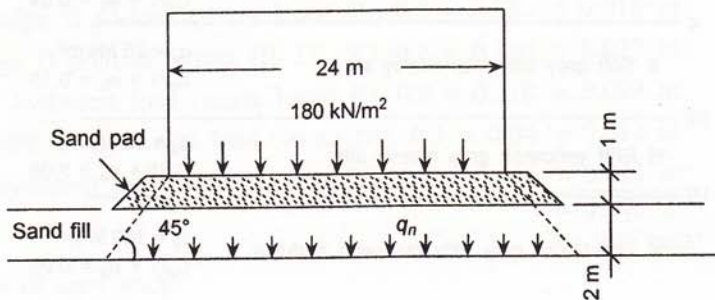
(d) Shear strength after consolidation under sand fill

Layer	Original $c_u (\text{kN/m}^2)$	$\Delta c_u (\text{kN/m}^2)$	Increased $c_u (\text{kN/m}^2)$
I	40	$0.3 \times 40 = 12$	52
II	25	12	37
III	60	12	72
IV	100	12	112
V	120	12	132

$$[c_u]_{AVG} = \frac{(4 \times 52) + (6 \times 32) + (5 \times 72)}{15} = 52 \text{ kN/m}^2$$

(15 m depth)

- (e) Bearing capacity of tank foundation  
Tank loading



$$\text{For } 18 \text{ m high tank, } q_n = \frac{180 \times 24^2}{30^2} + 2.0 = 135 \text{ kN/m}^2 \text{ (sand pad)}$$

- (f) Diameter of stone column = 500 mm

Spacing: 1.0 m c/c triangular grid

$$\text{Area} = 0.2 \text{ m}^2$$

$$\text{Influence area} = 0.866 (1)^2 = 0.866 \text{ m}^2$$

$$\text{Area ratio} = \frac{0.2}{0.866} \times 100 = 23\%$$

Capacity of stone column

$$q_{ult} = 25c_u = 25 \times 40 = 1000 \text{ kN/m}^2$$

Using Eq. (12.8)

$$\sigma_{vf} = \frac{1 + \sin \phi'}{1 - \sin \phi'} (\sigma_{ro} - u + Kc_u)$$

$$= 4.26 [(18 \times 2 - 10) \times 1.5 - 10 + 4 \times 40] = 805 \text{ kN/m}^2$$

[GWT 1 m BGL,  $K = 4$ ;  $\phi' = 38^\circ$ , and depth of bulging 2 m]

$$Q_{ult} \text{ per stone column} = 0.2 \times 805 = 161 \text{ kN}$$

$$Q_{all} \text{ per stone column} = \frac{Q_{ult}}{FS} = \frac{161}{2} = 80.5 \text{ kN}$$

Therefore, take it to be 100 kN per stone column.

- (g) Bearing capacity of treated ground,

$$\begin{aligned} q_{all} &= [100 + (0.866 - 0.2)(6 \times 50)/2.5]/0.866 \\ &= 208 \text{ kN/m}^2 > 135 \text{ kN/m}^2 \end{aligned}$$

## (h) Settlement of untreated soil

$$q_n = 135 \text{ kN/m}^2$$

Effective loaded area = 30 m diameter

$$\delta = \sum \frac{C_c}{1 + e_0} H \log \frac{p_o + \Delta p}{p_o}$$

(where  $p_o$  = effective overburden pressure after consolidation under sand fill.)

Layer	$H(\text{m})$	$p_o (\text{kN/m}^2)$	$\Delta p (\text{kN/m}^2)$	$\frac{C_c}{1 + e_0}$ [Boussinessq]	$\delta (\text{m})$
I	4	56	135	0.04	0.085
II	6	106	128	0.15	0.309
III	5	140	115	0.08	0.104
IV	9	196	95	0.05	0.077
V	8	264	74	0.03	0.026
					$\Sigma 0.601 \text{ m}$ ( $\approx 600 \text{ mm}$ )

## (i) Settlement of treated soil

Settlement reduction ratio

$$\beta = \frac{1}{1 + (n - 1)A_R} = 0.52$$

where

$$n = \text{stress concentration ratio} = 5$$

$$A_R = \text{area ratio} = 23\%$$

## (j) Settlement during hydrotest

Consider 100% for 10 m depth (by radial consolidation through stone columns) and 20% below 10 m depth

$$\begin{aligned}\delta_{\text{centre}} &= (0.52 \times 394) + (0.2 \times 207) \\ &= 208 + 40 = 248 \text{ mm} \approx 250 \text{ mm}\end{aligned}$$

## (k) Long-term settlement

Additional settlement will occur due to remaining 80% consolidation of soil below 10 m depth but under reduced operation load of oil having specific gravity 0.8).

$$\begin{aligned}\delta_{\text{centre}} &= 248 + (0.8 \times 200 \times 0.8) \\ &= 376 \approx 375 \text{ mm.}\end{aligned}$$

**REFERENCES**

- Barron, R.A. (1948), Consolidation of Fine-grained Soils by Drain Wells, *Trans. ASCE*, Vol. 113, pp. 718–734.
- Brown, R.E. (1978), Vibroflotation Compaction of Cohesionless Soils, *Journal of Geotechnical Division, ASCE*, Vol. 103, No. GT 12, pp. 1437–51.
- Dastidar, A.G., S. Gupta, and T.K. Ghosh (1969), *Application of Sandwick in a Housing Project*, Proceedings 7th International Conference on SMFE, Mexico, 2: pp. 59–64.
- Dastidar, A.G. (1985), Treatment of Weak Soils—An Indian Perspective, *Geotechnical Engineering*, Vol. 1, pp. 179–229.
- Datye, K.R. (1982), Simpler Techniques for Ground Improvement, 4th IGS Annual Lecture, *Indian Geotechnical Journal* Jan., 12(1): pp. 1–82.
- Datye and Nagaraju (1977), Design Approach and Field Control of Stone Columns, Proceedings 10th ICSMFE, Stockholm, Vol. 3.
- Dhar, P.R. (1976), *Soil Densification by Compaction Piles at a Refinery Site*, Symposium on Foundations and Excavations in Weak Soil, Calcutta.
- Engelhardt, K., W.A. Flynn, and A.A. Bayak (1974), Vibro-replacement Method to Strengthen Cohesive Soils in-situ, *ASCE National Structural Engineering Meeting*, Cincinnati, p. 30.
- Greenwood, D.A. (1970), *Mechanical Improvement of Soil below Ground Surface*, Proceedings Ground Engineering Conference, I.C.E., London, pp. 11–22.
- Hughes, J.M.O. and N.J. Withers (1974), Reinforcing of Soft Cohesive Soil with Stone Column, *Ground Engineering*, Vol. 7, No. 3, pp. 42–49.
- Hughes, J.M.O., N.J. Withers, and D.A. Greenwood (1975), A Field Trial of the Reinforced Effect of a Stone Column in Soil, *Geotechnique*, Vol. 25, pp. 34–44.
- Kjellman, W. (1948), *Accelerating Consolidation of Fine-grained Soils by means of Cardboard Wicks*, Proceedings 2nd International Conference on SMFE, Rotterdam, 2: pp. 302–305.
- Mitchell, J.K. and R.K. Katti (1981), *Soil improvement: State-of-the-art Report*, Proceedings 10th International Conference on SMFE, Stockholm, p. 163.
- Nayak, N.V. (1982), *Stone Columns and Monitoring Instruments*, Proceedings Symposium on soil and rock improvement: geotextiles, reinforced earth and modern piling techniques, Asian Institute of Technology, Bangkok, December 1982.
- Nayak, N.V. (1983), *Structures on Ground Improved by Stone Columns*, Proceedings International Symposium on Soil Structure Interaction, Roorkee, India.
- Pilot, G. (1977), *Methods of Improving the Engineering Properties of Soft Clay*, State-of-the-art Report, Symposium on soft clay, Bangkok.

- Som, N.N. (1995), *Consolidation Settlement of Large Diameter Storage Tank Foundations on Stone Columns in Soft Clay*, Proceedings International Symposium on compression and consolidation of clayey soils, Hiroshima, p. 653, Balkema Publishers.
- Som, N.N. (1999), *Stone Column Foundation for Large Area Loading—Some Case Studies*, Symposium on Thick Deltaic Deposits, Asian Regional Conference on Soil Mechanics and Geotechnical Engineering, Seoul, Korea.
- Thorburn, S. (1975), *Building Supported by Stabilised Ground*, Symposium on ground treatment by deep compaction, Institute of Civil Engineers, London.
- Tsytovich, N., V. Berezantzev, B. Dalmatov and M. Abelev (1974), *Foundation Soils and Substructures*, MIR Publishers, Moscow.



# **Earthquake Response of Soils and Foundations**

## **13.1 INTRODUCTION**

Earthquakes can cause extensive damage to foundations and structures built on them. Earthquake motions are initiated in the soil and they are instantaneously transmitted to the foundation causing adverse effect on the behaviour of the superstructure. Damage may occur due to instability of the soil which results in extensive ground movement including differential movement. While structural damage is ultimately manifested in tilt or damage or even collapse of the superstructure, the initiating cause can often be identified as the adverse response of the soil-foundation system under seismic forces.

Geotechnical considerations are, therefore, important in the development of an earthquake resistance design. It is not only the type of soil deposit that determines the kind of response to be expected during a strong earthquake. The type of structure also influences the seismic response. The field of geotechnical earthquake engineering is quite complex. Much of its applications are based on empirical studies made on the basis of case histories which illustrate the effect of earthquake on engineering structures.

## **13.2 EARTHQUAKE CHARACTERISTICS**

### **13.2.1 Magnitude**

The most widely used magnitude scale to define the severity of an earthquake was developed by Richter (1958). Accordingly, the magnitude of an earthquake is given by the logarithm of the amplitude on a Wood-Anderson torsion seismogram located at a distance of 100 km from the earthquake source. Thus,

$$M = \log(A/T) + f(\Delta, h) + C_s + C_r \quad (13.1)$$

where

$A$  = amplitude in (0.001) mm,

$T$  = period of seismic wave in seconds,

$f(\Delta, h)$  = correction factor for epicentral distance ( $\Delta$ ) and focal depth ( $h$ ),

$C_s$  = correction factor for seismological station, and

$C_r$  = regional correction factor.

Natural seismic events may have magnitude as high as 8.5 or 9. Magnitudes below 2.5 are not generally felt by humans. The frequency of occurrence of earthquake in a global scale (based on observations since 1990) is shown in Table 13.1.

**Table 13.1** Frequency of occurrence of earthquakes (since 1990)

Description	Magnitude	Average (Annual)
Great	8 and higher	1
Major	7–7.9	18
Strong	6–6.9	120
Moderate	5–5.9	820
Light	4–4.9	6200 (estimated)
Minor	3–3.9	49,000 (estimated)
Very Minor	<3.0	Magnitude 2–3 about 1000 per day Magnitude 1–2 about 8000 per day

### 13.2.2 Energy Release

The energy released by an earthquake has been related to the magnitude  $M$  by the equation

$$E = 10^{4.8 + 1.5M} \text{ Joules} \quad (13.2)$$

This energy is comparable to that of nuclear explosions. For example, a nuclear explosion of one mega ton releases energy of  $5 \times 10^{15}$  J. An earthquake of magnitude 7.3 would also release the energy equivalent of one mega ton nuclear explosion.

### 13.2.3 Intensity

The magnitude of an earthquake as obtained by the Richter's scale gives measure of the amount of energy released by the earthquake, not its damage potential. The intensity of an earthquake is a measure of the effect of an earthquake at a given location. Several intensity scales have been proposed, the most widely used being the Modified Mercalli Intensity (MMI) scale, as given in Table 13.2 (Newmann, 1954). The value assigned to the MMI scale gives qualitative description of the damages based on physical verification at site. The equivalent value of the magnitude by Richter's scale is given alongside the MMI in Table 13.2.

**Table 13.2** Modified Mercalli intensity (MMI) scale (abbreviated version)

Intensity	Evaluation	Description	Magnitude (Richter scale)
I	Insignificant	Only detected by instruments	1–1.9
II	Very light	Only felt by sensitive persons; oscillation of hanging objects	2–2.9
III	Light	Small vibratory motion	3–3.9
IV	Moderate	Felt inside buildings; noise produced by moving objects	4–4.9
V	Slightly strong	Felt by most persons; some panic; minor damages	
VI	Strong	Damages to nonseismic resistant structures	
VII	Very strong	People running; some damages in seismic resistant structures and serious damages to nonreinforced masonry structures	5–5.9

(Cont.)

Table 13.2 Modified Mercalli intensity (MMI) scale (abbreviated version), Cont.

Intensity	Evaluation	Description	Magnitude (Richter scale)
VIII	Destructive	Serious damage to structures in general	6-6.9
IX	Ruinous	Serious damage to structures; almost total destruction of nonseismic resistant structures	
X	Disastrous	Only seismic resistant structures remain standing	7-7.9
XI	Disastrous in extreme	General panic; almost total destruction; the ground cracks and opens	
XII	Catastrophic	Total destruction	8-8.6

### 13.2.4 Ground Acceleration

The intensity of ground motion during an earthquake is represented by the horizontal ground acceleration produced. The predominant effect of an earthquake is the horizontal forces that are produced in a structure. The horizontal ground acceleration  $\alpha$  gives a measure of this force, which can be expressed by  $\alpha W$ , (where  $W$  = weight of the structure) and acts at the centroid of the structure. This horizontal force is depicted in Fig. 13.1. I.S. 1893 (1983) gives the earthquake zones of India based on the horizontal ground acceleration and the vulnerability of an area to earthquakes.

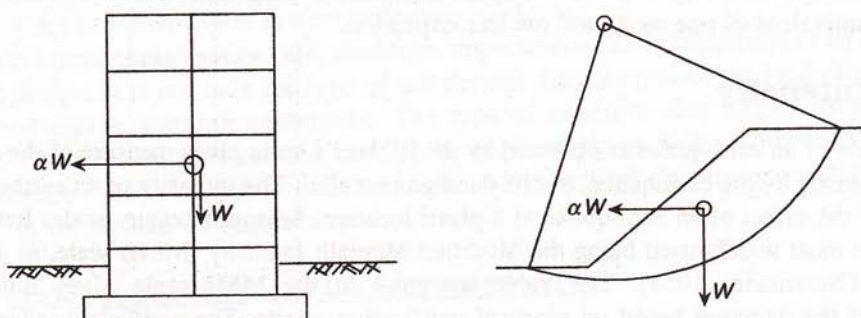


Fig. 13.1 Horizontal force due to earthquake.

### 13.2.5 Response Spectrum

Response spectra are typically used to portray the characteristics of the earthquake shaking at a site. Response spectrum shows the maximum response induced by the ground motions in damped single degree-of-freedom structures of different fundamental periods. Each structure has a unique fundamental period at which the structure tends to vibrate when it is allowed to vibrate freely, without any external excitation. The response spectrum indicates how a particular structure with its inherent fundamental period would respond to an earthquake ground motion. For example, measurement of ground motion in the 1985 Mexico City earthquake, response spectra shown in Fig. 13.2, shows that a low-period structure (say,  $T = 0.1$  s) experienced a maximum acceleration of  $0.14g$ , whereas a higher-period structure (say,  $T = 2.0$  s) experienced a maximum acceleration of  $0.74g$  for the same ground motions.

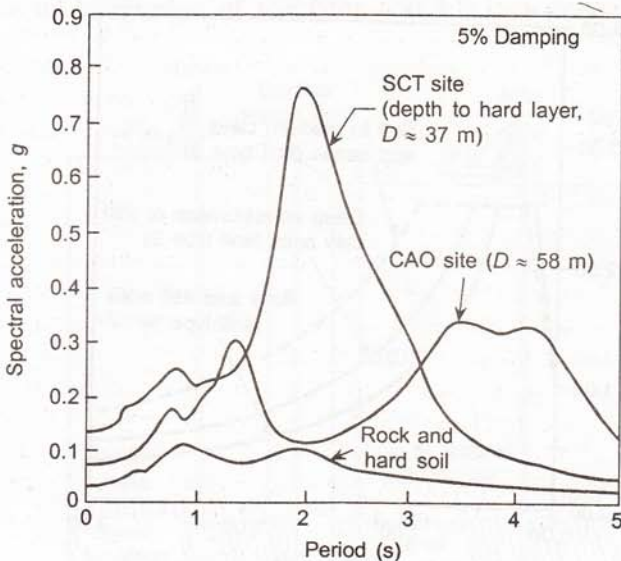


Fig. 13.2 Acceleration response spectrum as recorded in Mexico City earthquake, 1985 (Seed et al., 1987).

The response spectra shown in Fig. 13.2 illustrate the pronounced influence of local soil conditions on the characteristics of the observed earthquake ground motions. Since Mexico City was located approximately 400 km away from the epicentre, the observed response at rock and hard soil sites was fairly low (that is, the spectral accelerations were less than 0.1g for all periods). Damage was correspondingly negligible at these sites. At the Central Market site (CAO), spectral accelerations were significantly amplified to 0.3–0.35g at periods of around 1.3 s and within the range 3.5–4.5 s. Since buildings at the CAO site did not generally have fundamental periods within these ranges, damage was minor. The motion recorded at the SCT building site, however, indicated significant amplification of the underlying bedrock motions with a maximum horizontal ground acceleration (the spectral acceleration at a period of zero) over four times that of the rock and hard soil sites and with a spectral acceleration at  $T = 2.0$  s over seven times that of the rock and hard soil sites. Major damage including collapse, occurred to structures with fundamental periods ranging from about 1 s to 2 s near the SCT building site and in areas with similar subsurface conditions. At these locations, the fundamental period of the soil almost matched with that of the overlying structures, creating a near resonance condition that amplified the shaking and caused heavy damage.

The Uniform Building Code of USA (UBC, 1991) recommends the response spectrum, shown in Fig. 13.3, to determine the peak ground acceleration for a given fundamental period  $T$  for different soil conditions. For  $T > 0.5$  s, ground acceleration for deep soil strata is considerably higher than that for rock and hard soils. It is to be noted that the period of ground motion at a particular site is important in determining the effect of earthquake motion on the structure. If the fundamental period of a building is close to that of the site, a resonant condition is created. This amplifies the shaking and increases the potential to damage.

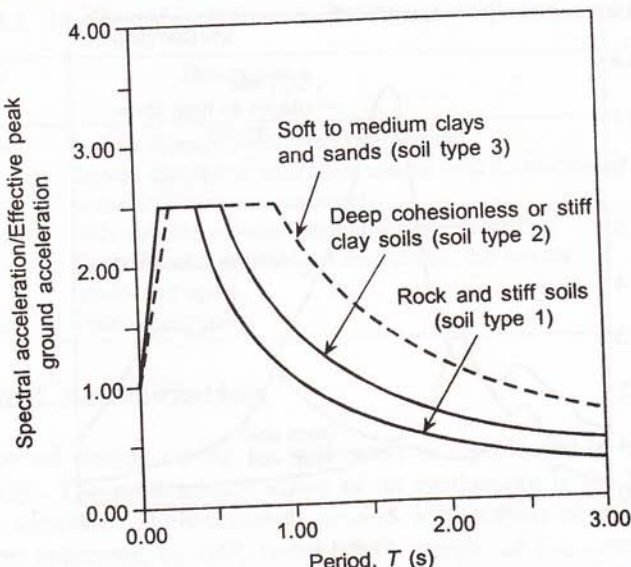


Fig. 13.3 UBC normalized acceleration response spectra (UBC, 1991).

### 13.3 EFFECTS OF EARTHQUAKE

Earthquakes affect soils in many ways. The major effects of earthquake on soils are:

1. Loose granular soils are compacted by ground vibration which cause large subsidence of the ground surface,
2. Compaction of loose granular soil may result in development of excess pore water pressure to cause liquefaction of the soil and lead to settlement and tilting of structures,
3. Combination of dynamic stress and induced pore water pressure may result in reduction of soil strength and cause bearing capacity failure and landslides in the earthquake area, and
4. Ground vibrations and shaking may cause structural damage even though the soils underlying the structure may remain stable during the earthquake.

### 13.4 GROUND SETTLEMENT

Vibration has long been recognized as an effective means of compacting granular soils. However, such compaction is associated with volume change of the soil and associated settlement of the ground surface. A measure of the ground subsidence caused by earthquake was obtained in the Alaska earthquake in 1964 (Grantz et al., 1964). A steel casing installed in firm rock in Homer, Alaska projected 30 cm above the ground surface. After the earthquake, the casing was seen to project 1.1 m above the ground indicating a subsidence of 0.8 m of the ground surface, as depicted in Fig. 13.4. Geological studies revealed that the rock surface had subsided by 0.6 m due to tectonic movements indicating a ground

subsidence of 1.4 m. A combination of 1.3 m settlement of rock due to tectonic movement and 1.3 m due to compaction of overlying soil led to a ground settlement of more than

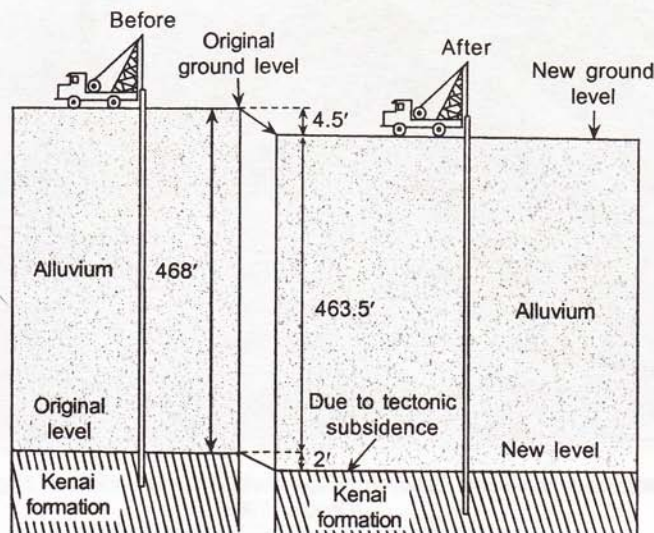


Fig. 13.4 Ground settlement around well casing at Homer in Alaska earthquake 1964 (Grantz et al., 1964).

2.6 m at Portage in the same earthquake in Alaska. This caused widespread flooding in the area during high tide periods and the town had to be relocated at a new location. Similar subsidence was noticed in other earthquakes also and the data is given in Table 13.3.

Table 13.3 Ground subsidence due to earthquake

Earthquake	Year	Rock subsidence (Tectonic) (m)	Ground subsidence (m)
Homer, Alaska	1964	0.6	1.4
Portage, Alaska	1964	1.3	2.6
Validina, Chile	1960	1.8	2.8
Niigata, Japan	1964	—	3.0

Ground settlement due to compaction of granular soil often leads to differential settlement of structures. A differential movement of more than a metre was noticed between a railroad bridge abutment, founded on deep piles, and the backfill placed directly on the ground surface during the Niigata earthquake of 1964. This is shown in Fig. 13.5. The bridge abutment, being founded on piles did not undergo much settlement but the granular backfill experienced major subsidence due to compaction by seismic vibrations. Field measurements have shown that vibrations induced by earthquakes are often responsible for causing significant structural damage resulting from differential settlement in a building frame. Field observations of earthquake induced settlement in saturated sandy soil are summarized in Table 13.4.



Fig. 13.5 Differential settlement between bridge abutment and backfill at Niigata earthquake 1964 (Ohsaki, 1966).

Table 13.4 Earthquake induced settlement in saturated soil

<i>Location and year</i>	<i>Magnitude of earthquake</i>	<i>Site</i>	<i>Thickness of sand layer (m)</i>	<i>Observed settlement (cm)</i>
Mexico, 1957	7.5	Mexico City	—	40
Tokachioki, 1968	7.9	Hachinohe	5.0	35
Niigata, 1964	7.5	Niigata C	9.0	20
Miagiken-oki, 1968	7.4	Arahama	9.0	20

Much of this settlement occurs due to horizontal motions induced by earthquakes. The stresses obtained by ground response analysis and the settlement obtained by cyclic shear stress give a basis for evaluation of the settlement potential of the ground during earthquakes (Seed and Silver, 1972).

### 13.5 LIQUEFACTION

A major damage to structures during earthquakes is caused by liquefaction in saturated fine sand and silt. This is seen as *sand boils* or *mud spouts* with associated ground cracks and development of quick sand-like condition over wide areas (Seed, 1968; Ambresey and Sarma, 1969). When liquefaction occurs buildings may sink into the ground. Lightweight structures may even 'float' up to the ground surface. A most vivid illustration of liquefaction was found in Niigata earthquake, Japan in 1964, shown in Fig. 13.6. The epicentre of the earthquake was located about 60 km from Niigata. Extensive liquefaction of the soil caused water to flow out of cracks and boils. Structures settled more than 1 m accompanied by severe tilting (refer Fig. 13.6). The recent Bhuj earthquake in India also presented vivid illustrations of liquefaction (Rao, 2001). Figure 13.7 depicts liquefaction in Bhuj earthquake, India, 2001.

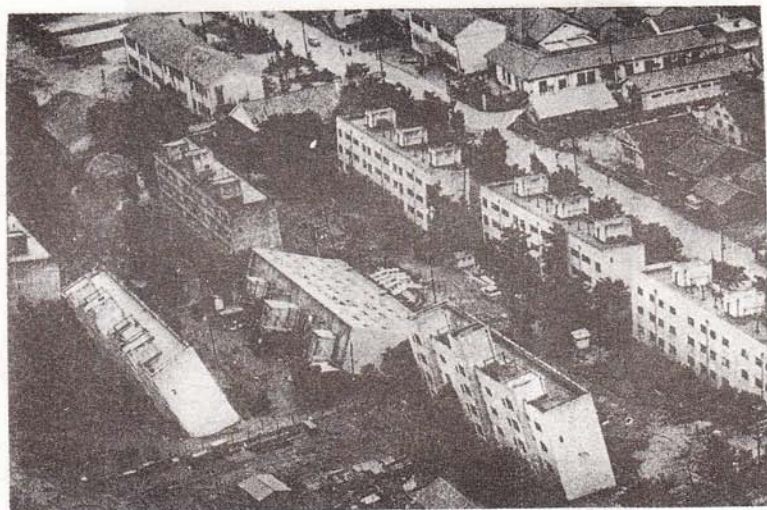
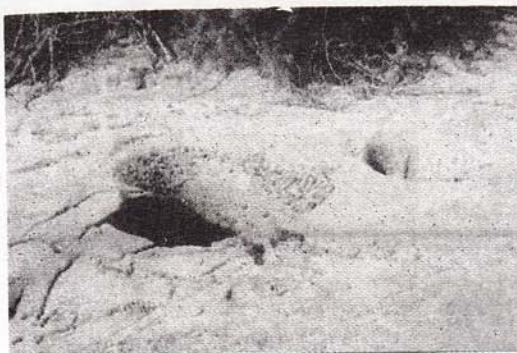
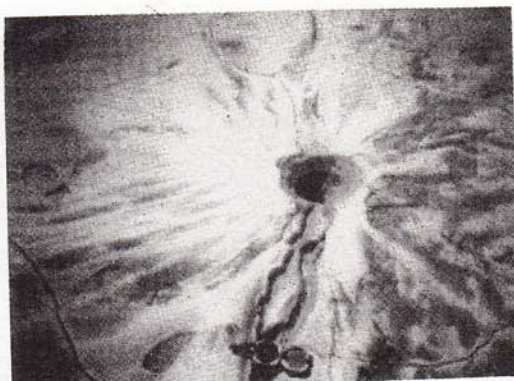


Fig. 13.6 Liquefaction in Niigata earthquake, 1964 (Ohsaki, 1966).

Liquefaction is caused in sand by ground vibration which tends to compact the sand and decrease its volume. If drainage does not occur, the tendency to decrease in volume results in increased pore water pressure. If the pore pressure builds up to an extent which is equal to the overburden pressure, the effective stress becomes zero and the soil loses its strength completely and gets into a liquefied state. Liquefaction may be initiated at the surface or at some depth below the ground surface. Once liquefaction occurs at some depth, the excess pore-pressure tends to dissipate by upward flow of water which, in turn, induces liquefaction in the upper layers of the soil.



**Fig. 13.7 Liquefaction in Bhuj earthquake, India, 2001 (Rao, 2001).**

### 13.5.1 Liquefaction Potential

The liquefaction potential of a soil depends on the relative density of the soil, percentage of fines present in the soil, effective confining pressure, depth of water table, and the ground acceleration produced by the earthquake.

For practical use, the liquefaction potential has been studied from a comparison of the shear stress developed in the soil at a given depth by an earthquake and the shear stress required to cause liquefaction, the latter being related to the relative density of the soil as measured by the SPT blow count  $N$  (blows/30 cm), as presented in Fig. 13.8 (Byrne, 1976). Kishida (1969) proposed a relationship between  $N$  value and depth, and indicated a boundary line between liquefaction and nonliquefaction, which is shown in Fig. 13.9. The data clearly show that liquefaction occurs mostly in soil with low relative density ( $D_r < 70\%$ ). Based on such field observations, a relationship between the cyclic stress ratio causing liquefaction and  $N$  value of sands containing different percentages of fines has been proposed, which is depicted in Fig. 13.10 (Seed et al., 1984).

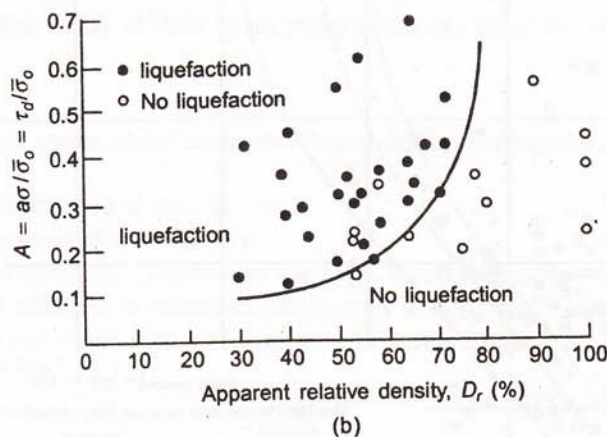
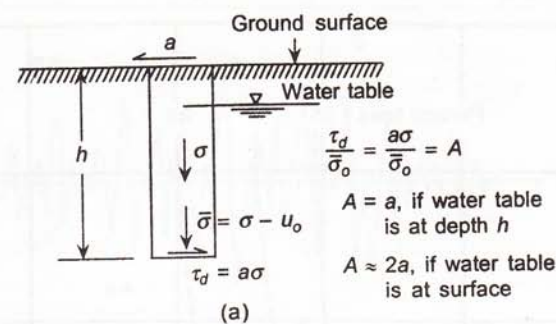


Fig. 13.8 Field observation of liquefaction (Byrne, 1976).

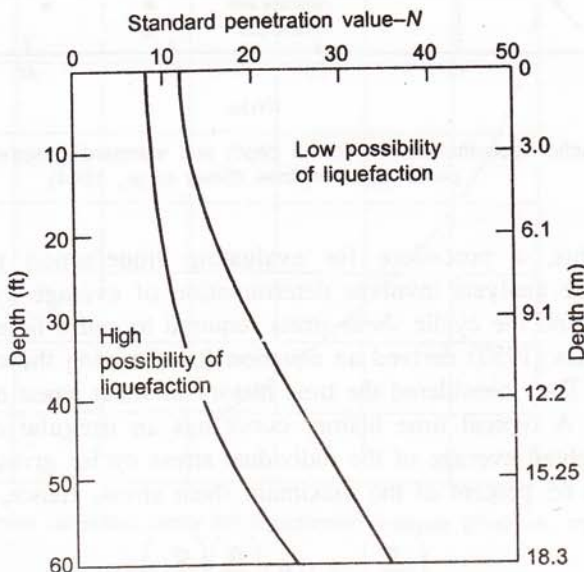


Fig. 13.9 Relationship between liquefaction potential and  $N$  value as a function of depth (Kishida, 1969).

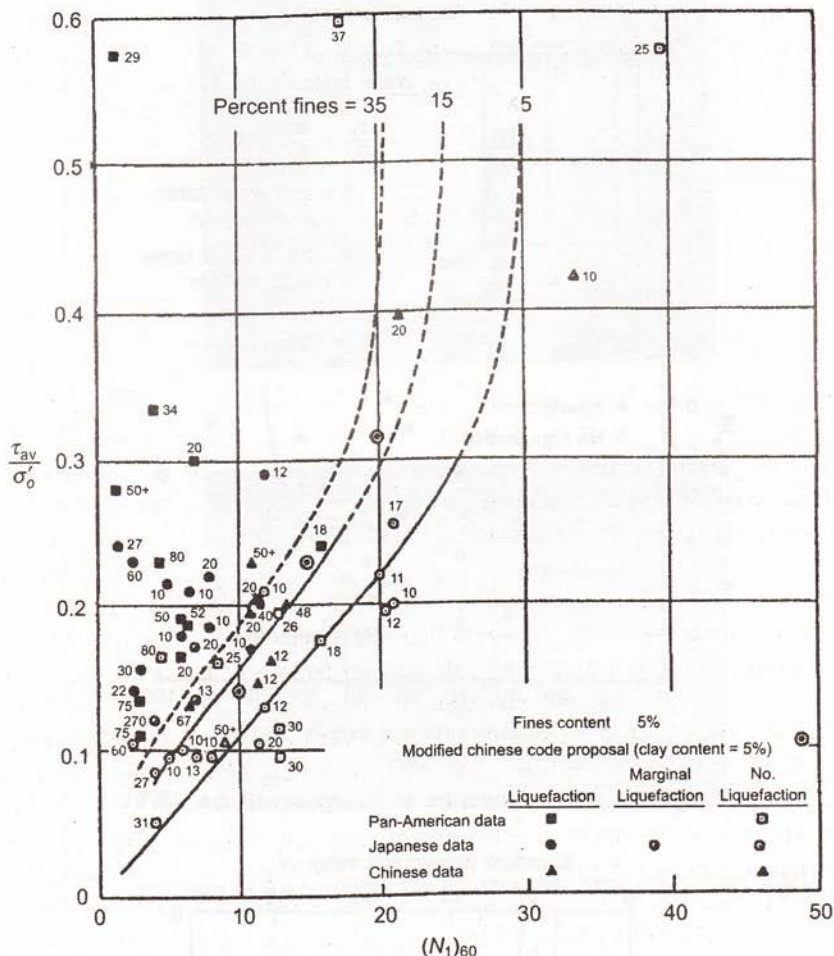


Fig. 13.10 Liquefaction potential as function of depth and standard penetration resistance for different percentages of fines (Seed et al., 1984).

Based on this, a procedure for evaluating liquefaction potential of a soil has been proposed. The analysis involves determination of average cyclic shear stress caused by the earthquake and the cyclic shear stress required to cause liquefaction.

Seed and Idriss (1982) derived an equation for obtaining the cyclic shear stress caused by an earthquake. They considered the time history of shear stress at any point in a soil due to an earthquake. A typical time history curve has an irregular distribution as shown in Fig. 13.11. A weighted average of the individual stress cycles gives the average shear stress  $\tau_{av}$  which is about 65 percent of the maximum shear stress. Hence,

$$\left( \frac{\tau}{\sigma'_o} \right)_d = 0.65 \left( \frac{\alpha}{g} \right) \left( \frac{\sigma_o}{\sigma'_o} \right) r_d \quad (13.3)$$

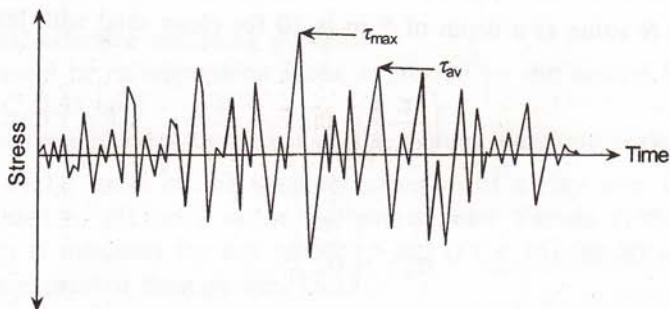


Fig. 13.11 Time history of shear stress during earthquake (Seed and Idriss, 1982).

where,

$$\left( \frac{\tau}{\sigma'_o} \right)_d = \text{average cyclic shear stress developed during earthquake,}$$

$\alpha$  = maximum ground acceleration,

$g$  = acceleration due to gravity,

$\sigma_o$  = total overburden pressure in the sand layer under consideration,

$\sigma'_o$  = initial effective overburden pressure at depth under consideration, and

$r_d$  = stress reduction factor (1.0 at ground surface to 0.8 at 5 m depth)  
(refer Fig. 13.12).

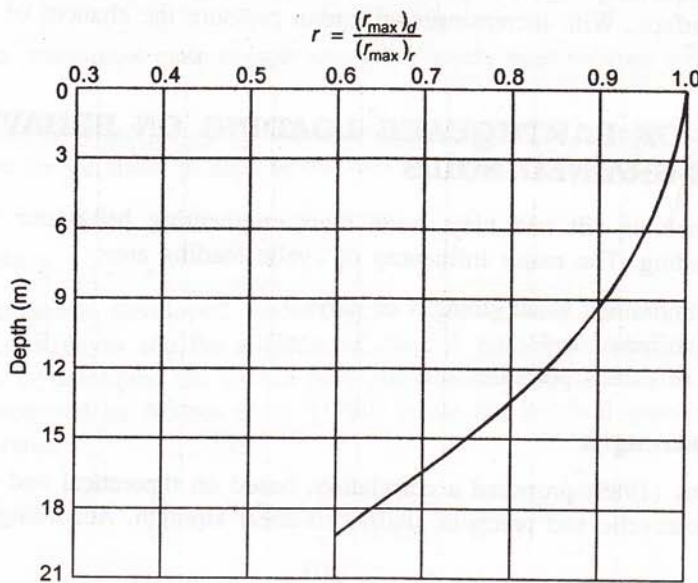


Fig. 13.12 Stress reduction factor for liquefaction analysis (Prakash, 1980).

For example, let us consider a site where the ground water table is at the ground surface and  $\alpha = 0.2 \text{ g}$ . At a depth of 5 m, the average cyclic stress ratio during earthquake works out as 0.29 [refer Eq. (13.3)].

The corrected  $N$  value at a depth of 5 m is 10 for clean sand with less than 5% fines. From Fig. 13.9,

$$\left( \frac{\tau}{\sigma_o} \right)_1 = 0.11$$

This gives,

$$\frac{\tau}{\sigma'_o} > \left( \frac{\tau}{\sigma'_o} \right)_1$$

Hence, liquefaction may occur at the site.

Table 13.5 gives the data on grain-size of the soil and depth of liquefaction in some well known earthquakes.

**Table 13.5** Liquefaction data

Location and year	Magnitude of earthquake	Grain-size $D_{10}$ (mm)	Depth of liquefaction (m)
Niigata, 1964	7.5	0.07–0.25	5
Mino-Owan, Japan, 1969	7.4	0.05–0.25	9
Jaltpan, Mexico, 1959	6.9	0.01–0.10	7
Alaska, 1964		0.01–0.1	8

It appears that liquefaction generally occurs in fine to medium sand within a depth of 10 m from ground surface. With increasing overburden pressure the chances of liquefaction usually decrease.

### 13.6 EFFECT OF EARTHQUAKE LOADING ON BEHAVIOUR OF FINE-GRAINED SOILS

Fine-grained soils such as silt and clay, have their engineering behaviour significantly affected by cyclic loading. The major influences of cyclic loading are:

- reduction of undrained shear strength of clays,
- reduction of stiffness, and
- development of excess pore-pressure.

#### Undrained shear strength

Van Eekelen and Potts (1989) proposed a correlation, based on theoretical and experimental work, between the postcyclic and precyclic undrained shear strength. Accordingly,

$$\frac{C_{uc}}{c_u} = \left( \frac{1 - u_e}{\sigma'_c} \right)^{k/\lambda} \quad (13.4)$$

where,

$C_{uc}$  = postcyclic undrained shear strength,

$c_u$  = precyclic undrained shear strength,

$u_e$  = excess pore-pressure due to cyclic loading,

$\sigma'_c$  = initial effective confining pressure,

$k$  = rebound or recompression index expressed on the natural logarithmic scale ( $= C_r/2.3$ ), and

$\lambda$  = compression index expressed on the natural logarithm scale ( $= C/2.3$ ).

The effect of cyclic stress on the strength reduction of a clay with initial zero shear stress has been related to plasticity index by Ishihara and Yasuda (1980). Almost 50% reduction in strength is indicated for low plasticity soil ( $PI < 15$ ) for 30 cycles of loading and this variation is expressed through Fig. 13.13.

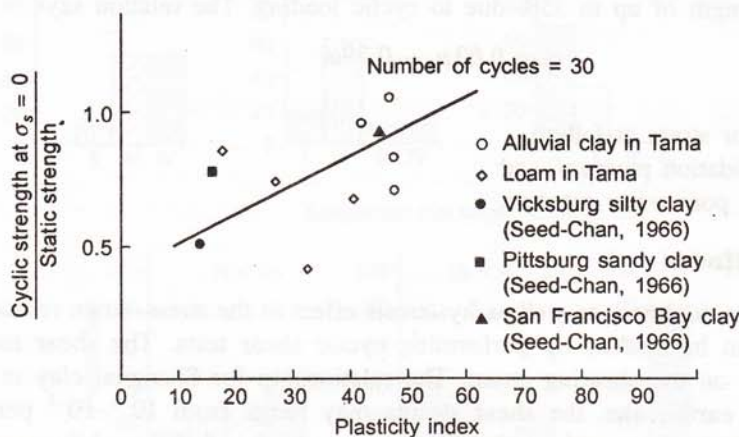


Fig. 13.13 Variation of cyclic strength ratio with plasticity index (Ishihara and Yasuda, 1980).

In general, the effect of cyclic stress on undrained shear strength has been found to be small when the cyclic strain is kept below half the precyclic failure strain (Thiers and Seed, 1969).

### Pore-pressure

Excess pore-pressure developed under cyclic loading may cause marked reduction in undrained shear strength and the stiffness of clay. A number of empirical correlations have been proposed to determine the excess pore-pressure developed in cyclic loading. One such relationship proposed by Matsui et al. (1980) relate the residual pore-pressure to the over consolidation ratio,

$$\frac{u_r}{\sigma_c} = \beta \left[ \log_{10} \left( \frac{\gamma_{c \max}}{A_1(OCR - 1)} + B_1 \right) \right] \quad (13.5)$$

where,

$u_r$  = residual pore-pressure,

$\sigma_c$  = effective confining pressure,

$\gamma_{c \max}$  = single amplitude maximum cyclic shear strain,

$OCR$  = overconsolidation ratio, and

$\beta$  = 0.45 (found experimentally).

Also,  $A_1, B_1 = f(PI)$  such that

PI	$A_1$	$B_1$
20	$0.4 \times 10^{-3}$	$0.6 \times 10^{-3}$
40	$1.1 \times 10^3$	$1.2 \times 10^{-3}$
55	$2.5 \times 10^{-3}$	$1.2 \times 10^{-3}$

Togrol and Guler (1984) proposed an empirical relation for normally consolidated clays to relate the deviator stress at failure to the excess pore-pressure and found reduction of undrained shear strength of up to 35% due to cyclic loading. The relation says

$$q_f = 0.63 p_c - 0.39 u \quad (13.6)$$

where,

$q_f$  = deviator stress at failure,  
 $p_c$  = consolidation pressure, and  
 $u$  = excess pore water pressure.

### Reduction of stiffness

Cyclic loading causes nonlinear as well as hysteresis effect in the stress-strain relationships of soils. The effect can be studied by performing cyclic shear tests. The shear modulus is, however, dependent on the shearing strain. The relationship for Shanghai clay is shown in Fig. 13.14. During earthquake, the shear strains may range from  $10^{-3}$ – $10^{-1}$  percent with different maximum strain in each cycle. Hence, two-thirds of the modulus measured at maximum strain is normally taken for design.

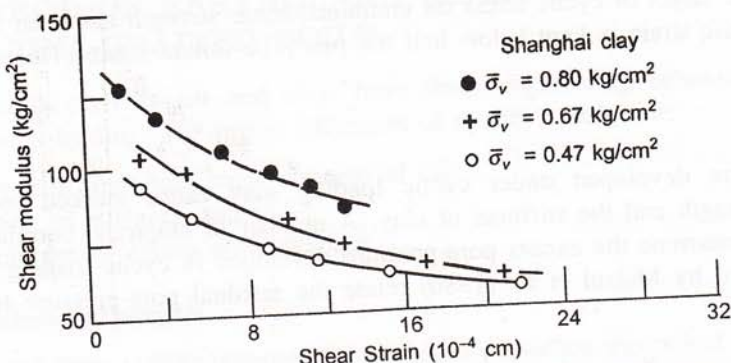


Fig. 13.14 Variation of shear modulus with strain (Seed and Idriss, 1969).

## 13.7 BUILDING DAMAGE DUE TO LIQUEFACTION

Seed et al. (1989) reported extensive study of the building damages that occurred in the Niigata earthquake, Japan, 1964. The subsoil consisted of sand having  $D_{10}$  of 0.07–0.25 mm and uniformity coefficient of 10. The buildings suffered on spread footings and piles. While 64% of buildings on spread footings suffered medium to heavy damage, 55% of the

buildings on piles also reported similar damage. Apparently, the piles had little effect in reducing damage by the earthquake. Figure 13.15 shows a correlation of damage to the standard penetration resistance of the soil at the base of the foundation or the pile tip. When the sand underlying the footings had  $N < 15$ , the buildings suffered heavy damage but for  $N$  values between 20–25 the damage was less. Similar data were obtained for buildings supported on piles. Heavy damage occurred when the  $N$  value at the pile tip was less than 15.

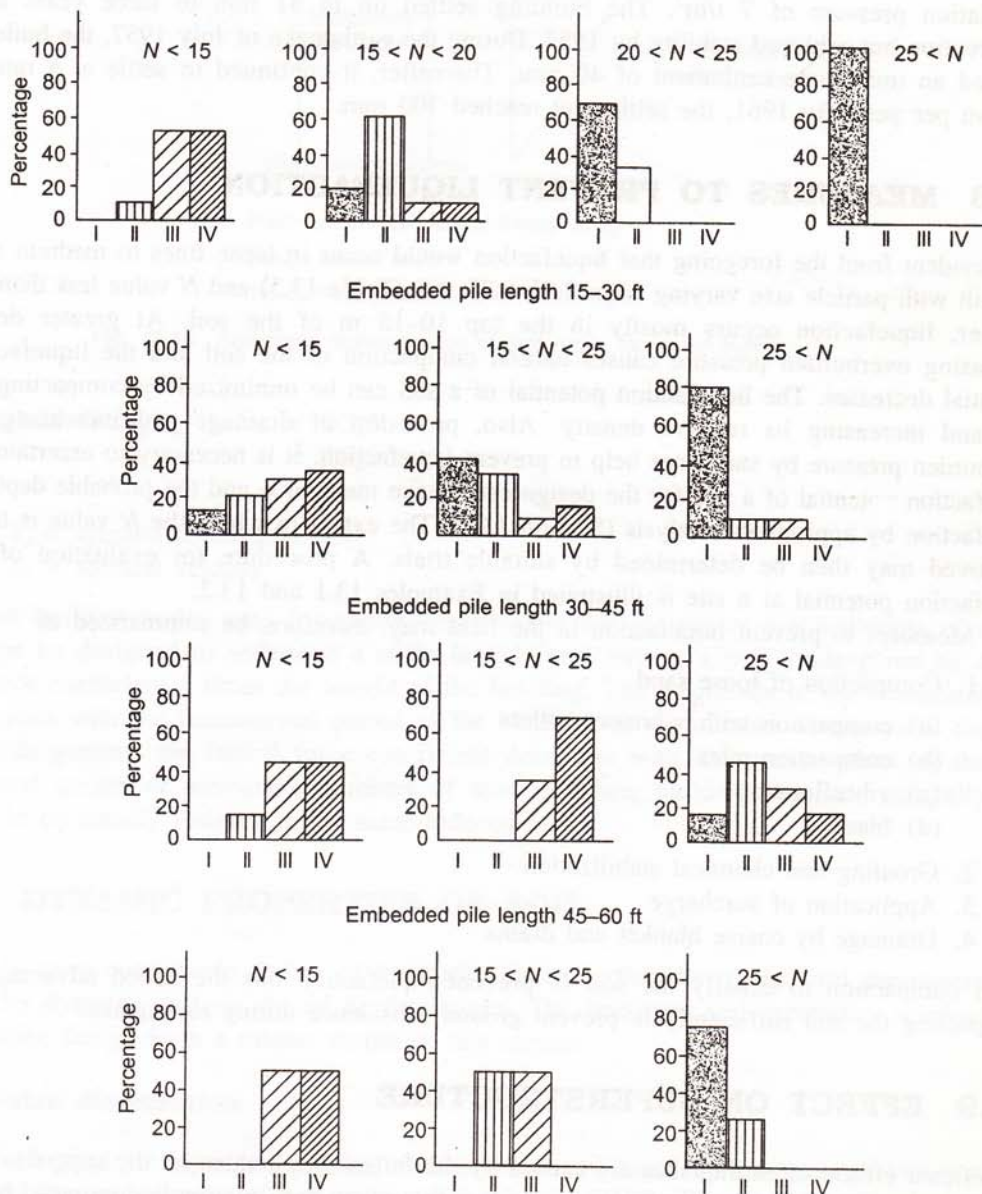


Fig. 13.15 Building damages due to liquefaction (Kishida, 1965).

For  $N > 25$ , the damage to the buildings was less. Similar data have been reported for building damages in Alaska earthquake (Ross et al., 1969) and Jaltipan earthquake (Marsal, 1961). The field data clearly indicate that liquefaction has generally occurred in cohesionless soil with 10% size varying 0.01 to 0.25 mm with uniformly coefficient of 2–10. Also, such sand having  $N < 15$  appears most vulnerable to liquefaction. Zeevaert (1989) describes a case history of foundation settlement of a raft foundation in Mexico City. The building was constructed in 1952 on a buoyancy raft foundation 6.5 m below ground surface with a net foundation pressure of  $7 \text{ t/m}^2$ . The building settled up to 51 mm in three years after construction but achieved stability by 1957. During the earthquake of July 1957, the building showed an immediate settlement of 40 mm. Thereafter, it continued to settle at a rate of 30 mm per year. By 1961, the settlement reached 700 mm.

### **13.8 MEASURES TO PREVENT LIQUEFACTION**

It is evident from the foregoing that liquefaction would occur in loose fines to medium sand and silt with particle size varying from 0.01–0.25 mm (Table 13.5) and  $N$  value less than 15. Further, liquefaction occurs mostly in the top 10–15 m of the soil. At greater depth, increasing overburden pressure causes natural compaction of the soil and the liquefaction potential decreases. The liquefaction potential of a soil can be minimized by compacting the soil and increasing its relative density. Also, provision of drainage and increasing the overburden pressure by surcharge help to prevent liquefaction. It is necessary to ascertain the liquefaction potential of a site for the design earthquake magnitude and the probable depth of liquefaction by appropriate analysis (Section 13.4). The extent to which the  $N$  value is to be improved may then be determined by suitable trials. A procedure for evaluation of the liquefaction potential at a site is illustrated in Examples 13.1 and 13.2.

Measures to prevent liquefaction in the field may, therefore, be summarized as

1. Compaction of loose sand
  - (a) compaction with vibratory rollers
  - (b) compaction piles
  - (c) vibroflotation
  - (d) blasting
2. Grouting and chemical stabilization
3. Application of surcharge
4. Drainage by coarse blanket and drains

Field compaction to densify the soil to prevent liquefaction has the added advantage of compacting the soil sufficiently to prevent ground subsidence during earthquake.

### **13.9 EFFECT ON SUPERSTRUCTURE**

Significant effects of earthquakes are caused by the forces they induce on the superstructure. If it is considered that the response of a structure to a given base motion is dominated by the influence of the first mode then the maximum lateral forces on a structure would have the

approximate distribution, as shown in Fig. 13.16, decreasing from a maximum at the top and zero at the base. The potential damaging effect of a base motion may be considered to be proportional to the product of the force developed and the period for which it acts, that is,

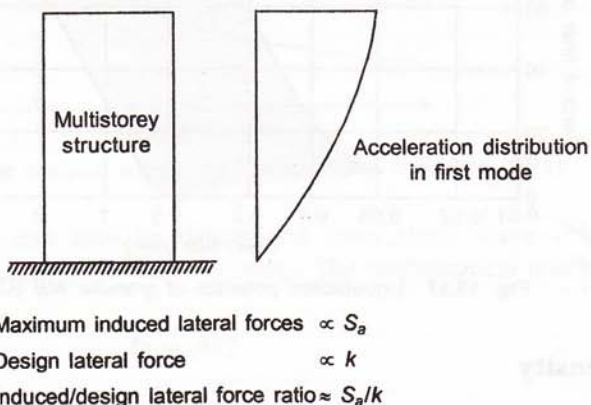


Fig. 13.16 Schematic representation of first mode forces on building.

$$\begin{aligned}\text{Potential damaging factor} &\propto WS_a T \\ &\propto WS_v\end{aligned}$$

where,

$S_a$  = spectral acceleration and

$S_v$  = spectral velocity.

Most building codes used for earthquake-resistant design require that buildings of a given type be designed to withstand a static lateral force having a magnitude given by a lateral force coefficient  $k$  times the weight of the building. The magnitude of the coefficient usually varies with the fundamental period of the building, or the number of storeys in the building. In general, the lateral force coefficient decreases with increasing values of the fundamental period or increasing numbers of storeys. Thus, buildings are not generally designed to be equally resistant to the same induced forces.

## 13.10 DYNAMIC PROPERTIES OF SOIL

In order to carry out seismic design of foundation in an earthquake region, soil parameters required for dynamic analysis should be determined. The important soil parameters relevant to earthquake design form a subject matter of this section.

### Particle-size distribution

Figure 13.17 gives the liquefaction potential of granular soil based on grain-size distribution as obtained from experiences of past earthquakes (Oshaki, 1970). The grain-size distribution of the soil may be determined by standard tests.

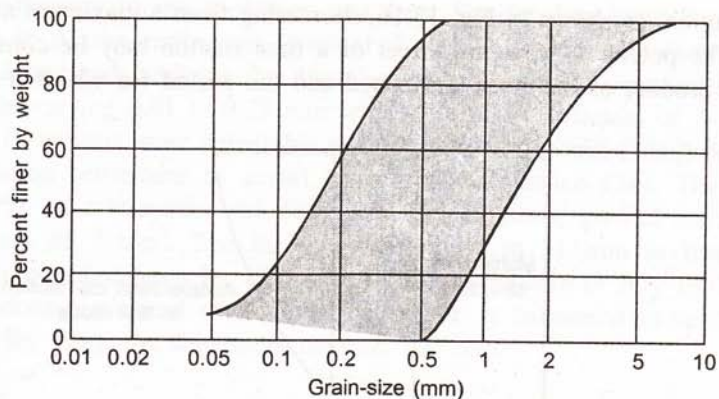


Fig. 13.17 Liquefaction potential of granular soil (Oshaki, 1970).

### Relative density

The relative density of granular soil expresses the degree of compaction and is given by the expression

$$D_r = \frac{e_{\max} - e}{e_{\max} - e_{\min}} \quad (13.7)$$

$$= \frac{\gamma_{\max}(\gamma - \gamma_{\min})}{\gamma(\gamma_{\max} - \gamma_{\min})} \quad (13.8)$$

where,

$e_{\max}$ ,  $e_{\min}$  = maximum and minimum void ratios,

$\gamma_{\max}$ ,  $\gamma_{\min}$  = maximum and minimum unit weights of soil

$e$  = in-situ void ratio, and

$\gamma$  = in-situ unit weight.

The maximum and minimum void ratio of the soil may be determined in the laboratory with the relative density apparatus and the in-situ density from field density tests.

### Shear modulus

The shear modulus  $G$  of the soil is determined from the modulus of elasticity obtained from triaxial tests as

$$G = \frac{E}{1 + v} \quad (13.9)$$

where,  $v$  = Poisson's ratio.

The shear modulus can also be determined from cyclic triaxial tests. The test gives the cyclic stress-strain relationship of the soil and the shear modulus is determined for the appropriate stress level. Normally two-thirds of the modulus measured at maximum strain is used for earthquake design. Typical relationship between shear modulus and shear strain is given in Fig. 13.18. During earthquake, the developed shear stress may range from  $10^{-3}$ - $10^{-1}\%$ .

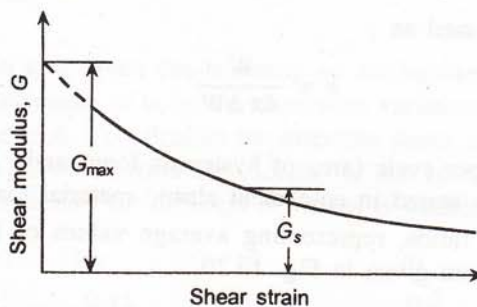


Fig. 13.18 Shear modulus versus shear strain (Seed and Idriss, 1971).

In the field, shear modulus can also be determined from shear wave velocity test by charging an explosive and measuring the wave velocity. The mathematical relationship is then given by

$$G = \rho V_s^2 \quad (13.10)$$

where,

$\rho$  = density of soil and

$V_s$  = shear wave velocity.

### Damping factor

Two different damping phenomena are related to soils—material damping and radiation damping. Material damping takes place when any vibration wave travels through the soil. It is related to the loss of vibration energy resulting from hysteresis in the soil. Damping is generally expressed as a fraction of critical damping and thus, referred to as damping ratio. Figure 13.19 is a graphical representation of calculation of the damping ratio.

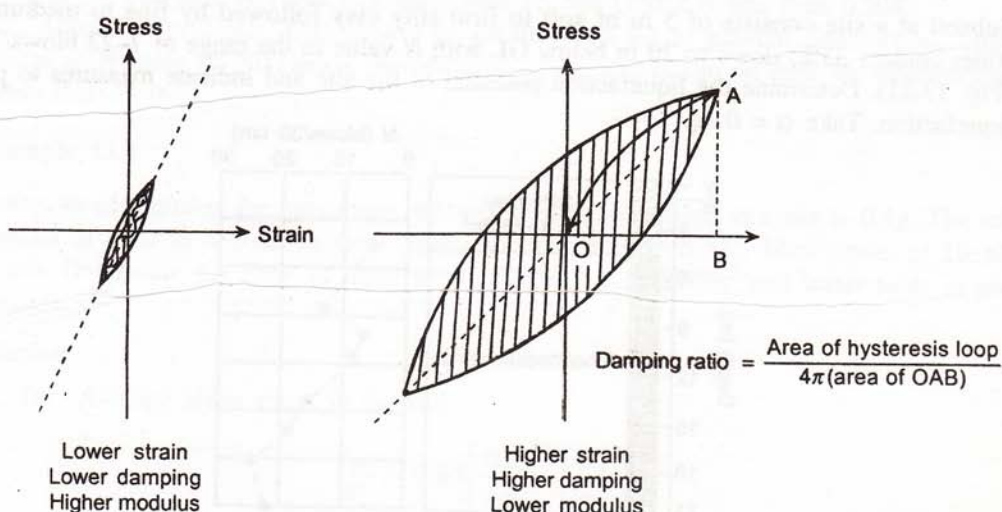


Fig. 13.19 Calculating damping ratio (Seed and Idriss, 1970).

The damping ratio is expressed as

$$\varepsilon = \frac{W}{4\pi \Delta W}$$

where,

$W$  = energy loss per cycle (area of hysteresis loop) and

$\Delta W$  = strain energy stored in equivalent elastic material (area OAB in Fig. 13.19).

Typical material damping ratios, representing average values of laboratory test results on sands and saturated clays, are given in Fig. 13.20.

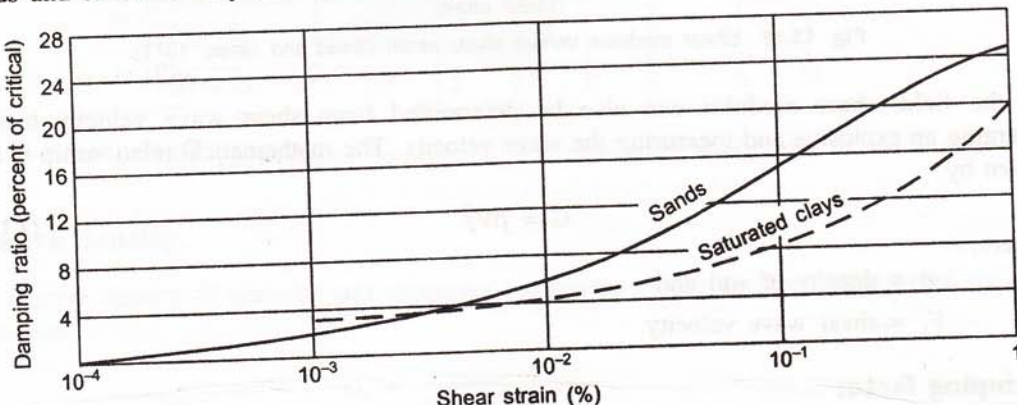


Fig. 13.20 Material damping ratio (Seed and Idriss, 1970).

Radiation damping is a measure of the loss of energy through radiation of vibration waves from the source. It is related to the geometrical properties of the foundation. This is generally used for design of machine foundations.

### Example 13.1

Subsoil at a site consists of 5 m of soft to firm silty clay followed by fine to medium sand (fines content 35%) down to 20 m below GL with  $N$  value in the range of 7–22 blows/30 cm, (Fig. 13.21). Determine the liquefaction potential of the site and indicate measures to prevent liquefaction. Take  $\alpha = 0.2g$ .

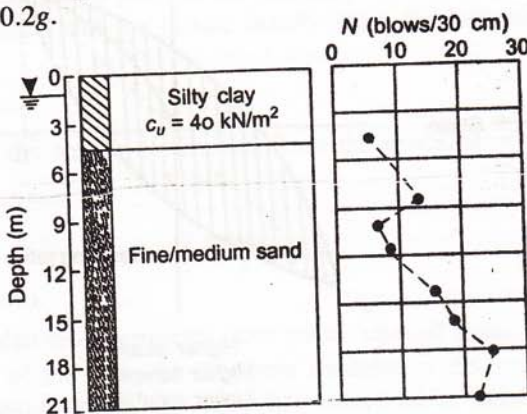


Fig. 13.21 Subsoil condition.

Liquefaction analysis may be done using the procedure of Seed et al. (1989).

Table 13.7 Calculation of cyclic stress ratio

Depth (m)	$\alpha_{\max}/g$	$\sigma_o$ (kN/m <sup>2</sup> )	$\sigma'_o$ (kN/m <sup>2</sup> )	$r_d$	$\tau/\sigma'_o$
3	0.1	54	24	0.98	0.143
6	—	108	48	0.96	0.140
9	—	162	72	0.94	0.137
12	—	216	95	0.85	0.124
15	—	270	120	0.74	0.108
18	—	324	144	0.64	0.094
21	—	378	168	0.60	0.088

(b) Shear stress ratio causing liquefaction (see Fig. 13.10)

For  $N = 10$  and 15% fines

$$\frac{\tau_{av}}{\sigma'_o} = 0.15$$

with  $FS = 1.2$

$$\left( \frac{\tau_{av}}{\sigma'_o} \right)_{all} = \frac{0.15}{1.2} = 0.124$$

The data are plotted in Fig. 13.22. It is seen that liquefaction potential exists in the top 12 m of the deposit.

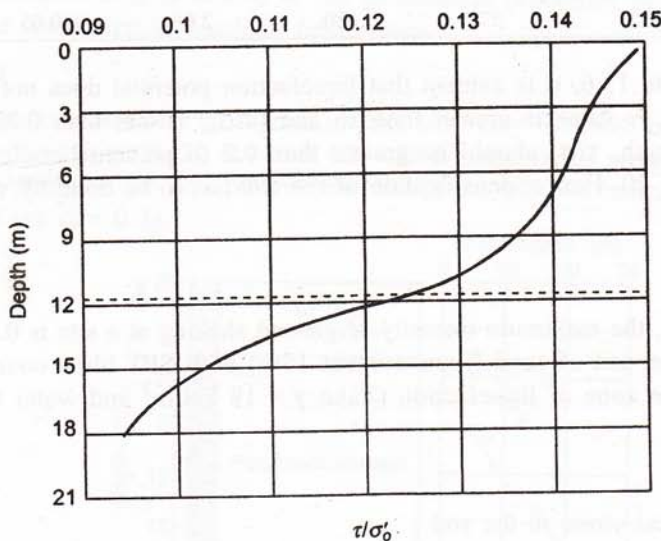


Fig. 13.22 Zone of liquefaction.

**REFERENCES**

- Ambreseys, N. and S.K. Sarma (1969), *Liquefaction of Soils induced by Earthquakes*, Bulletin of the Seismological Society of America, Vol. 59, No. 2, pp. 651–664.
- Byrne, P.M. (1976), An Evaluation of the Liquefaction Potential of the Frazer Delta, *Canadian Geotechnical Journal*, **15**, No. 1, pp. 32–46.
- Grantz, A., G. Flafker, and R. Kachedoorian, (1964),—*Alaska's Good Friday Earthquake*, March 27, 1964, Geological Survey, US Dept. of Interior. Circular 491, Washington, DC
- IS 1893 (1983), *Code of Practice for Design of Earthquake Resistant Structures*, Bureau of Indian Standards, New Delhi.
- Ishihara, K. and S. Yasuda (1980), *Cyclic Strengths of Undisturbed Cohesive Soils of Western Tokyo*, Int. Symp. on Soils under Cyclic and Transient Loading Swansea, A.A. Balkema, pp. 57–66.
- Kishida, H. (1969), Damage of Reinforced Concrete Buildings in Niigata City with special reference to Foundation Engineering, *Soil and Foundation Engineering*, **6**, No. 1, Tokyo, Japan.
- Marsal, R.J. (1961), *Behaviour of a Sandy Uniform Soil during the Jaltipan Earthquake*, Mexico, Proceedings Fifth International Conference on Soil Mechanics and Foundation Engineering, Paris, France.
- Matsui, T., H. Ohara, and T. Ito (1980), Cyclic Stress–Strain History and Shear Characteristics of Clay, *Journal of the Geotechnical Engineering Division*, ASCE, **106**, No. 10, pp. 1011–1020.
- Newmann, N.M. (1965), Earthquake Effects on Dams and Embankments, *Geotechnique*, Vol. 15, No. 2, pp. 139–160.
- Ohsaki, Yorihiko (1966), Niigata Earthquake 1964—Building Damage and Soil Condition, *Soils and Foundations*, VI, No. 2, pp. 14–37.
- Oshaki, Y. (1970), Effects of Sand Compaction on Liquefaction during the Tokachioki Earthquake, *Soils and Foundations*, Vol. 10, No. 2, pp. 112–128.
- Prakash, S. (1980), *Soil Dynamics and Machine Foundation*, Sarita Prakashan, Roorkee.
- Rao, K.S. (2001), Magnitude Scales and Related Issues of Earthquakes, *IGS News*, Vol. 33, No. 3–4, Indian Geotechnical Society, New Delhi.
- Richter, C.F. (1958), *Elementary Seismology*, W.H. Freeman, San Francisco.
- Ross, G.A., H.B. Seed, and R.R. Migliaccio (1969), Bridge Foundation Behaviour in Alaska Earthquake, *Journal of the Soil Mechanics and Foundations Division*, ASCE, **95**, No. SM-4, pp. 1007–1036.
- Seed, H.B. (1968), Landslides during Earthquake due to Soil Liquefaction, *Journal of the Soil Mechanics and Foundations Division*, ASCE, **94**, No. SM-5, pp. 1053–1122.

- Seed, H.B., K. Tokimatsu, L.F. Harder and R.M. Chung (1984), *The Influence of SPT Procedures in Soil Liquefaction Resistance Evaluations*, Report No. UBC/EERC-84/15, Earthquake Engineering Research Centre, University of California, Berkeley, California.
- Seed, R.B., S.E. Dickenson, M.F. Riemer, J.D. Bray, N. Sitar, J.K. Mitchell, I.M. Idriss, R.E. Kayen, A. Kropp, L.F. Harder and M.S. Power (1989), *Preliminary Report on the Principal Geotechnical Aspects of the October 17, 1989 Loma Prieta Earthquake*, Earthquake Engineering Research Centre, Report No. UCB/EERC-90/05, University of California.
- Seed, H.B. and I.M. Idriss (1971), Simplified Procedure of Evaluating Soil Liquefaction Potential, *Journal of Soil Mechanics and Foundation Division*, ASCE, Vol. 97, No. SM 9, pp. 1249-1273.
- Seed, H.B. and I.M. Idriss (1982), *Ground Motions and Soil Liquefaction during Earthquakes*, Monograph Series, Earthquake Engineering Research Institute, Berkeley, California.
- Seed, H.B. and M.L. Silver (1972), Settlement of Dry Sands during Earthquakes, *Journal of the Soil Mechanics and Foundations Division*, ASCE, 98, No. SM-4, pp. 381-397.
- Seed, H.B. and K. Tokimatsu (1987), Evaluation of Settlements in Sands due to Earthquake Shaking, *Journal of Geotechnical Engineering*, 113, No. 8, pp. 861-878.
- Thiers, R.G. and H.B. Seed (1969), *Strength and Stress-Strain Characteristics of Clays subjected to Seismic Loading Conditions*, Vibration Effects of Earthquakes on Soils and Foundations, ASTM STP 450.
- Togrol, E. and E. Guler (1984), Effect of Repeated Loading on the Strength of Clay, *Soil Dynamics and Earthquake Engineering*, 3, No. 4, pp. 184-190.
- UBC (1991), *Uniform Building Code*, USA.
- Van Eekelen, H.A.M. and D.M. Potts (1989), The Behaviour of Drammen Clay under Cyclic Loading, *Geotechnique*, 28, No. 2, pp. 173-196.
- Zeevaert, L. (1989), Foundation Problems in Earthquake Region, Chapter 17 of *Foundation Engineering Handbook*, Ed. H.Y. Fang, CBS Publishers, New Delhi.



# Construction Problems

## 14.1 INTRODUCTION

Foundation design is made on the basis of available knowledge about the structure to be built and the subsoil condition available at the given site. The structural design is done in a way to suit the facilities to be created for a given architectural layout. In general, the loads that are imposed on the soil can be evaluated fairly accurately. Foundation design requires evaluation of the safe bearing capacity and settlement, both immediate and long term. These factors require knowledge of the subsoil characteristics which are determined from an appropriate site investigation. However, soil being deposited at a site by natural geological processes over long periods of time, there are inherent variations which may not be fully reflected by even an elaborate subsoil investigation. Hence, simplifying assumptions are made about boundary conditions and average soil properties are to be assigned to the different strata for working out the detailed design. Also, the land use pattern of the area surrounding the site determines the vulnerability of existing buildings. Different degrees of precaution are to be taken to implement a given design without causing any distress to adjoining structures. The job of the foundation engineer does not, therefore, end at producing a design only. It is equally important to determine if any problems are to be anticipated during construction and work out proper construction procedure and remedial measures in time.

The construction problems vary widely and are often site specific. However, some general problems associated with foundation construction are discussed in this chapter.

## 14.2 COMMON CONSTRUCTION PROBLEMS

When a foundation design has been finalized, the job is given to a construction agency for doing the construction. Inevitably the work requires excavation of varying depth and magnitude. The problems multiply when excavation is to be made below the ground water table. The major construction problems, therefore, arise as a result of

1. stability of excavations,
2. dewatering, and
3. effect of adjoining structures.

### 14.3 STABILITY OF EXCAVATION

Excavation is done manually or by mechanical scrapers depending on the magnitude of earth work involved. Manual expansion is mostly adopted for foundation construction. Use of mechanical scrapers gives faster progress but they are not suitable for excavations in small areas since the ramp roads needed for the scrapers to move in and out of the cut need space. Mechanical scrapers are best suited to large area of shallow excavation.

Depending on the availability of space surrounding a construction site, an excavation with side slopes or braced cuts may be adopted. Sloped excavation only involves earth work for a stable slope designed from appropriate slope stability analysis. Figure 14.1 depicts excavation with side slopes. But a stable slope needs sufficient free space in the vicinity of the construction area. In particular, if there are existing buildings close to the area, excavation with side slopes does not become feasible. Therefore, in build up areas, braced cut is adopted.

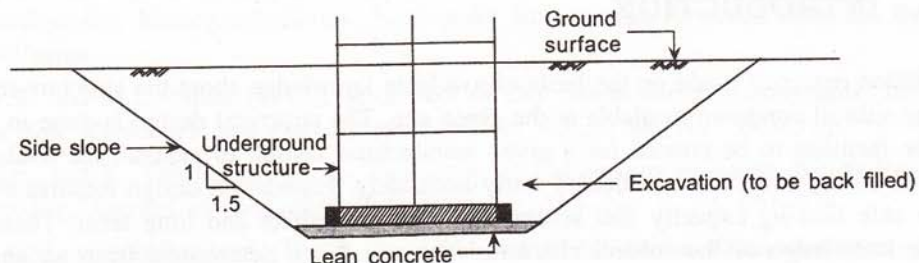


Fig. 14.1 Excavation with side slopes.

Braced cuts essentially consist of making vertical walls in the soil and suitably propping them by steel struts as the excavation is done. When the final excavation level is reached, the foundation is cast and backfilling done to restore the original ground surface as the struts are progressively removed, as presented in Fig. 14.2.

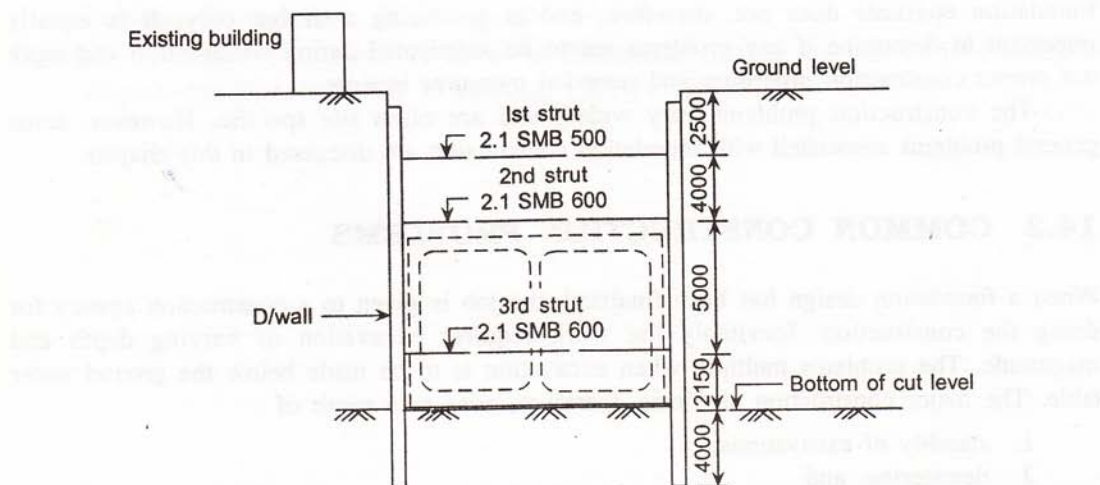


Fig. 14.2 Braced cut.

For shallow footings and raft foundations, the depth of excavation seldom exceeds 2 m and elaborate support is not required. However, if heterogeneous fill exists near the ground surface, side protection with timber planks and small struts should be sufficient.

Deep excavation for two or three basements (excavation depth: 6–10 m) would require adequate lateral support with diaphragm walls or contiguous bored piles and struts. Because of large excavation width, it may not be feasible to have horizontal struts which would tend to deflect under their own weight. In such cases, inclined props supported between the diaphragm wall and the already cast base raft at the centre may be adopted. Otherwise, a number of H-piles may be driven at close intervals and the struts be made to span among them to reduce the effective length. Figure 14.3 depicts inclined props to support diaphragm wall and Fig. 14.4 shows struts in wide cuts.

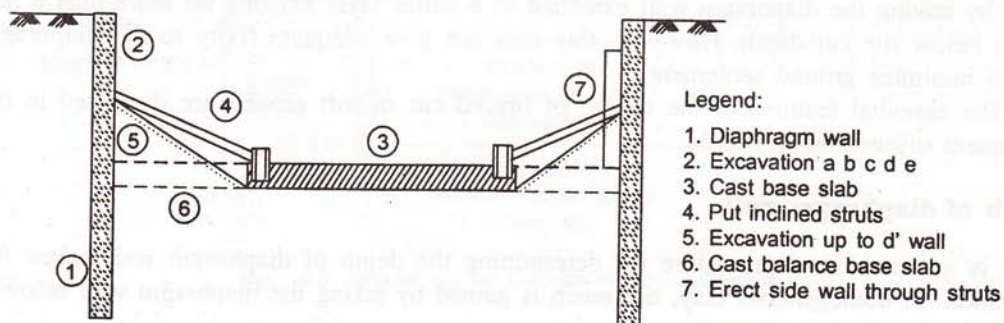


Fig. 14.3 Inclined props to support diaphragm wall.

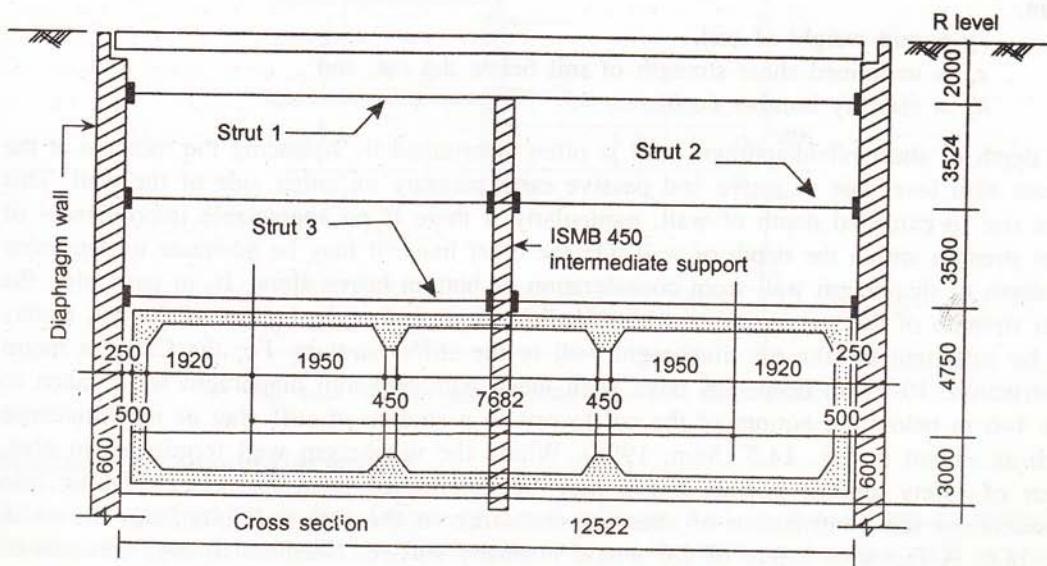


Fig. 14.4 Struts in wide cuts.

### 14.3.1 Design of Braced Cuts

The design of braced excavation involves two distinct yet interrelated features, namely

- stability of the excavation, ground movement, control of water into the excavation, effect on adjoining structures, and so on and
- design of structural elements, that is, diaphragm wall or sheet pile, struts or anchors and so forth.

Although the overall stability of braced cuts in soft ground does not depend to any great extent on the number and spacing of struts or anchors, they very much influence the pattern of ground movement expected in a given situation. The depth of diaphragm wall/ sheet pile determines both the stability of the system and the ground movement associated with it. Depending on the subsoil stratification, one may get adequate stability against bottom heave by having the diaphragm wall extended to a stiffer layer existing no more than a few metres below the cut depth. However, this may not give adequate fixity to the diaphragm wall to minimize ground settlement.

The essential features of the design of braced cut in soft ground are discussed in the subsequent subsections in details.

#### Depth of diaphragm wall

There is no established procedure for determining the depth of diaphragm wall below the excavation. In homogeneous clay, not much is gained by taking the diaphragm wall below a critical depth, which is given by

$$N_c = \frac{\gamma H}{c_u} \quad (14.1)$$

where,

$\gamma$  = unit weight of soil,

$c_u$  = undrained shear strength of soil below the cut, and

$N_c$  = stability number ( $\approx 6$ ).

The depth of sheet pile/diaphragm wall is often determined by balancing the moment at the bottom strut level due to active and passive earth pressure on either side of the wall. This gives rise to extended depth of wall, particularly if there is no appreciable improvement of shear strength within the depth of wall. On the other hand, it may be adequate to determine the depth of diaphragm wall from consideration of bottom heave alone. If, in particular, the shear strength of the soil improves within shallow depth below the bottom of the cut, it may just be sufficient to take the diaphragm wall to the stiffer stratum. For the Calcutta metro construction, 10–14 m deep cuts have been made with 600 mm diaphragm walls taken to only 4–6 m below the bottom of the cut to rest in a stratum of stiff clay or medium/dense sand, as shown in Fig. 14.5 (Som, 1998). Where the diaphragm wall terminates in clay, factor of safety against bottom heave may be determined from Eq. (14.2), taking into consideration the contribution of shearing resistance at the soil–wall interface, shown in Fig. 14.6. A factor of safety of 2.0 would normally suffice. Needless to say, presence of struts, whatever the number, does not contribute to safety against bottom heave.

$$F = \frac{c_{u4}N_c + \gamma_3 D_2 + \gamma_4 D_f + \sum c_u(H + D_2 + D_f)/D_1}{\sum \gamma(H + D_2 + D_f)} \quad (14.2)$$

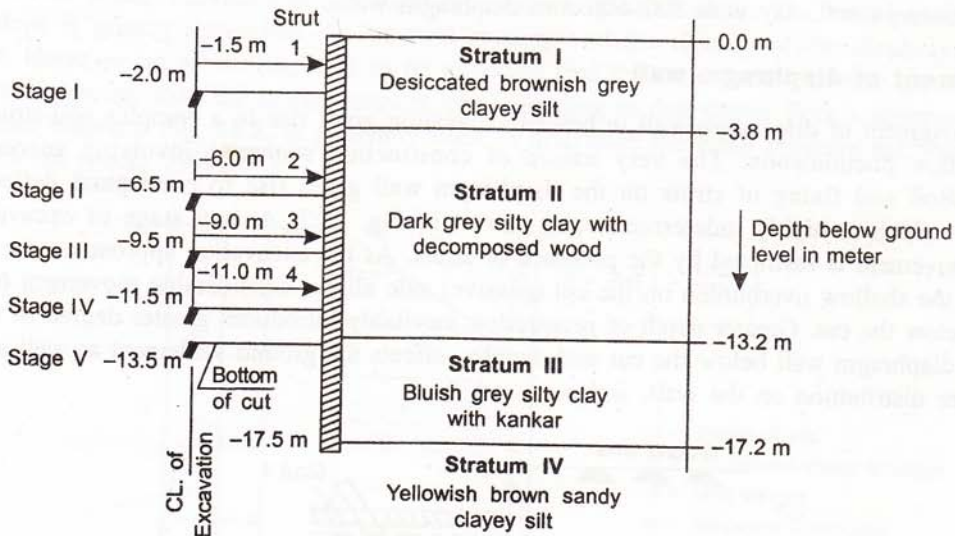


Fig. 14.5 Braced cut for Calcutta metro construction.

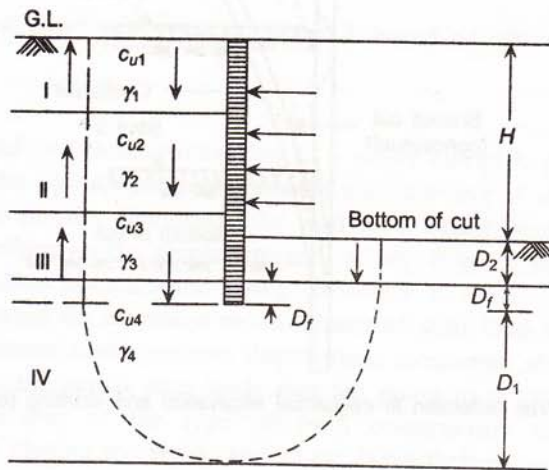


Fig. 14.6 Stability against bottom heave in stratified soil.

### Number and spacing of struts

Struts are required to prevent failure of the diaphragm wall in flexure and to minimize lateral deflection of the wall. The diaphragm wall and the struts make up a rigid structural system which prevent excessive ground movement. Obviously, greater the number of struts,

better is the rigidity of the system. On the other hand, too many struts create obstruction to the construction work. In general, a spacing of 3–4 m between struts may be adopted. Field measurements indicate that the settlement increases rapidly for unsupported cut depth of more than 4 m. Available case histories also suggest an optimum strut spacing of 3–4 m for deep excavations in soft clay with 500–600 mm diaphragm walls.

### Movement of diaphragm wall

The movement of diaphragm wall in braced excavation gives rise to a complex soil-structure interaction phenomenon. The very nature of construction sequence involving successive excavation and fixing of struts on the diaphragm wall gives rise to conceptual deflection pattern which is highly indeterminate, as shown in Fig. 14.7. At any stage of excavation, wall movement is restricted by the presence of struts. As the excavation approaches the final depth, the shallow overburden on the cut (passive) side allows considerable movement of the wall below the cut. Greater depth of penetration inevitably introduces greater degree of fixity in the diaphragm wall below the cut and thereby, affects the ground settlement as well as the pressure distribution on the wall.

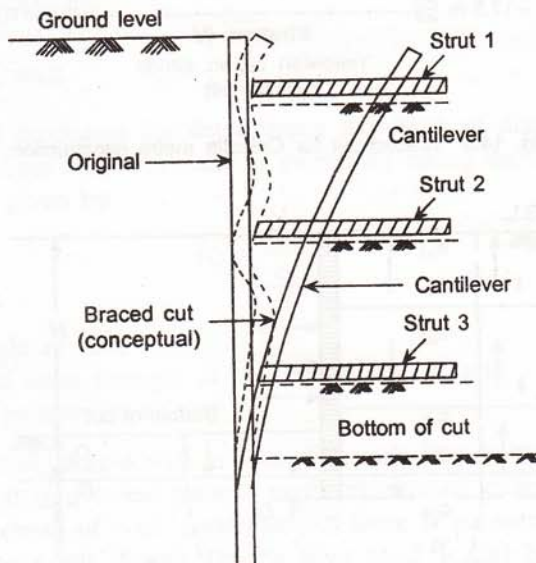


Fig. 14.7 Wall deflection in sequential excavation and strutting (conceptual).

### Earth pressure

One of the most complex aspects of the behaviour of braced cuts in cohesive soil is the distribution of earth pressure on the diaphragm wall. This has important effect on the structural design of both the diaphragm wall and the struts. Obviously, the distribution of earth pressure on either side of the diaphragm wall corresponds to the  $K_o$ -stresses before the excavation commences (Som and Raju, 1989). The first stage of excavation allows the diaphragm wall to move freely as a cantilever although the rigidity of the wall may not

allow the earth pressure to come down to the active value by the time the first strut is placed—normally, 2–3 m below ground level. Thereafter, the movement of diaphragm wall is restricted by the presence of the strut and stress concentration occurs in the vicinity of the strut as excavation is done below. Similar phenomenon occurs at the second and subsequent strut levels when excavation is continued below the respective struts. The earth pressure that develops is greatly dependent on the strut spacing and the rigidity of the diaphragm wall itself. However, at all stages, it is to be expected that the total earth pressure on the wall would be greater than the active pressure corresponding to that depth. Peck's apparent earth pressure diagram, Fig. 14.8, is generally used to determine the earth pressure distribution in braced cut (Peck, 1969).

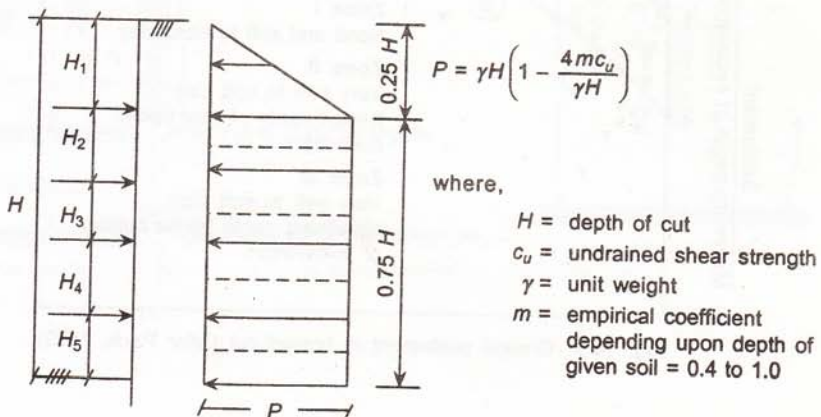


Fig. 14.8 Apparent earth pressure diagram in braced cut (after Peck, 1969).

## Strut load

Estimation of strut load in braced excavation is a rather complex problem. The strut load depends primarily on the rigidity of the diaphragm wall, spacing of struts and, of course, the soil parameters at a given site. Obviously, the strut load would be a function of the lateral earth pressure that develops on the diaphragm wall at any stage of excavation. But the latter is a highly indeterminate phenomenon being primarily a function of the interface soil structure interaction. Based on extensive measurement of strut load in the Chicago subway, Peck proposed the apparent earth pressure distribution, mentioned above, for the estimation of strut load. However, the actual strut loads that are going to develop in a given situation may only be characteristic of the type of wall, construction methodology, speed of construction, manner of placing the struts, and so on. Nevertheless, an empirical procedure as proposed by Peck still appears to be the best way of estimating the strut load for initial design (refer Fig. 14.8).

## Ground settlement

Ground settlement is the surface manifestation of the subsoil deformation in a braced cut. Both the magnitude of settlement and the zone of influence are of importance in determining whether adjacent buildings are going to be adversely affected by the construction. The

variation of ground settlement for the final cut level may be obtained from Peck's normalized plot for braced cut with sheet pile supports in different types of soil, as depicted in Fig. 14.9. Different zones of settlement proposed by Peck are shown as zones I, II, and III for different soil conditions below the cut (Peck, 1969).

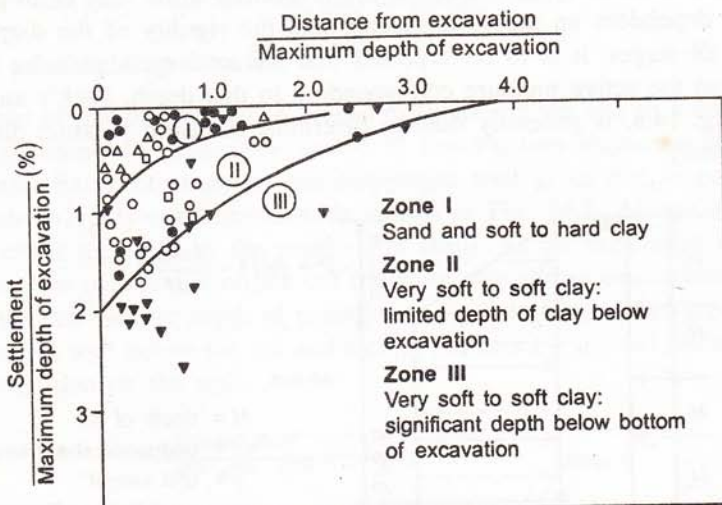


Fig. 14.9 Ground settlement in braced cut (after Peck, 1969).

## 14.4 DEWATERING

Dewatering is required for any deep excavation to facilitate construction of basements, power houses, pumping stations, and so on. Theoretically, any excavation below ground water table would necessitate some kind of dewatering. However, low permeability soils, for example, clay and silty clay ( $K < 10^{-6}$  cm/s) do not present much problem with seepage because the discharge is generally small and elaborate dewatering is not required. For medium to high degree of permeability ( $K > 10^{-5}$  cm/s), suitable dewatering scheme has to be worked out.

The basic purpose of dewatering is to control seepage into the excavation either by pumping the water out of the excavation or by lowering the water table sufficiently below the bottom of the cut till the underground works are over. The extent of dewatering depends on the subsoil stratification, presence of water bearing stratum, aquifer parameters, and in-situ permeability.

### 14.4.1 Rate of Seepage

The first requirement in a dewatering job is to estimate the rate of seepage into the excavation for a certain degree of dewatering. For this, the excavation is considered as a large circular well from which water is pumped out to affect the desired ground water lowering. For a fully or partially penetrating well, as shown in Fig. 14.10, the rate of pumping is given by the well equation.

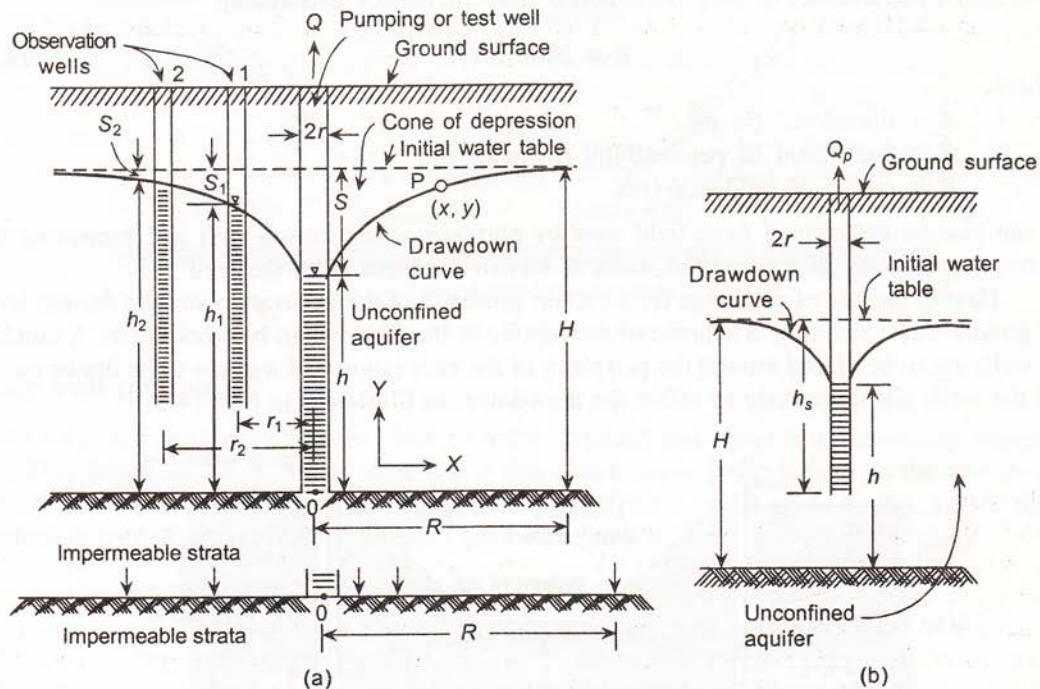


Fig. 14.10 Discharge from wells.

(a) Fully penetrating well [refer Fig. 14.10 (a)]

$$Q = \frac{\pi K (H^2 - h^2)}{\log_e(R/r)} \quad (14.3)$$

(b) Partially penetrating well [refer Fig. 14.10 (b)]

$$Q_p = Q \left[ \frac{h_s}{H} \left( 1 + 7 \sqrt{\frac{r}{2h_s}} \cos \frac{\pi h_s}{2H} \right) \right] \quad (14.4)$$

where,

 $Q$  = discharge from a fully penetrating well in an unconfined aquifer ( $\text{m}^3/\text{s}$ ), $Q_p$  = discharge from a partially penetration well in an unconfined aquifer ( $\text{m}^3/\text{s}$ ), $K$  = coefficient of permeability of soil ( $\text{m}/\text{s}$ ), $H$  = height of ground water above the top of aquifer before drawdown (m), $h$  = height of water in the well above the top of aquifer after drawdown (m), that is, drawdown =  $H - h$  (m), $r$  = radius of well or equivalent well (m), $R$  = radius of influence (m), and $h_s$  = penetrating of well below water table (m).

The radius of influence  $R$  may be obtained from Sichardt's expression

$$R = 3000 S \sqrt{K} \quad (14.5)$$

where,

$S$  = drawdown (in m),

$K$  = coefficient of permeability (in m/s), and

$R$  = radius of influence (m).

$R$  can also be determined from field tests by pumping water from a well and measuring the drawdown in a set of observation wells at known distances from the well.

Having the rate of discharge for a certain geometry of the excavation and the desired level of ground water lowering, a scheme of dewatering in the field has to be worked out. A number of wells are to be placed around the periphery of the excavation and water is to be drawn out of all the wells simultaneously to effect the drawdown, as illustrated in Fig. 14.11.

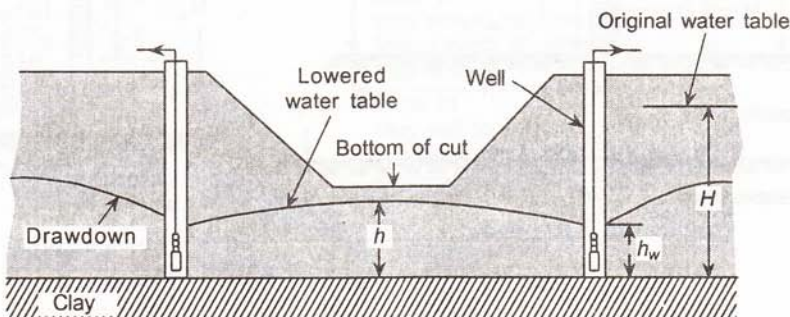


Fig. 14.11 Dewatering from an excavation.

#### 14.4.2 Methods of Dewatering

The common dewatering methods for field application are

- (a) Sump pumping
- (b) Deep well pumping
- (c) Well point dewatering

##### Sump pumping

If the soil consists of cohesive material having low permeability, shallow trenches are dug along the outer edge of the excavation to collect the water and conduct it to shallow sumps from which it is pumped out. Figure 14.12 is a schematic representation of sump pumping. This method is particularly suitable in clay and silty clay where the rate of seepage is low. Water is to be pumped out at the same rate at which seepage is occurring. The pump capacity is to be determined for the rate of discharge, the lift, and location of the discharge point.

This method is inexpensive and easy to operate. However, if ground water flows towards the excavation with high gradient, there is risk of soil loss and slope failure. The greatest depth to which water table may be lowered by this method is 5–6 m below the pump level. For greater depth, pumps are re-installed at intermediate depths.

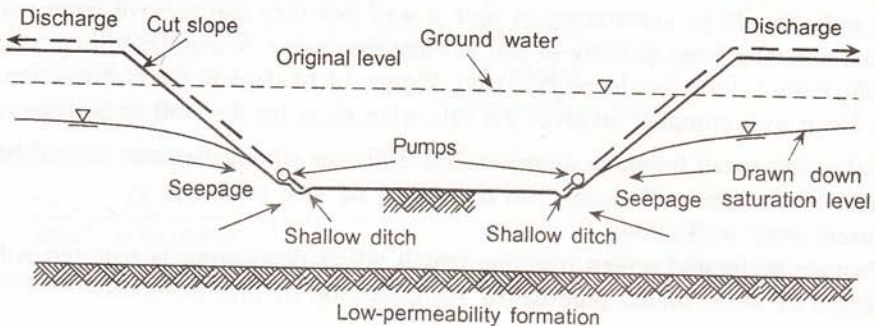


Fig. 14.12 Sump pumping.

### Deep well pumping

Deep wells are installed along the sides of the excavation and water is continuously pumped out. This brings down the water table and a drawdown curve passing through the bottom of the cut is obtained. The diagrammatic representation of the same is given in Fig. 14.13. This method is particularly suitable for highly permeable soil such as sand and silty sand.

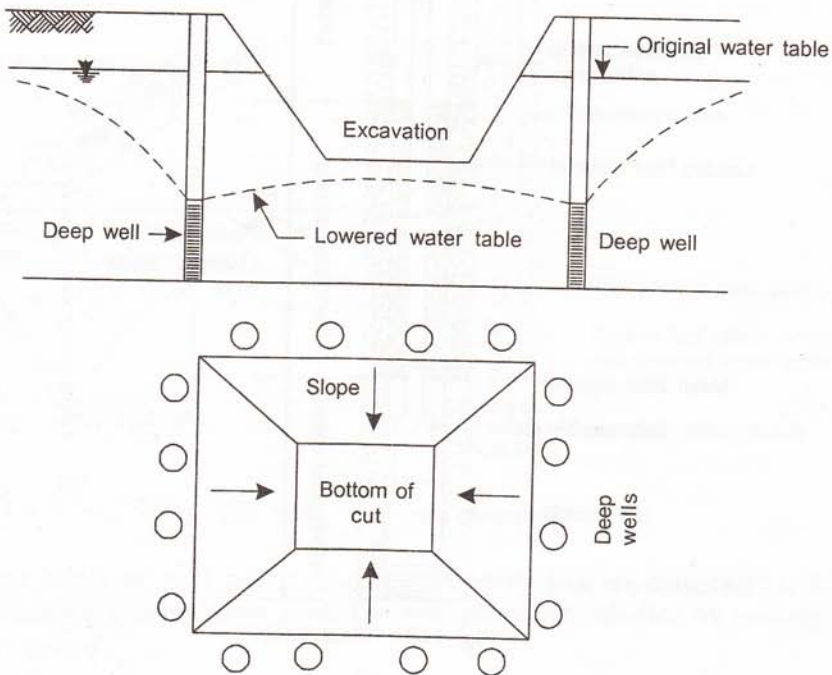


Fig. 14.13 Deep well pumping.

The method is sufficiently flexible. A group of wells is first installed and the effect of pumping is observed. If sufficient control is not achieved additional wells and pumps can be installed. Standby pumps and power supplies should be on hand in case of breakdown of equipment and drop of power supply.

Deep wells should be constructed in such a way that they can remove large volumes of water without allowing large quantity of soil to enter the casing. When the soil consists of fine sand and silt, a sand filter should be provided. Figure 14.14 depicts the construction of such deep wells. Deep well pumping involves the following steps for the well to be constructed.

- (i) Take sink cased borehole diameter 200–300 mm whose diameter should be greater than that of the well casing and depending on size of pump.
- (ii) Insert inner well casing.
- (iii) Provide perforated screen over the length where dewatering is required with 3.5 m length of unperforated pipe below for collection of fine materials.

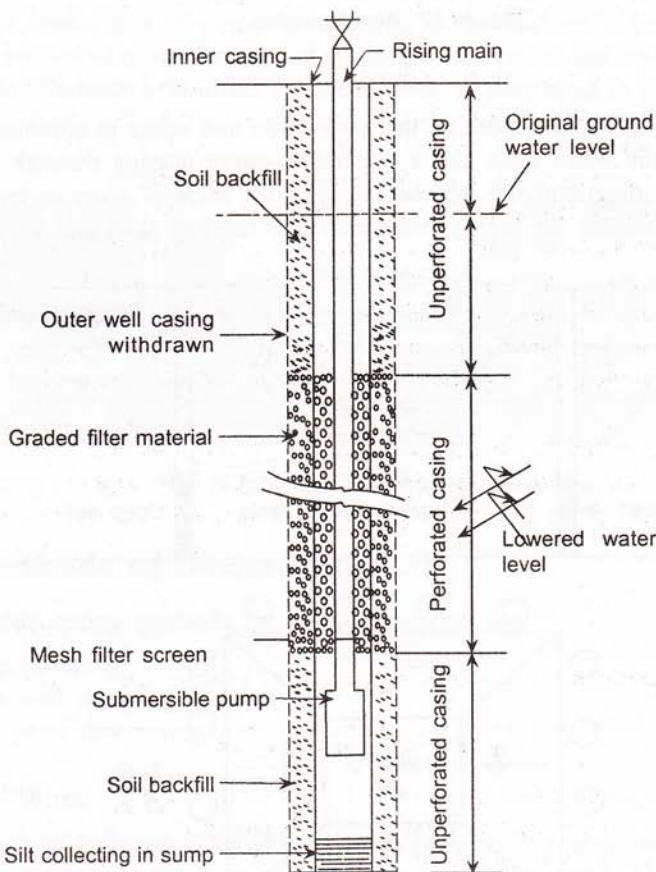


Fig. 14.14 Deep wells.

- (iv) Place graded gravel between casing and outer borehole casing over the dewatering length.
- (v) Fill the space above the screen by soil.
- (vi) Water is then ‘surged’ by a boring tool to promote flow of water back and forth through the filter and fines collected at the bottom are bailed out.
- (vii) Insert submersible pump.

The filter is designed on the conventional filter criteria suggested by Terzaghi which is

$$(a) \frac{D_{15} \text{ (of filter)}}{D_{85} \text{ (of soil)}} < 4 \quad (\text{Piping criterion})$$

$$(b) \frac{D_{15} \text{ (filter)}}{D_{15} \text{ (soil)}} > 5 \quad (\text{Permeability criterion})$$

For slotted or perforated pipes,

$$(c) \frac{D_{85} \text{ (filter)}}{\text{width or diameter of hole}} > 1$$

to prevent soil loss through the openings.

### Well point dewatering

This consists of installation of a number of well points, usually 1 m long, around the excavation. They are connected by vertical riser pipes to a header pipe on the ground which, in turn, is connected to a pump. The ground water is drawn by the pump into the header pipe through the well points and discharged there. The well points are installed at 1–1.5 m spacing, as shown in Fig. 14.15.

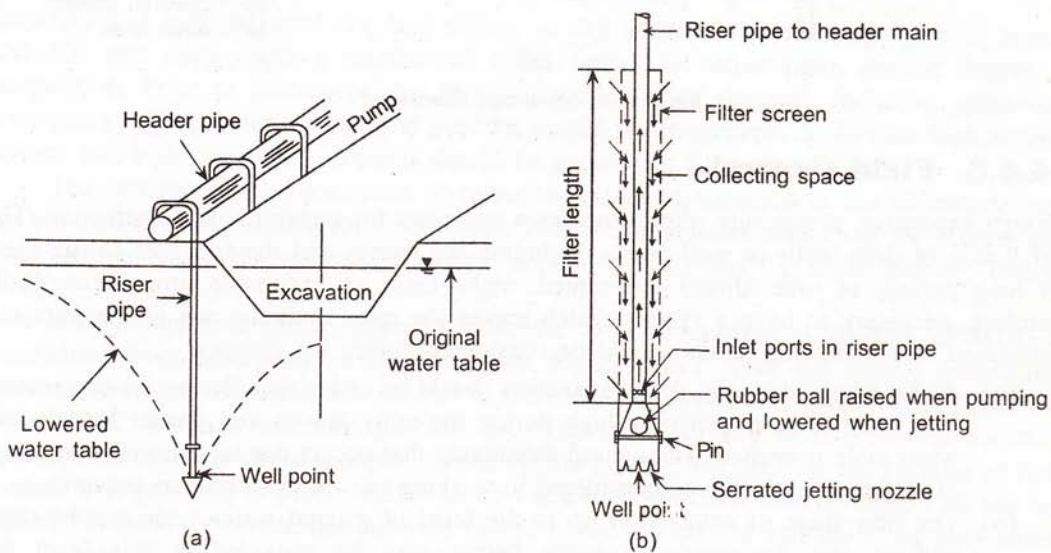


Fig. 14.15 Well point dewatering.

The filter wells or well points usually consist of a 1 m long screen, 60–75 mm diameter surrounding a central riser pipe. The well points are installed by pushing or jetting them into the ground.

Capacity of a single well point with 16 m riser pipe = 10 litres/min. (approx.)

The spacing of well points depends on the permeability of soil and the time available for affecting the drawdown. The spacings normally adopted for different soil types are as follows:

Fine to medium sand      0.75–1.0 m

Silty sand of low permeability      1.5 m

Well point dewatering is suitable in both fine and silty sands. In highly previous soil, the spacing required to handle the water may be too small and impractical. Well points are not generally suitable for clays because of slow water seepage.

Well points can lower a water table to a maximum of 6 m below the header pipe. For lowering water table to greater depth, multiple stage well point system may be adopted. Under average conditions, any number of stages can be used, each stage lowering the water table by about 5 m. A typical set-up for a two stage system is shown in Fig. 14.16. Multistage well point may be used for greater depth of dewatering but this requires additional header pipe, additional pumps, and larger excavation width for the provision of berms.

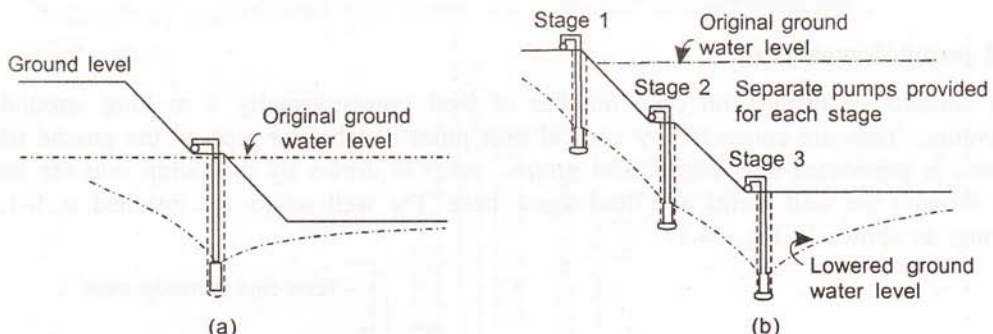


Fig. 14.16 Multistage dewatering.

#### 14.4.3 Field Control

Though expensive, dewatering often becomes a necessity for underground construction. The installation of deep wells or well points, including the pumps and the fuel cost to run them for long periods of time almost interrupted, make them an expensive proposition. It is, therefore, necessary to have a system which makes the most optimum use of the pumping installation. The following points should be considered during the process:

- As far as possible, any deep excavation should be undertaken during the dry season. The water table is generally high during the rainy season and greater lowering of water table is needed. The natural dewatering that occurs due to seasonal fluctuation of water table should be considered in working out the construction sequence.
- The first stage of excavation up to the level of ground water table can be done without any dewatering. Suitable berms may be provided at this level for installation of deep wells/well points before commencing further excavation.
- The rate of discharge obtained by using well equation gives only an indication of the rate of discharge to be expected for a given drawdown. There is no need to put all the deep wells/well points into operation right at the beginning.
- Initially a limited number of wells may be commissioned and depending on field observation, further wells may be added taking into consideration the gradual excavation process. The number of wells required for a certain depth of cut may be installed initially. Further, additions may be done as the depth of cut is increased.
- Adequate number of standby pumps should be available at site particularly when concreting is in progress so that any pump breakdown may be compensated without loss of time.

- (f) The effect of ground subsidence on adjacent structures due to dewatering should be evaluated and adequate precautions taken to prevent major damage.

## 14.5 LAND FILLING

In many construction projects, low lying areas are to be reclaimed to raise the formation level of the ground. Even in an apparently high ground, often there are ponds and depressions which had been filled up in the past. In general, except for large scale land reclamation, not much attention is given to such landfilling. All kinds of materials, including garbage and rubbish are used to fill up these areas. A few years after filling when grass has grown on the land, there is no apparent indication of filling and problems arise only during construction. Any load bearing fill should be done with care and all data pertaining to the filling, namely type of soil, method of compaction, date of filling, and so on, should be properly recorded so that the relevant data pertaining to the foundation design are available during design.

### 14.5.1 Cohesive Fill

Cohesive soil may be used for land filling in dry areas. Compaction is done in layers, 250–300 mm thick, with a number of roller passes to achieve the desired degree of compaction. Prior to placement, the physical properties of the soil, including grain-size, consistency limits, water content and the like should be determined. Soils with high organic content and high expansive potential should be avoided in filling work.

The compaction characteristics of cohesive soil are determined in the laboratory from the standard or modified Proctor Compaction Test. Representative soils from the borrow area are tested to obtain the optimum moisture content (OMC) and the maximum dry density (MDD).

Most compaction specifications provide for field compaction at 90–95% of MDD as determined from laboratory compaction tests. Figure 14.17 gives the typical compaction curve for clayey soil. Higher compaction in the modified proctor test gives higher MDD and lower OMC than the standard proctor test. The curve of dry density versus moisture condition for zero air voids is superimposed on the proctor test data for the purpose of field control. It is generally a good practice to have the field moisture content slightly on the wet side of the OMC to ensure that all void spaces of the compacted soil are filled with water.

It may be noted here that not all soils yield the same type of compaction curve as shown in Fig. 14.17. Lee and Suedkamp (1972) reported the test results of 35 samples and suggested four types compact ion curves that are shown in Fig. 14.18. They also gave some guidelines for predicting the nature of compaction curve based on the liquid limit of the soil (Table 14.1).

**Table 14.1** Type of compaction centre

Liquid limit of soil	Nature of compaction curve (Fig. 14.18)
30–70	Type I
< 30	Type II and III
> 70	Type III and IV

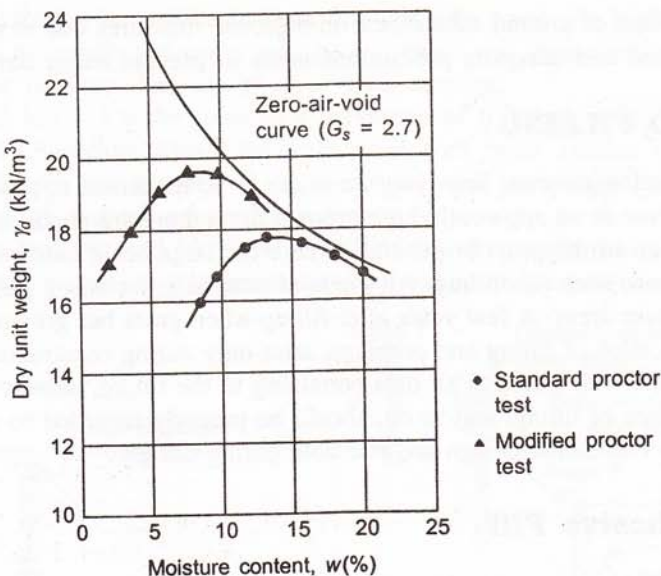


Fig. 14.17 Dry density versus moisture content relationship from Proctor test.

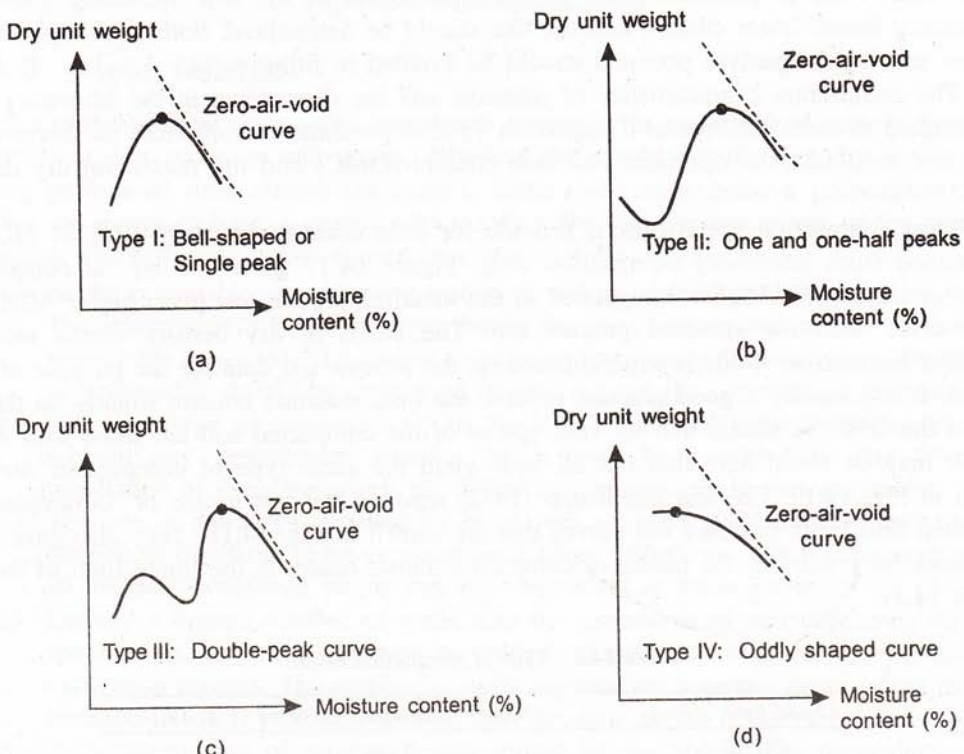


Fig. 14.18 Typical moisture density relationships of cohesive soil (after Lee and Suedkamp, 1972).

It may however be understood that irrespective of the type of compaction curve, the highest value of MDD as marked by point A should be taken for specifying the field compaction parameters in cohesive soil.

### 14.5.2 Granular Fill

Granular soil, predominantly sand, happens to be the most suitable material for land filling. Well graded sand ( $D_{60}/D_{10} > 4$ ) gives good compaction when saturated and vibrated. These give high bearing capacity and low settlement potential and sand appears to be best suited for under water filling.

The compaction of granular soil is determined by the relative density, defined as

$$R_p = \frac{e_{\max} - e}{e_{\max} - e_{\min}} \times 100\% \quad (14.6)$$

where,

$e_{\max}$  = maximum void ratio under loose condition,

$e_{\min}$  = minimum void ratio under dense condition, and

$e$  = void ratio achieved at site.

In terms of dry density, the relative density can be expressed as

$$R_p = \left( \frac{\gamma_d - (\gamma_d)_{\min}}{(\gamma_d)_{\max} - (\gamma_d)_{\min}} \right) \left( \frac{(\gamma_d)_{\max}}{\gamma_d} \right) \quad (14.7)$$

where,

$\gamma_d$  = dry density achieved in the field,

$(\gamma_d)_{\max}$  = maximum dry density as determined in the laboratory, and

$(\gamma_d)_{\min}$  = minimum dry density as determined in the laboratory.

For field compaction, a relative density of at least 80% should be specified. This can be easily achieved by placing the loose sand in 300 mm layers, flooding it with water and then compacting it with vibratory rollers to layers 250 mm thick.

Numerous buildings have suffered damages due to inadequate attention given to the ground filling in the construction area. Som and Sahu (1993) report the collapse of a 4-storey building soon after construction near Calcutta. The building was supported on a central raft with two-way interconnected strip placed 5.3 m below the ground which had indicated a bowl-shaped profile sloping across the building. A differential excavation was made to locate the foundation below the lowest point. Subsequent filling on the foundation put an overburden pressure of varying magnitude across the building area. This caused a non-uniform foundation pressure varying from  $16 \text{ t/m}^2$  on western side to  $11 \text{ t/m}^2$  on the eastern side of the foundation, as shown in Fig. 14.19. The factor of safety against bearing capacity failure was only 1.5. This is believed to have led to significant yielding of the soil and the building tilted towards the western face due to heavier stress concentration. Subsequent consolidation settlement (the building collapsed almost 3 years after start of construction) appears to have led to further tilting of the building and an estimated angular distortion of 1/86 occurred towards the western side as against a permissible angular distortion of 1/300 for

conventional RCC framed structures. Analysis of the building frame and the nondestructive tests on concrete had shown that the beams and columns were not adequately designed to withstand the additional stresses due to excessive angular distortion. The failure of individual structural members, one by one, appears to have led to the ultimate collapse of the building.

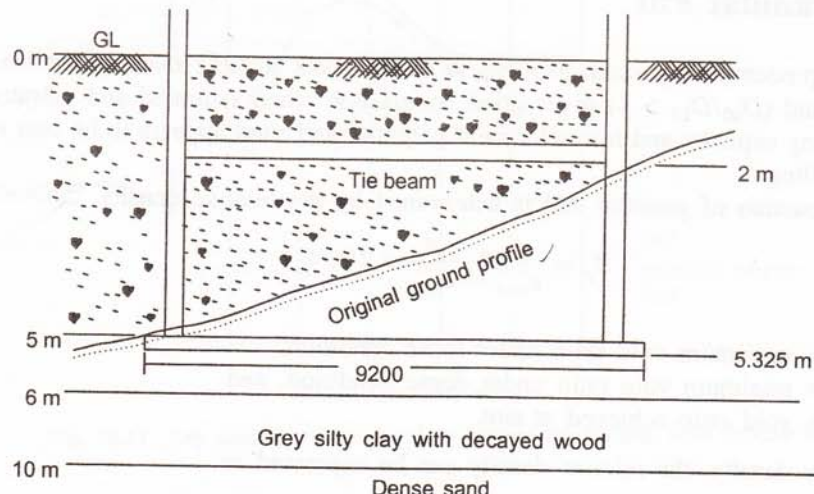


Fig. 14.19 Foundation on differential filling (Som and Sahu, 1993).

Som (2000) reported the severe tilt in a 4-storey residential building built on filled up soil. The subsoil consisted of 2 m top soil followed by 3 m of rice mill waste which was used to fill up the low lying ditches in the area. No soil tests were done before construction. The building was provided with RCC raft foundation with a net bearing pressure of  $50 \text{ kN/m}^2$ , as shown in Fig. 14.20.

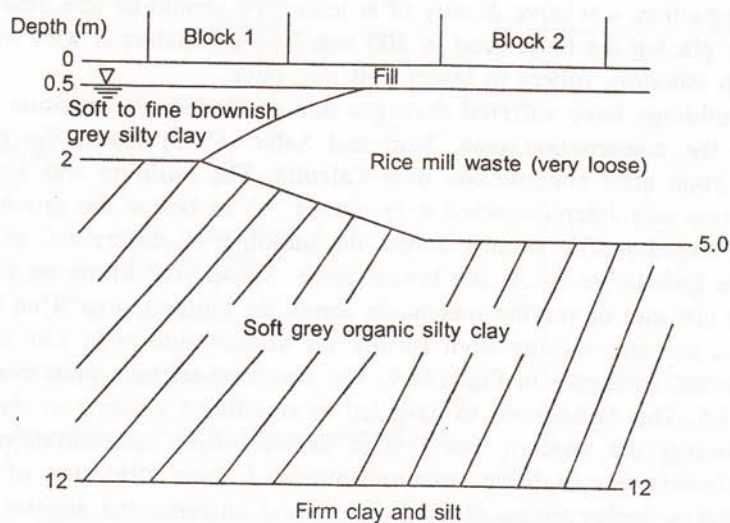


Fig. 14.20 Building tilt on filled up soil.

The building started to tilt soon after construction and in spite of cement grouting in the surrounding area, it went on to tilt by as much as 800 mm within one year after construction due to the compression of the fill. Subsequently, counterbalancing weight on the heaved up portion and removal of soil from underneath by pumping water through perforated pipes inserted below the building gradually brought the building back to verticality, although the ground floor ended up 800 mm below the surrounding ground.

Major land reclamation is done in submerged ground or even on the sea bed by sand filling. Sand compacts well under water and provides good foundation bed for structures to be built subsequently. Salt Lake City near Calcutta was reclaimed in the early sixties by pumping dredged silty sand from the river Hooghly on soft clay 2–3 m depth of sand was sedimented on the low lying land to raise the ground surface and also to provide good foundation for one or two storeyed residential buildings (refer Fig. 14.19). In recent years, Kansai international airport in Osaka, Japan has been built on an airport island created on the sea bed by reclamation with 150 million cu m of sand fill (Soda, 2001). The sea bed soil consists of 20 m thick alluvial clay with further depth of alluvial clay and sand, gravel extending to several hundred metres below the sea bed, the depth of reclaimed soil being 30 m. Sand drains were installed in the sea bed prior to land filling to force the compressible clay to undergo consolidation during the reclamation itself. A pilot construction area was set up before the full scale reclamation. Settlement studies were made to evaluate the settlement potential of the reclaimed ground. Such observational method helped to build and monitor the foundations of the airport structures.

## 14.6 EFFECT ON ADJOINING STRUCTURES

Underground construction at any location affects surrounding areas by way of ground movement, vibration and the like. Every construction has a zone of influence and facilities existing without this zone are liable to get affected. Whether these will be any damage to a building will depend on the severity of such influence and the condition of the building.

Excavation during construction may cause damage to existing structures due to the effects of ground movement in the vicinity of the excavation. It is to be remembered that an existing building has, in all probability, undergone settlement under its own weight and has probably reached the limit of permissible settlement already. Any additional settlement would, therefore, take the building beyond permissible limits and damages may occur. Proper bracing system has, therefore, to be adopted to protect the sides of the excavation.

As a general rule, the ground settlement due to braced excavation extends to a distance of three times the depth of the cut, as depicted in Fig. 14.21. All buildings within this zone should be thoroughly surveyed. Wherever necessary, photographs should be taken to assess the condition of the building. Settlement points should be established on the buildings plinth and measurements taken with reference to suitable benchmarks to monitor the movement during and after construction. These will provide valuable evidence if claims of damage are to be faced subsequently.

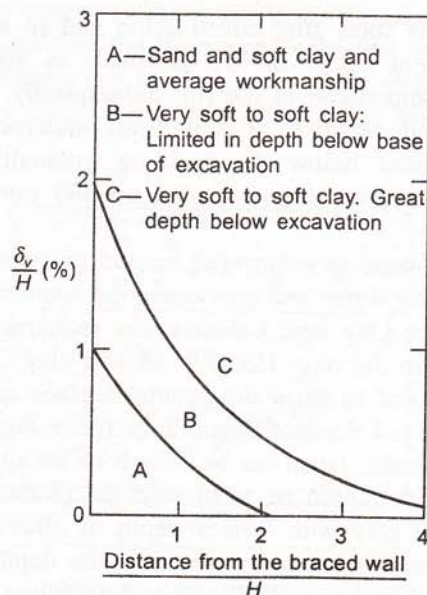


Fig. 14.21 Influence zone in braced cut.

Time is the essence of underground construction. Faster the underground works are completed, lesser will be the problems of settlement. Deep excavation should never be kept open for long periods of time as this invites additional settlement and damage to adjoining structures. Figure 14.22 shows the effect of Calcutta metro construction on a building close

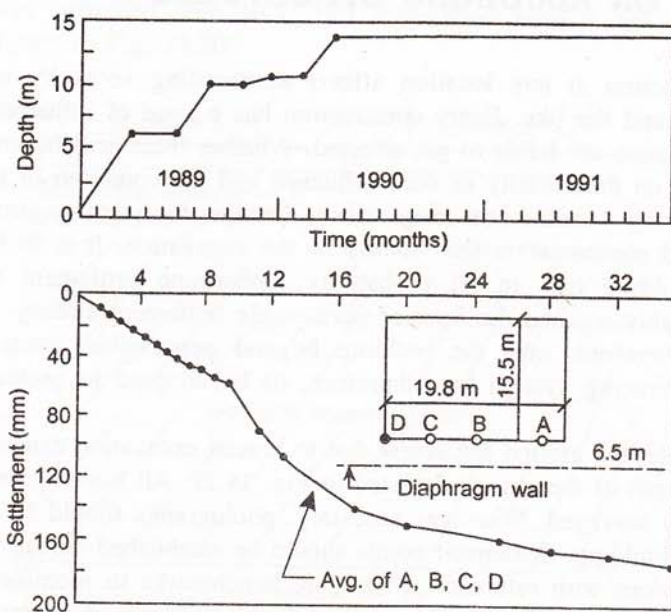


Fig. 14.22 Effect of time on building settlement adjacent to braced cut.

to the diaphragm wall. For various reasons, the metro work was stopped repeatedly at this section and the construction took the best part of three years. The excavation was kept open for 90 days at 8 m depth and thereafter for almost two years at 14 m depth. It may be noticed that out of a total settlement of 172 mm, no less than 93 mm had occurred during stoppages of construction. The data clearly show the effect of time on ground settlement adjacent to a braced cut.

#### 14.6.1 Effect of Vibration

Vibrations caused by construction operations such as blasting, pile-driving, compaction by drop hammer, compaction piles, and so on can damage existing structures and equipment if not designed to resist such motions. The peak particle velocity near a building due to a source of single impact is shown in Fig. 14.23 (Mayne et al., 1982).

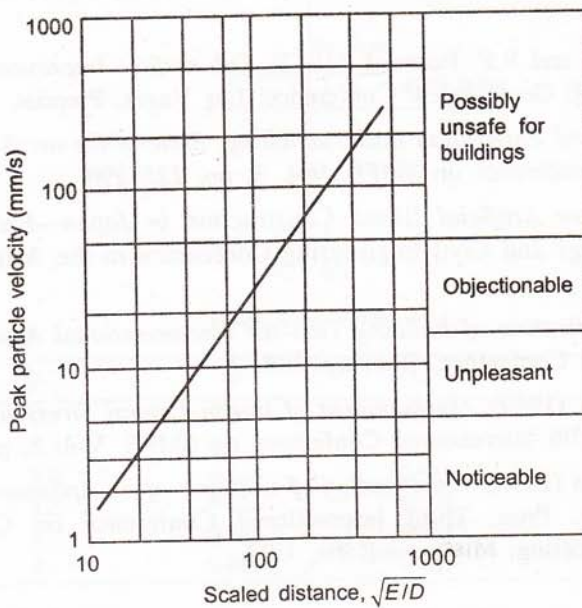


Fig. 14.23 Particle velocity versus distance due to a single impact (after Mayne et al., 1982).

A safe upper limit for small buildings, is given as

$$v = 70 \left( \frac{E}{10D^2} \right)^{0.56} \quad (14.8)$$

where,

$E$  = energy per blow in KJ, and

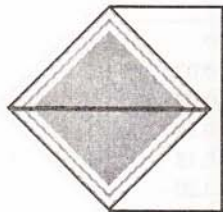
$D$  = distance between the source and the structure under consideration.

A maximum peak particle velocity of 50 mm/s is normally considered safe for conventional buildings.

If the vibration level is intolerable, the soil foundation system may be modified to minimize the effect of vibration. This may be done by providing vibration barriers. Trenches may be made around the vibration source for *active isolation* or may be made near the object to form *passive isolation*. For active isolation, the depth of trench should be 0.6 times the distance from the structure. This would reduce the ground motion to one quarter of the amplitude of 'no trench' condition. For passive isolation, a semicircular plan area behind the trench at a distance  $L_R$  with the depth of trench equal to  $1.33L_R$  would give effective isolation.

## REFERENCES

- Lee and R.J. Suedkamp (1972), *Characteristics of Irregular Shaped Compaction Curves of Soils*, Highway Research Record No. 381, National Academy of Seeing, Washington DC, pp. 1-9.
- Mayne, P.W., J.S. Jones and R.P. Fedosick (1982), *Sub-surface Improvement due to Impact Densification*, ASCE Geotechnical Conference, Las Vagas, Preprint, Session B 2.
- Peck, R.B. (1969), *Braced Excavation and Tunnelling. State-of-the-art Report*, Proceedings 5th International Conference on SMFE, Vol. 3, pp. 225-290.
- Soda, S. (2001), *Offshore Artificial Island Construction in Japan—Example of Offshore Airports*, Proceedings 2nd Civil Engineering Conference in the Asian Region, Tokyo. p. 77.
- Som, N.N. (2000), *Rectification of Building Tilt—An Unconventional Approach*, Proceeding Indian Geotechnical Conference, Bombay, Vol. 2.
- Som, N. and I.R.K. Raju (1989), *Measurement of in-situ Lateral Stress in Normal Calcutta Soil*, Proceedings 12th International Conference on SMFE, Vol. 3, pp. 1519-1522.
- Som, N.N. and R.B. Sahu (1993), *Investigation of Collapse of an Apartment Building due to Differential Filling*, Proc. Third International Conference on Case Histories in Geotechnical Engineering, Missoorie-Rolla, USA.



# Appendix

- (a) Vertical stress influence coefficient for uniform circular load

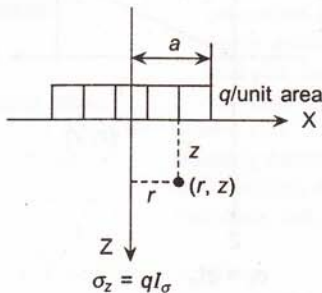
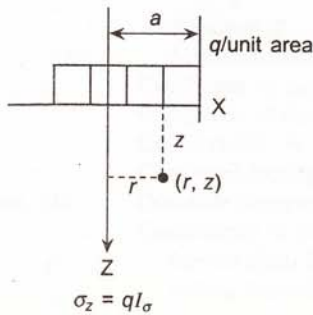


Table A.1 Values of  $I_\sigma$

$z/a \diagup r/a$	0	0.5	1.0
0	1.000	1.000	1.000
0.5	0.910	0.790	0.417
1.0	0.646	0.560	0.332
1.5	0.424	0.375	0.256
2	0.286	0.258	0.196
4	0.087	0.083	0.075

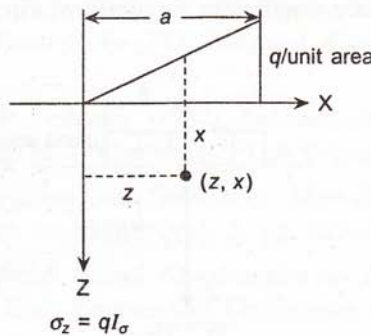
- (b) Vertical stress influence coefficient for uniformly distributed strip load



**Table A.2** Values of  $I_\sigma$ 

$z/a \diagup x/a$	0	0.5	1.0	1.5	2
0	1.00	1.00	0.50	0	0
0.5	0.96	0.90	0.49	0.09	0.02
1.0	0.82	0.73	0.38	0.25	0.08
1.5	0.67	0.61	0.45	0.27	0.15
2	0.55	0.51	0.41	0.29	0.18
3	0.39	0.40	0.30	0.28	0.20
4	0.31	0.30	0.25	0.26	0.22

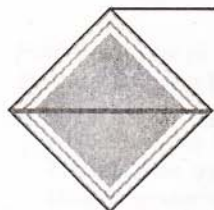
(c) Vertical stress influence coefficient for triangular load



$$\sigma_z = qI_\sigma$$

**Table A.3** Values of  $I_\sigma$ 

$z/a \diagup x/a$	0	0.5	1	2
0	0	0.5	0.5	0
0.5	0.13	0.41	0.35	0.03
1	0.16	0.28	0.25	0.07
2	0.13	0.16	0.15	0.08



# Index

- Aerial photographs, 34  
Allowable load on piles from static analysis, 218  
Allowable settlement, 73  
Angle of shearing resistance, 14  
Apparent cohesion, 14  
Approximate method of determining verticle stress, 106  
Atterberg limits, 5  
    Liquid limit, 5  
    Plastic limit, 5  
    Shrinkage limit, 5  
  
Band drains, 310  
Basement raft, 181  
Bearing capacity, 70, 117, 177  
    allowable, 71, 166  
    from field tests, 131  
    of non-homogeneous soil, 127  
Bearing capacity analysis  
    bearing capacity factors, 124  
    depth factors, 126  
    Hansen's method, 126  
    inclination factors, 126  
    local shear failure, 126  
    Meyerhof's method, 125  
    Prandtl's analysis, 120  
    shape factors, 126  
    Skempton's method, 125  
    Terzaghi's analysis, 122  
    Vesic's method, 126  
Black cotton soil, 294  
Bored and cast-in-situ piles in cohesionless soil, 212  
Bored piles, 201  
    in cohesive soil, 205  
    in cohesionless soil, 205  
  
Boring, 34  
    auger boring, 35  
    percussion drilling, 36  
    rotary drilling, 36  
    trial pits, 34  
    wash boring, 34  
Braced cuts, 374  
Building damage due to liquefaction, 360  
Bulk density, 4  
Buoyancy raft, 68, 177  
  
Caissons, 266  
    box, 266  
    open, 266  
    pneumatic, 266  
Capacity of pile group, 224  
Causes of defect in piles, 246  
Cellular raft, 180  
Chemical and mineralogical data, 60  
Chemical injection and grouting, 306  
Chemical test on water samples, 60  
Choice of foundation type, 70  
Classification of swelling potential, 297  
Clay minerals, 2  
    Illite, 2  
    Kaolinite, 2  
    Montmorillonite, 2, 295  
Coefficient of earth pressure at rest, 77, 144  
Coefficient of consolidation, 25  
Cohesive fill, 387  
Combined footing, 66, 164  
Common construction problems, 371  
Components of well foundation, 268  
    bottom plug, 269  
    cutting edge, 269

- dredge hole, 269  
 intermediate/top plug, 270  
 steining, 269  
 well cap, 270  
 well curb, 269
- Concrete piles, 200  
 Consistency, 61  
 Consolidation, 63  
     coefficient of, 25  
     degree of, 25  
     rate of, 24  
 Consolidation settlement, 142  
 Conventional raft, 67, 175  
 Critical depth, 216  
 Cyclic shear stress, 356
- Damage limits  
     for load bearing walls, 74  
     of angular distortion, 74
- Damages due to differential settlement, 72  
     architectural, 72  
     combined structural and architectural, 73  
     structural, 72  
     visual effects, 73
- Darcy's law, 12  
 Deep foundations, 68  
     piers and caissons, 69  
     pile foundation, 68
- Degree of saturation, 4  
 Depth correction, 142  
 Depth  
     of boreholes, 52  
     of diaphragm wall, 374  
     of fixity, 233  
     of footing, 165  
     of penetration, 376
- Design criteria, 70  
 Design for equal settlement, 172  
 Design  
     of braced cuts, 374  
     of raft foundation, 175
- Design parameters, 63  
 Dewatering, 378  
     methods of, 380  
         deep well pumping, 381  
         field control, 384  
         sump pumping, 380  
         well point dewatering, 383
- Differential free swell, 295  
 Dimensioning footing foundations, 170
- Driven piles, 201  
     cast-in-situ, 201  
     in cohesionless soil, 205  
     in cohesive soil, 204
- Dry density, 4  
 Dynamic properties of soil, 363  
     damping factor, 365  
     particle-size distribution, 363  
     radiation damping, 365  
     relative density, 364  
     shear modulus, 364
- Dynamics of pile driving (dynamic analysis), 219  
     ENR formula, 220  
     Hiley formula, 220  
     Janbu's formula, 221  
     limitations of dynamic analysis, 222  
     Simplex formula, 221  
     wave equation, 222
- Earth pressure, 376  
 Earthquake, 346  
     Alaska, 351  
     Bhuj, 354  
     Niigata, 352, 353  
     energy release, 347  
     intensity, 347  
     magnitude of, 346  
     modified Mercalli Intensity, 347  
     Richter scale, 346
- Effect of  
     adjoining structures, 371  
     earthquake on fine-grained soils, 358  
     ground water table, 168  
     ground water table on bearing capacity, 130  
     swelling, 294  
     time on building settlement adjacent to braced cut, 390  
     vibration, 391
- Effective stress parameters, 63  
 Effects of earthquake, 350  
 Efficiency of pile group, 223  
 Elastic parameters, 27  
 Elastic theory, 152  
 End bearing, 213  
     in cohesionless soil, 213  
     in cohesive soil, 213
- End bearing piles, 199  
 Engineering properties, 60  
     of soil, 12  
 Expansive soils, 10, 296  
 Factors affecting bearing capacity, 129

- Failure mechanism, 118  
 general shear failure, 119  
 local shear failure, 119  
 punching shear failure, 119
- Field control for preloading, 313  
 Field measurement for preloading, 310  
 Field testing of soils, 40  
   direct shear test (In-situ), 47  
   dynamic cone penetration test, 43  
   Menard pressuremeter, 49  
   plate bearing test, 48  
   pressuremeter test, 49  
   standard penetration test, 41  
   static cone penetration test, 44  
   Vane shear test, 46  
 Floating foundation, 178  
 Flocculated structure, 3, 305  
 Forces acting on well foundation, 272  
 Foundation design in expansive soil, 298  
   chemical stabilization, 302  
   CNS layer, 301  
   controlling swelling, 300  
   impervious apron, 300  
   measures to withstand settlement, 302  
   surcharge loading, 301  
   under-reamed piles, 298
- Foundations  
   deep, 65, 68  
   on clay, 138  
   on sand, 152  
   raft or mat, 67  
   shallow, 66
- Free-swell test, 294  
 Friction piles, 200  
 Frictional resistance, 206  
   in cohesionless soil, 210  
   in cohesive soil, 207
- Fundamental period, 349
- Geological survey reports and maps, 34  
 Geophysical methods, 34  
 Grain-size distribution, 7  
 Granular fill, 387  
 Granular soil  
   structure of, 305  
 Gross and net soil pressure: safe bearing capacity, 131  
 Gross ultimate bearing capacity, 70  
 Ground acceleration, 348
- Ground improvement in granular soil, 326  
   compaction piles, 332  
   control of field work, 332  
   dynamic consolidation, 328  
   heavy tamping or drop hammer, 326  
   trial ground improvement, 333  
   vibrocompaction, 330
- Ground improvement  
   principles of, 304
- Ground settlement, 350, 377  
 Ground treatment in cohesive soil, 306  
 Ground water table, 51  
 Groundwater, 10  
   aquifer, 10  
   aquifuge, 11  
   aquitard, 11  
   capillary zone, 11  
   recharge, 10  
   water table, 10  
   zone of saturation, 11
- Honeycombed structure, 3
- I.S. code method, 240  
 Immediate settlement, 140  
 Indian standard classification system, 8  
 Influence of stress-path, 148  
 Influence zone in braced cut, 390  
 Information required from soil investigation, 55  
 In-situ compressibility, 28  
 In-situ stress, 76  
 Integrity testing of piles, 246  
 Interference effect, 172  
 Intergranular pressure, 15  
 Isobar, 91  
 Isolated footing, 66, 164
- Laboratory test data, 60  
 Laboratory tests, 51  
 Lacey's silt factor, 271  
 Land filling, 385  
 Large area loading, 325  
 Lateral stability of wells, 273  
   Bombay method, 275  
   bulkhead concept, 273  
   IRC method, 275  
 Layout and number of boreholes, 51  
 Limitations of theoretical analysis, 129

- Limits of consistency, 5  
 Liquefaction, 352  
 Liquefaction potential, 354  
 Liquidity index, 5  
 Load carrying capacity of stone column, 323  
 Load versus settlement relationship, 117  
 Load test on piles, 247  
     constant rate of penetration (CRP) test, 249  
     maintained load test, 248  
     procedure of, 248
- M.I.T. classification system, 7  
 Measurement of shear strength, 18  
 Measures to prevent liquefaction, 362  
 Mohr-Coulomb equation, 17  
 Movement of diaphragm wall, 376
- Negative skin friction, 242  
     clay overlying sand fill, 243  
     neutral point, 243  
     sand fill overlying clay, 244
- Net permissible bearing pressure, 75  
 Net ultimate bearing capacity, 70  
 Newmark's chart, 89  
 Nonlinear soil, 103  
 Normal Calcutta deposit, 9  
 Normally consolidated clays, 23  
 Number and spacing of struts, 375
- Open drive samplers, 38  
 Organic soils, 9  
 Overconsolidated clays, 23
- Peat, 9  
 Pedological data, 34  
 Permeability, 12  
 Permissible settlement, 74  
 Pile behaviour under axial load, 201  
 Pile capacity from in-situ soil tests, 203  
 Pile driving analyzer, 251  
 Pile group subjected to vertical load and moment, 226  
 Pile groups, 223  
     in cohesionless soil, 230  
     in cohesive soil, 228  
 Piles, 199  
     in cohesionless soil, 205  
     in cohesive soil, 204
- testing of, 245  
 timber, 200
- Pile spacing, 225  
 Piles under horizontal forces, 232  
 Piston sampler, 38  
 Planning of exploration programme, 51  
 Plasticity chart, 6  
 Plasticity index, 5  
 Plate load test, 153  
 Pore-pressure, 14  
     coefficients, 16
- Porosity, 4  
 Pre-consolidation pressure, 28  
 Preloading with vertical drains, 306  
 Preservation of samples, 39  
 Pressure bulb, 91  
 Pressure-void ratio relationships, 22  
 Principle of effective stress, 13
- Radius of influence, 379, 380  
 Rammed stone column, 316  
 Rate  
     of discharge, 380  
     of seepage, 378  
     of settlement, 151
- Reclaimed ground, 389  
 Reconnaissance study, 33  
 Relative density, 8  
 Response spectrum, 348  
 Responsibility of designer, 55  
 Rigidity of footings: contact pressure, 92
- Sampling, 37  
     from boreholes, 37  
     from trial pits, 37
- Sand drains, 309  
     drain diameter, 308  
     drain spacing, 308  
     types of vertical drains, 309
- Sand wicks, 309  
 Scour depth, 270  
 Semi-empirical method, 152  
 Sensitivity of clays, 21  
 Settlement analysis  
     methods of, 139
- Settlement  
     of pile groups, 228  
     of stone column foundations, 324
- Settlement criteria, 71  
 Settlement reduction ratio, 324

- Shear strength of soils, 17  
 Site investigation, 32  
     stages of, 33  
 Sloped excavation, 372  
 Soil  
     aeolian, 1  
     estuarine, 1  
     glacial, 1  
     lacustrine, 1  
     marine, 1  
     residual, 1  
     sedimentary, 1  
 Soil classification, 7  
 Soil deposits of India, 29  
 Soil profile, 59  
 Soil test report, 55  
 Stability of excavation, 372  
 Stabilization of boreholes, 36  
     by casing, 36  
     by drilling fluid, 36  
     by water, 36  
 Standard penetration test, 41  
 Static analysis, 203  
 Static cone test, 153  
 Steel piles, 200  
 Stone columns, 314  
 Stress concentration factor, 325  
 Stress distribution in non-homogeneous soils, 94  
     multilayer systems, 99  
     non-homogeneous medium, 100  
     rigid base system, 94  
     single elastic layer on a rigid base, 96  
     three-layer systems, 97  
     two layers with different elastic parameters, 95  
     two-layer system, 94  
 Stress increment ratio, 148  
 Stresses due to foundation loading, 78  
     Boussinesq analysis: point load, 78  
     embankment type loading, 87  
     triangular load, 86  
     uniform line load, 85  
     uniform strip load, 85  
     vertical stresses below uniform circular load, 83  
     vertical stresses below uniform rectangular load,  
         81  
 Stresses during loading and consolidation in the  
     field, 146  
 Stress-path, 143  
     settlement analysis, method of, 149  
 Strip footing, 67, 164  
 Structural capacity of piles, 196  
 Structural design  
     of footings, 174  
     of raft foundation, 182  
         elastic method, 182  
         rigid method, 182  
 Strut load, 378  
 Submerged density, 4  
 Swelling pressure, 296  
  
 Testing of soil, 40  
     classification tests, 40  
     engineering properties, 40  
 Three-phase system, 3  
 Total normal pressure, 14  
 Types of compaction curve, 387  
 Triaxial test, 19  
     consolidated drained test, 20  
     consolidated undrained test, 19  
     unconsolidated undrained test, 19  
  
 Ultimate lateral resistance, 234  
 Under-reamed piles, 194, 210  
 Undrained shear strength, 62  
     of clays, 20, 358  
 Unified soil classification system, 8  
 Uniform building code of USA, 349  
 Uniformity coefficient, 7  
 Unit weight, 4  
 Unrestrained swell test, 295  
 Uplift resistance of piles, 231  
  
 Validity of Darcy's law, 13  
 Vibroflotation, 315  
 Void ratio, 4  
  
 Water content, 4  
 Weathering, 1  
 Well Foundations, 266  
 Well sinking, 283  
 Well/caisson, 65